

Bifurcations in stochastic equations with delayed feedback

Mathieu Gaudreault

Department of Physics
McGill University
Montréal, Québec, Canada

June 2011

A thesis submitted to McGill University in partial fulfillment of the
requirements for the degree of Doctorate of Physics

© 2011 Mathieu Gaudreault

Acknowledgements

This project would not have been possible without the support of many people. Many thanks to my advisor, Professor Jorge Viñals, for his patience and availability. His knowledge always gives me motivation and creative ideas through my research. Thanks also to collaborators that were involved in various parts of this project, Françoise Lépine, François Drolet, and Juliana Berbert. Computational resources have been provided by Clumeq, SciNet, and Msi. Support from friends is also an important aspect. In that matter, I would like to acknowledge Elvis Pandzic, Adriano Ferrari, and Xusheng Zhang.

Abstract

The bifurcation diagram of a model stochastic differential equation with delayed feedback is presented. We are motivated by recent research on stochastic effects in models of transcriptional gene regulation. We start from the normal form for a pitchfork bifurcation, and add multiplicative or parametric noise and linear delayed feedback. The latter is sufficient to originate a Hopf bifurcation in that region of parameters in which there is a sufficiently strong negative feedback. We find a sharp bifurcation in parameter space, and define the threshold as the point in which the stationary distribution function $p(x)$ changes from a delta function at the trivial state $x = 0$ to $p(x) \sim x^\alpha$ at small x (with $\alpha = 1$ exactly at threshold). We find that the bifurcation threshold is shifted by fluctuations relative to the deterministic limit by an amount that scales linearly with the noise intensity.

Analytical expressions for pitchfork and Hopf bifurcation thresholds are given for the model considered. Our results assume that the delay time τ is small compared to other characteristic time scales, not a significant limitation close to the bifurcation line. A pitchfork bifurcation line is found, the location of which depends on the conditional average $\langle x(t)|x(t - \tau) \rangle$, where $x(t)$ is the dynamical variable. This conditional probability incorporates the

combined effect of fluctuation correlations and delayed feedback. We also find a Hopf bifurcation line which is obtained by a multiple scale expansion around the oscillatory solution near threshold. We solve the Fokker-Planck equation associated with the slowly varying amplitudes and use it to determine the threshold location. In both cases, the predicted bifurcation lines are in excellent agreement with a direct numerical integration of the governing equations. Contrary to the known case involving no delayed feedback, we show that the stochastic bifurcation lines are shifted relative to the deterministic limit and hence that the interaction between fluctuation correlations and delay affect the stability of the solutions of the model equation studied.

Moreover, we obtain the characteristic correlation time associated to the model. In particular, the validity of the common assumption of statistical independence between the state at time t and that at $t - \tau$ is examined. We find that the correlation time diverges at the model's bifurcation line, thus signalling the failure of statistical independence near threshold. We determine the correlation time both by numerical integration of the governing equation, and analytically in the limit of small τ . The correlation time T diverges as $T \sim a^{-1}$, where a is the control parameter so that $a_c = 0$ is the bifurcation threshold. The small- τ expansion correctly predicts the location of the bifurcation threshold, but there are systematic deviations in the magnitude of the correlation time.

Abrégé

Le diagramme de bifurcation d'une équation différentielle stochastique incluant une échelle de temps retardée est présenté. Nous sommes motivés par des recherches récentes portant sur des modèles de régulation des gènes. Nous débutons avec la forme normale d'une bifurcation de type fourchette auquel est ajoutée un terme stochastique de manière paramétrique ainsi qu'un terme linéaire incluant le délai. Ce dernier terme introduit une bifurcation de type Hopf où le délai négatif est particulièrement fort dans l'espace des paramètres. Une bifurcation abrupte est trouvée et nous définissons le seuil de bifurcation comme étant le point dans l'espace des paramètres pour lequel la fonction de distribution stationnaire $p(x)$ change d'une fonction delta autour de l'origine à $p(x) \sim x^\alpha$ pour x petit (avec $\alpha = -1$ exactement au seuil). Nous démontrons que le seuil de bifurcation est modifié par les fluctuations comparé à la limite déterministique par une valeur qui suit une relation linéaire avec l'intensité du bruit.

Des expressions analytiques pour les seuils de bifurcation de type fourchette et Hopf du modèle considéré sont présentées. Nos résultats assument que le temps retardé τ est petit comparé aux autres temps caractéristiques du système, une limitation qui n'est pas significative près de la ligne de bifurca-

tion. L'expression pour la bifurcation de type fourchette est déterminée suite à une expansion stochastique de Taylor. La location de cette bifurcation dépend de la moyenne conditionnelle $\langle x(t)|x(t-\tau) \rangle$, où $x(t)$ est la variable dynamique. Cette probabilité conditionnelle comprend les effets combinés des fluctuations corrélées et du retardement rétroactif. Nous déterminons aussi une expression pour la bifurcation de type Hopf obtenue à l'aide d'une expansion des échelles de temps autour de la solution près du seuil. Nous obtenons une équation de Fokker-Planck associée à la dynamique des amplitudes des oscillations et nous utilisons celle-ci pour déterminer la location du seuil. Contrairement au cas sans délai, nous démontrons que la location des lignes de bifurcation est modifiée comparé à la limite déterministique et donc que l'interaction entre les corrélations des fluctuations et le délai affectent la stabilité des solutions du modèle étudié.

De plus, nous obtenons le temps de corrélation caractéristique associé au modèle. En particulier, la validité de l'hypothèse d'indépendance statistique entre l'état au temps t ainsi qu'au temps $t - \tau$ est examinée. Nous trouvons que le temps de corrélation diverge à la bifurcation, signalant l'infirmité de l'indépendance statistique au seuil de bifurcation. Nous déterminons le temps de corrélation par une intégration directe de l'équation gouvernant le modèle ainsi qu'analytiquement dans la limite où le délai est petit. Le temps de corrélation T diverge suivant une relation du type $T \sim a^{-1}$, où a est le paramètre de contrôle et où $a_c = 0$ est la location de la bifurcation. L'expansion dans la limite où le délai est petit prédit correctement la location du seuil de bifurcation. Néanmoins, des déviations systématiques dans la magnitude du temps de corrélation sont observées entre les deux résultats.

Table of Contents

List of Figures	xi
List of Tables	xiii
1 Introduction	1
2 Stochastic bifurcation	15
2.1 Algorithm for delay stochastic differential equation	15
2.2 Stochastic bifurcation	18
2.3 Normal form of a pitchfork bifurcation	24
3 Stochastic bifurcation of delayed equations	31
3.1 Delayed feedback induces oscillation	32
3.2 Stationary density for small time delay	45
3.3 Expansion under Stratonovich calculus	53
4 Multiple time scale expansion	59
4.1 Van der Pol oscillator with delayed feedback	60
4.2 Multiple time scale expansion of a SDDE	78
5 Numerical stability analysis	93
5.1 Pitchfork bifurcation	95
5.2 Hopf bifurcation	100
6 Correlation time near threshold	103
6.1 Correlation time	104
6.2 Numerical determination of the correlation time	108

7	Conclusions	119
A	Ito and Stratonovich calculus	125
B	Fokker-Planck equation	131
B.1	Ito interpretation	131
B.2	Stratonovich interpretation	133
C	Integration method with delay	139
D	Jung-Risken theory	147
	Bibliography	165

List of Figures

1. Introduction	1
2. Stochastic bifurcation	15
2.1 Growth exponent of $\dot{x}(t) = ax(t) + \eta(t)$	21
2.2 Growth exponent of $\dot{x}(t) = ax(t) + x(t)\xi(t)$	24
2.3 Histogram of $\dot{x}(t) = ax(t) - x^3(t) + \eta(t)$	26
2.4 Histogram of $\dot{x}(t) = ax(t) - x^3(t) + x(t)\xi(t)$	29
3. Stochastic bifurcation of delayed equations	31
3.1 Real branches of the Lambert function	34
3.2 Growth exponent of linear equations with delay	36
3.3 Bifurcation of $\dot{x}(t) = ax(t) + bx(t - \tau)$	37
3.4 Bifurcation of linear stochastic equations with delay	44
4. Multiple time scale expansion	59
4.1 Phase portrait of the delayed VDP oscillator	66
4.2 Probability density of the VDP oscillator	70
4.3 Exponent of the power law of the VDP oscillator	75
4.4 Bifurcation diagram of the VDP oscillator	76
4.5 Hopf frequency of the VDP oscillator	77
5. Numerical stability analysis	93
5.1 Bifurcation of $\dot{x}(t) = ax(t) + bx(t - \tau) - x^3(t) + x(t)\xi(t)$. . .	94

5.2	Pitchfork bifurcation with delay	95
5.3	Histogram of $\dot{x}(t) = ax(t) + bx(t - \tau) - x^3(t) + x(t)\xi(t)$	96
5.4	Power law fit around the pitchfork branch	97
5.5	Bifurcation threshold a_c from $p(x)$	98
5.6	Average conditional drift $\langle x_\tau x \rangle$	99
5.7	Probability density around the Hopf branch	101
5.8	Exponent of the power law around the Hopf branch	102
6. Correlation time near threshold		103
6.1	Theoretical correlation time	109
6.2	Correlation function without delayed feedback	110
6.3	Correlation time of the Stratonovich model	111
6.4	Correlation time of the Stratonovich model scaled	112
6.5	Correlation function with delayed feedback	113
6.6	Correlation time with delayed feedback	114
6.7	Correlation time with delayed feedback scaled	115
6.8	Correlation time as a function of the time delay	116
Conclusions		119
A. Ito and Stratonovich calculus		125
B. Fokker-Planck equation		131
C. Integration method with delay		139
D. Jung-Risken theory		147

List of Tables

D. Jung-Risken theory	147
D.1 Coefficients $M_n^{(\nu)}$ of the moment.	154
D.2 Coefficients $K_n^{(\nu)}(0)$ of the correlation function	156
D.3 Coefficients $T_n^{(\nu)}$ of the scaled correlation time	157

Chapter 1

Introduction

At the cellular level, information encoded in the gene results into a phenotype through the processes of transcription and translation [1, 2, 3]. In the former process, the genetic code in DNA is transcribed to sequence of nucleotides called messenger RNA (mRNA). The latter process involves translation of the code carried by mRNA to an amino acid sequence during protein synthesis. Generated proteins then interact with other molecular species or other proteins. The ensemble of a given set of such interactions produces a given phenotype. Some proteins, the transcription factors, regulate the activity of genes. They bind to the promoter region of a gene in order to promote or inhibit transcription. The expression level of a given gene coding for these transcription factors may affect the activity of several genes. Genes are thus interconnected into complex networks that are self-regulated. The regulated genes, the transcription factors, and their interactions form a scheme that is generically referred to as the gene regulation network. Each phenotype is associated with a complex network of gene interactions. For this reason, the study of the dynamics of gene regulatory networks has become one of the main active research fields in theoretical biophysics today.

Gene networks are determined experimentally from gene expression profiles [4, 5]. Gene expression profiling is a measure of the activity or the expression of thousand of genes in parallel in order to have a global picture of the function of the genes considered. The activity of genes under study is measured by DNA microarray technology. Microarray is a two dimensional grid in which each microscopic spot contains a specific concentration of a fragment of DNA sequence. The concentration of mRNA's produced by transcription are measured either from fluorophore-, silver- or chemi-luminescence labelling technology. Microarray experiments can be classified into two groups: time-course experiments and perturbation experiments. The former are done to observe changes of gene activity in time in order to understand time-dependent process in the cell. The latter are performed to observe the effects of a given input on the cell and are used to understand the difference between cell types or responses to these inputs.

Some gene regulation networks are known in great detail, such as the lysis/lysogeny cycle regulation of bacteriophage- λ [6], the endomesoderm development network in Sea Urchin [7], and the segment polarity network in *Drosophila* development [8, 9]. The first two are mostly representations of the relationship between the genes while the last one involves quantitative models. Other gene networks are available in databases but in less detail such as in the KEGG [10] or in the EcoCyc [11] databases. The huge amount of experimental data in databases provides a framework suitable for modelization of these networks.

Several generic characteristics of gene networks emerge from the experiments. It has been observed that the topology of the network is sparse [12]. In order words, the average number of edges per nodes is much smaller than the

total number of nodes. Genes are thus regulated by a small number of other genes, about 2-4 in bacteria [13] and 5-10 in eukaryotes [14]. Moreover, the distribution of connectivity of nodes tend to follow a power law [15]. Networks showing this property are called scale-free. Furthermore, gene networks are robust to fluctuations in their parameters [9, 16] and there is strong evidence that only specific topologies allow such robustness [9, 15]. Finally, stochasticity is an integral part of gene networks as it is an intrinsic property of biochemical reactions [17, 18, 19].

Several methods exist to model the dynamics of gene networks. One of such model is called the Boolean network [20, 21]. Each gene, input, and output in the network is considered as a node in this method. Each node can either be on or off. On the one hand, if the node is a gene, “on” corresponds to the case where the gene is being expressed. On the other hand, if the node is an input or output, “on” represents the case in which the molecular species is present. Time is then modeled as discrete steps changing the state of the network. However, this model is qualitative as it cannot give predictions about the level of expression of genes in the system.

An alternative description that can yield quantitative predictions models gene networks as networks of chemical reactions [22, 23]. In fact, a state variable and a rate of synthetization or degradation are attributed to each component of the network. For example, a given protein can be synthesized at the rate $s > 0$ and degraded at the rate $a > 0$, corresponding to the chemical reactions,



where $n > 0$ is the number of protein molecules. A Master Equation can be associated to each network of chemical reactions [22, 23]. The Master Equation describes the time evolution of the probability distribution function over a discrete number of states. The states are defined by the number of molecules of the molecular species present in the network. For example, the Master Equation associated with the network defined by Eqs. (1.1) and (1.2) is,

$$\frac{\partial}{\partial t} p(n, t) = s\Omega(\mathbb{E}^{-1} - 1)p(n, t) + a(\mathbb{E} - 1)[np(n, t)] , \quad (1.3)$$

where Ω is the volume of the system, and where \mathbb{E} is the raising operator, $\mathbb{E}f(n) = f(n + 1)$. The dynamic evolution of the probability $p(n, t)$ is numerically simulated by using an algorithm devised by Gillespie [24].

The expression level of the genes can be approximated by a continuous function, and the network modeled by a set of Langevin equations when the number of molecule is large [22, 23]. A Langevin equation describes the stochastic time evolution of the concentration of a given molecular species in this context. It is defined as

$$\dot{x}(t) = f[x(t)] + g[x(t)]\xi(t) , \quad (1.4)$$

where $x(t)$ is the concentration of a molecular species at time t , where $f[x(t)]$ and $g[x(t)]$ are respectively the drift and the diffusion coefficient, and where $\xi(t)$ is a random process. Properties of Langevin equation are introduced in Appendix A. The continuous representation of genetic networks is investigated in this thesis, as well as the dynamics of the network as modeled by stochastic differential equations.

The field of stochastic differential equations is very mature [25, 26, 27, 28, 29, 30, 31, 32]. Two different calculi have been introduced in the literature,

one is due to Ito [33, 34], the other one to Stratonovich [35]. Existence and uniqueness of solutions to stochastic differential equations have been established in [36, 37]. The two calculi are introduced in Appendix A. Note that they are equivalent to each other under some transformation rules. These rules are presented in Appendix A. Even if the two interpretations are equivalent to each other, a distinction can be made depending on the physical situations modeled. In fact, it has been pointed out that the Stratonovich interpretation is appropriate when white noise is considered as the limiting case of the colored noise existing in the system [29, 38, 39, 40, 41, 42]. This observation has been confirmed experimentally [43]. On the other hand, the Ito interpretation is appropriate if the stochastic equation is considered as a continuous time limit of a discrete problem [44].

Gene expression is intrinsically a stochastic process [17, 18, 19]. It is widely accepted that the noise relevant to gene expression can be decomposed into *intrinsic* and *extrinsic* sources [45, 18, 46, 47]. On the one hand, intrinsic noise is inherent to the system and is due to the stochastic nature of biochemical reactions. This type of noise is introduced by adding a stochastic term to a differential equation describing the time evolution of the concentration of the molecular species. The noise is then said to be additive. On the other hand, extrinsic noise is due to the interaction with the environment and includes fluctuations in the reaction rates of the biochemical reactions. For example, the variability of activity of mRNAs between transcription and translation can be considered as an extrinsic source of noise in protein production [48, 49]. Fluctuating reaction rates can be introduced in Langevin equations by adding a stochastic component to the reaction rates. In this case, the noise is said to be parametric or multiplicative as random terms multiply the variables that

specify the state of the system. Both intrinsic and extrinsic sources of noise are investigated in this thesis, modeled by Langevin equations for which the noise enters either additively or multiplicatively.

This thesis focuses on biological regulation processes involving a feedback motif. Some reactions are not instantaneous [1, 2, 3] and the concentration of a given molecule at time t might depend on its state at a time $t-\tau$, where $\tau > 0$ is the time delay. For example, delay might be attributable to the time required for a protein to cross the membrane or to a conformational change of a protein. Another example is DNA transcription which is a fast process as compared to the time required for the transcription factor to appear as a functional unit in the cell. The mathematical theory of delay differential equations is extensively developed [50, 51, 52, 53, 54, 55, 56, 57]. The presence of delayed feedback changes drastically the solutions of the system and makes the governing models rarely tractable analytically. However, delay differential equations lead to rich dynamics such as oscillations, limit cycles, and Hopf bifurcations. The study of delay differential equations is an important topic with several applications in applied Mathematics, Physics (lasers [58, 59], liquid crystals [60]), Physiology (neural networks [61, 62, 63, 64, 65, 66], neuronal and cardiac tissue activity [67, 68]), and even Economics (agricultural commodity prices [69, 70]).

Stochastic processes without any time delay contributions can generally be modelled as Markov process. A Markov process is a random process that is only dependent on its present state [71, 72]. It simplifies analytical calculations because the transition probabilities between two states are delta-correlated [73]. This is no longer true for systems in which time delays are important because their state at time t depends at least on their past state at time $t-\tau$. Delays in stochastic models of gene regulation network have been mostly

ignored due to their non Markovian nature.

Our study is in part motivated by a model of protein degradation first introduced by Bratsun et al. [74]. It has been observed experimentally that the FRQ protein in *Neurospora crassa* degrades in the cell according to two time scales [75, 76]. *Neurospora crassa* is a type of red bread mold of the phylum *Ascomycota*. It is used in Biology as a model organism because it is easy to grow and its haploid life cycle makes genetic analysis simple since recessive traits show up in the offspring. The FRQ protein is known to be involved in the regulation of the period of the circadian rhythm as well as in the regulation of temperature compensation. It has been measured that the FRQ protein degrades in the cell because of dilution at a rate of $0.3 h^{-1}$. It has been also observed that protein degrades after multiple phosphorylation steps at a rate of $1 h^{-1}$. In fact, phosphate groups are added to one end of the protein so that it becomes a target of the ubiquitin proteosome machinery. The latter degradation mechanism is thus delayed relative to the former. The network representing this process is modeled by the following chemical reactions,



where s , a , and b are positive reaction rates and where $n > 0$ is the number of proteins. The double arrow in Eq. (1.7) represents a delayed reaction. Associated with this network of chemical reactions is a Master Equation [74,

77],

$$\begin{aligned} \frac{\partial}{\partial t} p(n, t) = & s\Omega(\mathbb{E}^{-1} - 1)p(n, t) + a(\mathbb{E} - 1)[np(n, t)] \\ & + b \sum_{m=0}^{\infty} mH(n)p(n, t; m, t - \tau), \end{aligned} \quad (1.8)$$

where $p(n, t; m, t - \tau)$ is the joint probability of having n molecule at time t and m molecules at time $t - \tau$, and where the step function $H(n) = 1$ if $n > 0$ and $H(n) = 0$ otherwise is added to ensure that there is at least one molecule in the system. One can expand this equation by using the inverse system size expansion of van Kampen [23]. The solution $n(t) = \Omega x(t) + \Omega^{1/2} \zeta(t)$ for large Ω is split into the deterministic solution $x(t)$ and a fluctuation $\zeta(t)$ around the deterministic solution. Substitution of this change of variable into Eq. (1.8) and collecting terms at leading order $\Omega^{1/2}$ leads to the deterministic equation,

$$\dot{x}(t) = s - ax(t) - bx(t - \tau). \quad (1.9)$$

This equation has a fixed point located at $x^* = s/(a+b)$. Equation (1.9) is the starting point of our study. We have first chosen the fixed point to be located at $x^* = 0$ by setting $s = 0$. The rate constants in the differential equation a and b are allowed to be either positive or negative, representing creation or degradation respectively. The bifurcation diagram of Eq. (1.9) with $s = 0$ is known [44] and is discussed in Chapter 2. It turns out that the solution is unstable above a certain threshold in the space of parameters and diverges to infinity. For this reason, we have added a nonlinear cubic term to this equation, which saturates the solution to a finite value above threshold and makes the stochastic analysis mathematically well posed. Furthermore, we have investigated the inclusion of noise into Eq. (1.9). On the one hand, additive

noise is known not to play a major role in the stability of the reaction (given by the location of a bifurcation threshold), which is unchanged as compared to the deterministic equation [44]. On the other hand, we are interested to know if correlations induced by parametric noise couple with delayed feedback, and perhaps modify the nature and location of the bifurcation. We therefore focus in this thesis on the following Langevin equation,

$$\dot{x}(t) = ax(t) + bx(t - \tau) - \gamma x^3(t) + x(t)\xi(t) + \eta(t) , \quad (1.10)$$

where a is a control parameter, b is the intensity of the feedback loop of time delay $\tau > 0$, γ is a constant and may differentiate between linear ($\gamma = 0$) and nonlinear ($\gamma \neq 0$) equation, and where $\xi(t)$ and $\eta(t)$ are two Gaussian white noise stochastic processes with mean $\langle \xi(t) \rangle = \langle \eta(t) \rangle = 0$ and correlation $\langle \xi(t)\xi(t') \rangle = 2D\delta(t - t')$, $\langle \eta(t)\eta(t') \rangle = 2K\delta(t - t')$, and $\langle \xi(t)\eta(t') \rangle = 0$ for all t and t' , where D and K are respectively the intensity of the stochastic process $\xi(t)$ and $\eta(t)$. We interpret Eq. (1.10) under the Stratonovich interpretation of stochastic calculus, as opposed to the stochastic calculus developed by Ito.

We focus in this thesis on the stability and bifurcation of stochastic differential equations with delay. Bifurcation thresholds separate regions in parameter space of different qualitative dynamics [78, 79, 80]. In fact, a system of differential equations is said to undergo a *bifurcation* when a slight continuous change of one parameter in the equation causes a qualitative change in the nature of the solutions and the stability of any fixed point. Stability in the vicinity of a fixed point x^* is studied by linearizing the flows around x^* . Consider the differential equation

$$\dot{x}(t) = f[x(t)] , \quad (1.11)$$

and let x^* be a fixed point of Eq. (1.11). Define $q(t) = x(t) - x^*$ as a small perturbation away from the fixed point. The time evolution of the new variable is then $\dot{q}(t) = \dot{x}(t) = f[x(t)] = f[q(t) + x^*]$. Take the Taylor expansion of the last expression around x^* ,

$$f[q(t) + x^*] = f(x^*) + q(t) \frac{\partial}{\partial q} f(x^*) + \mathcal{O}(q^2). \quad (1.12)$$

Since $f(x^*) = 0$, we then have,

$$\dot{q}(t) \approx q(t) \frac{\partial}{\partial q} f(x^*), \quad (1.13)$$

where we have neglected higher order terms $\mathcal{O}(q^2)$, a correct assumption if $\partial_q f(x^*) \neq 0$. Equation (1.13) is a linear equation in the variable $q(t)$ and is called the linearization of Eq. (1.11) around the fixed point x^* . It shows that the perturbation $q(t)$ grows exponentially if $\partial_q f(x^*) > 0$ and the solution is said to be *unstable*. The perturbation decays to zero if $\partial_q f(x^*) < 0$ and corresponds to an *stable* fixed point. If $\partial_q f(x^*) = 0$, quadratic terms $\mathcal{O}(q^2)$ cannot be neglected and a nonlinear stability analysis must be done.

In the absence of delay and fluctuations, Eq. (1.10) has a *supercritical pitchfork* bifurcation. The normal form of a pitchfork bifurcation is [80]

$$\dot{x}(t) = rx(t) - x^3(t), \quad (1.14)$$

where r is a control parameter. When $r < 0$, $x^* = 0$ is the only fixed point, and is stable. When $r > 0$, it is unstable. Two new fixed points appear in this range $x^* = \pm\sqrt{r}$, which are stable.

Introduction of a time delay term allows an oscillatory instability: a *super-*

critical Hopf bifurcation. This type of bifurcation occurs when a stable spiral changes to an unstable spiral surrounded by a small, nearly elliptical limit cycle. Since Hopf bifurcations involve oscillatory solutions, it appears only in systems that have dimensionality equal or bigger than 2. The normal form of a supercritical Hopf bifurcation is [80]

$$\dot{z}(t) = \lambda z(t) - bz(t)|z^2(t)|, \quad (1.15)$$

where $z(t)$ and $b = \alpha + i\beta$ are complex, and where $\lambda \in \mathbb{R}$ is a parameter. A supercritical Hopf bifurcation occurs for $\alpha < 0$ and $\lambda > 0$. On the other hand, a *subcritical* is possible if $\alpha > 0$ and $\lambda < 0$.

The bifurcation threshold of Eq. (1.10) and of its limits such as its linearization ($\gamma = 0$) or without delayed feedback ($b = 0$) are investigated both by computing moments of $x(t)$, or from the stationary probability distribution function $p(x)$. Stationary probability distribution functions are analytically determined from the associated Fokker-Planck equation [81]. While the Langevin equation describes the time evolution of the state variable, the Fokker-Planck equation describes the time evolution of the probability of being in a state x at time t . To every Langevin equation is an associated Fokker-Planck equation [23, 73, 22]. The derivation of the Fokker-Planck equation in both Ito and Stratonovich interpretations for Markovian equations are well known. We review the mathematical steps involved in this derivation in Appendix B in order to generalize both derivations to the case involving delayed feedback.

We are particularly interested in the following issues: It is known that the bifurcation threshold of Eq. (1.10) without delayed feedback ($b = 0$) is independent of the intensity of the noise D [82]. We would like to know if

delayed feedback and parametric noise couple and modify the nature and the location of the bifurcation. It is also known that the correlation time for the dynamical variable x without delayed feedback ($b = 0$) diverges at threshold with exponent -1 with respect to the control parameter [83]. We are interested to know if this result holds with delayed feedback.

This thesis is organized as follows. The bifurcation diagram of Eq. (1.10) is determined numerically by using a new second order numerical integration method that we have developed and that includes time delay. The algorithm is introduced in Chapter 2 while the mathematical steps involved in the derivation are shown in Appendix C. In order to verify the accuracy of our numerical method, several limits of Eq. (1.10) are investigated both analytically and numerically. The known limit of no feedback ($b = 0$) is briefly reviewed in Chapter 2. The bifurcation threshold of the moments of these equations is known analytically and is compared to our numerical results.

In the case of delayed feedback, the bifurcation threshold of the first moment of the stochastic equation is known [84, 55, 68, 85, 44] as shown in Chapter 3. We verify that additive noise ($D = 0$ and $K \neq 0$) does not affect the location of the bifurcation threshold whereas multiplicative noise ($D \neq 0$ and $K = 0$) shifts its location by an amount that scales with the intensity of the randomness. Furthermore, it is shown that the Fokker-Planck equation with delayed feedback is not closed. Time delay induces the presence of a non-Markovian term in the Fokker-Planck equation, precluding the analytical determination of stationary densities. The non-Markovian term can be expanded in Taylor series under the assumption that the time delay is small compared to other characteristic time scales in the system. We review two expansion schemes already existing in the literature [86, 87, 88]. It is

known that an expansion in the small time delay is valid only to first order in τ [89, 56, 57], leading to a Markovian first order differential equation. One dimensional differential equation cannot generate oscillation, and thus analytical results obtained in Chapter 3 are only valid in the vicinity of the pitchfork bifurcation. Expansion of delay terms in Taylor series around $\tau = 0$ leads to a singular perturbation. Although this expansion leads to the correct results to first order in τ , it completely fails to produce a Hopf branch.

We extend in Chapter 4 a method based on a multiple time scale expansion of the solution [90, 91, 92, 93, 94] to obtain equations for the stochastic time evolution of the envelope of the oscillation of both linear delayed equations with additive and parametric noise as well as for the van der Pol oscillator. The method is first applied to the van der Pol oscillator extended to allow delay terms in the model. The location of the Hopf bifurcation threshold in the limit of no time delay is known for this model, and is a way to verify the validity of our approximation scheme. In essence, we assume that the solution evolves over two time scales: The oscillations evolving over a fast time scale and their envelopes, evolving over a slow time scale. Fast time scales are eliminated by averaging over a period, leading to a stochastic differential equation for the time evolution of the envelopes. The location of the bifurcation threshold is found from the stationary probability distribution function. In addition, the method allows an expression of the Hopf frequency in the presence of fluctuations. Our theoretical predictions are in excellent agreement with numerical results obtained by integrating the governing equation of the model. The same expansion procedure is then applied to Eq. (1.10) and the Hopf bifurcation line determined. We show that unlike the case of no delay, the bifurcation line depends on the amplitude of the fluctuations, which generally destabilize the

trivial state $x^* = 0$.

A complete numerical analysis of Eq. (1.10) with multiplicative noise only ($K = 0$) is given in Chapter 5. We show excellent agreement between numerical and analytical results even for a range of parameter beyond the regime of small time delay.

Chapter 6 addresses the calculation of the correlation time of the state variable x . An analytical expression for the correlation time of Eq. (1.10) without delayed feedback ($b = 0$) and parametric noise only ($K = 0$) is known as the *Jung-Risken theory* [83]. The mathematical steps involved in the derivation of the correlation time in this theory are summarized in Appendix D. However, this theory requires the transition probabilities to be Markovian. We have used the approximate one dimensional expression for small time delay derived in Chapter 3 in order to compare our numerically determined correlation time with delayed feedback to the Jung-Risken theory extended to accommodate delay. We find that a divergent correlation time is recovered at the new pitchfork bifurcation line obtained when delay is included in the calculation. The correlation time is seen to diverge as σ^{-1} near threshold, where σ is a control parameter ($\sigma_c = 0$ is the location of the threshold). There are however numerical discrepancies with the numerical evaluation of the correlation time.

Chapter 2

Stochastic bifurcation

We review in this chapter earlier results on stochastic bifurcation theory which will form the basis of our analysis of stochastic equations with delay. These known results will also be used to verify a new second order algorithm that we have developed to numerically integrate stochastic delay differential equations. In particular, we discuss the different ways to define the stochastic bifurcation threshold, and the mathematical difficulties associated with linearization near threshold. The latter, of course, is standard procedure in conventional (or deterministic) bifurcation theory.

2.1 Algorithm for delay stochastic differential equation

Numerical integration of differential equations requires the discretization of time in small steps of Δt . The discretized equation becomes a *difference equation* that can be solved iteratively. Integration of stochastic differential equation is more challenging and an abundant literature has been developed on the subject (see for example [38]). However, no numerical methods have been developed to integrate stochastic *delay* differential equation to order greater

than 1 (example of first order methods can be found in [95, 86, 87, 88]). First order methods are computationally expensive because they require a small time step Δt to achieve convergence. In order to reduce the computational effort, we have extended a known second order numerical integration method for stochastic differential equations [96] and included time delay in the algorithm. The mathematical steps are summarized in Appendix C. In the case of delay terms involving a delay time τ , the algorithm needs to take into account trajectories into the past over an interval of 2τ . With additive noise only ($D = 0$ and $K \neq 0$), the algorithm used to integrate Eq. (1.10) is,

$$\begin{aligned}
x(t + \Delta t) = & x(t) \left(1 + a\Delta t + \frac{1}{2}a^2\Delta t^2 \right) + H_1(t, \Delta t) \\
& + aH_2(t, \Delta t) + bH_2(t - \tau, \Delta t) - 3\gamma x^2(t)H_2(t, \Delta t) \\
& + bx(t - \tau)(1 + a\Delta t)\Delta t - \gamma x^3(t)(1 + 2a\Delta t)\Delta t \\
& + \frac{1}{2}b^2x(t - 2\tau)\Delta t^2 + \frac{3}{2}\gamma^2x^5(t)\Delta t^2 \\
& - \frac{3}{2}\gamma bx(t - \tau)x^2(t)\Delta t^2 - \frac{1}{2}b\gamma x^3(t - \tau)\Delta t^2 ,
\end{aligned} \tag{2.1}$$

whereas for multiplicative noise only ($D \neq 0$ and $K = 0$), the algorithm is,

$$\begin{aligned}
x(t + \Delta t) = x(t) & \left[1 + a\Delta t + a^2 \frac{\Delta t^2}{2} + (1 + a\Delta t)G_1(t, \Delta t) \right. \\
& \left. + \frac{1}{2}(G_1(t, \Delta t))^2 \right] \\
& + bx(t - \tau) \left[\Delta t + a\Delta t^2 + \Delta t G_1(t, \Delta t) - G_2(t, \Delta t) \right. \\
& \left. + G_2(t - \tau, \Delta t) \right] \\
& - \gamma x^3(t) \left[2a\Delta t^2 + [G_1(t, \Delta t) + 1]\Delta t + 2G_2(t, \Delta t) \right] \\
& - \gamma x^2(t)x(t - \tau) \left(\frac{3b\Delta t^2}{2} \right) - \gamma x^3(t - \tau) \left(\frac{b\Delta t^2}{2} \right) \\
& + \gamma^2 x^5(t) \left(\frac{3\Delta t^2}{2} \right) + x(t - 2\tau) \left(b^2 \frac{\Delta t^2}{2} \right) .
\end{aligned} \tag{2.2}$$

where $G_1(t, \Delta t)$, $G_2(t, \Delta t)$, $H_1(t, \Delta t)$, and $H_2(t, \Delta t)$ are stochastic integrals defined by,

$$G_1(t, \Delta t) = \sqrt{2D\Delta t}\Psi_1(t) , \tag{2.3}$$

$$G_2(t, \Delta t) = \sqrt{\frac{2D}{3}\Delta t^3} \left[\frac{\sqrt{3}}{2}\Psi_1(t) + \frac{1}{2}\Psi_2(t) \right] , \tag{2.4}$$

$$H_1(t, \Delta t) = \sqrt{2K\Delta t}\Psi'_1(t) , \tag{2.5}$$

$$H_2(t, \Delta t) = \sqrt{\frac{2K}{3}\Delta t^3} \left[\frac{\sqrt{3}}{2}\Psi'_1(t) + \frac{1}{2}\Psi'_2(t) \right] , \tag{2.6}$$

where $\Psi_1(t)$, $\Psi_2(t)$, $\Psi'_1(t)$, and $\Psi'_2(t)$ are random numbers normally distributed with zero mean and variance one. These random numbers are generated by using the Box-Muller algorithm [97].

The accuracy of the algorithm is defined in terms of its approximation to the exact solution as a power of Δt . An algorithm is thus said to be of the

n^{th} order if the error is of the order $\mathcal{O}(\Delta t^n)$. In our case, we have expanded $x(t + \Delta t)$ to second order in Δt so that the error at each step is $\mathcal{O}(\Delta t^3)$. The cumulative error is proportional to the total number of steps, which is itself proportional to the inverse step size. Thus, the total error of our method is of the order $\mathcal{O}(\Delta t^2)$, and is called a second order algorithm.

2.2 Stochastic bifurcation

Consider the deterministic differential equation,

$$\dot{x}(t) = ax(t) , \quad (2.7)$$

where a is a constant called the control parameter. The solution of Eq. (2.7) is

$$x(t) = x(0)e^{at} , \quad (2.8)$$

where $x(0)$ is the initial condition. The solution grows to infinity if $a > 0$ and decays to zero if $a < 0$. The bifurcation point is thus located at $a_c = 0$. Consider the stochastic counterpart of Eq. (2.7) by adding a noise term,

$$\dot{x}(t) = ax(t) + \eta(t) , \quad (2.9)$$

where $\eta(t)$ is a Gaussian white noise with mean $\langle \eta(t) \rangle = 0$ and correlation $\langle \eta(t)\eta(t') \rangle = 2K\delta(t - t')$, where K is the intensity of the noise. The bifurcation threshold of Eq. (2.9) can be investigated either from the stationary probability distribution function or from the time evolution of the moments. The stationary density can be obtained analytically from the Fokker-Planck equation associated to Eq. (2.9). In fact, there is a Fokker-Planck equation associated to every Langevin equation [23, 73, 22]. The mathematical steps

involved in the derivation of the Fokker-Planck equation given a Langevin equation are shown in Appendix B. Using those results, the Fokker-Planck equation associated to Eq. (2.9) is obtained from Eq. (B.32) with $f(x) = ax$ and is

$$\frac{\partial}{\partial t} p(x, t) = -\frac{\partial}{\partial x} [axp(x, t)] + K \frac{\partial^2}{\partial x^2} p(x, t) . \quad (2.10)$$

The stationary probability distribution function $p_s(x)$ of Eq. (2.10) is found by using Eq. (B.9) with $g(x) = 1$ and leads to,

$$p_s(x) = \mathcal{N} \exp\left(\frac{a}{2K}x^2\right) , \quad (2.11)$$

where \mathcal{N} is a normalization constant. The solution is not normalizable if $a > 0$. The bifurcation threshold is hence not well defined as the stationary distribution function does not exist as $a > 0$.

The bifurcation threshold may be defined from the statistical moments of $x(t)$. Analytical expression for the time evolution of the moments of Eq. (2.9) is found from the Fokker-Planck equation [Eq. (2.10)]. By definition of the ensemble average [98],

$$\frac{\partial}{\partial t} \langle x^n(t) \rangle = \frac{\partial}{\partial t} \int_{-\infty}^{\infty} x^n p(x, t) dx = \int_{-\infty}^{\infty} x^n \frac{\partial}{\partial t} p(x, t) dx . \quad (2.12)$$

Substitute Eq. (2.10) in Eq. (2.12) and integrate by parts. Assuming further that the probability distribution function vanishes at $x = \pm\infty$ yields,

$$\frac{\partial}{\partial t} \langle x^n(t) \rangle = na \langle x^n(t) \rangle + Kn(n-1) \langle x^{n-2}(t) \rangle . \quad (2.13)$$

The solution of Eq. (2.13) is obtained in integral form,

$$\langle x^n(t) \rangle = e^{nat} \left[\langle x^n(0) \rangle + Kn(n-1) \int_0^t ds \langle x^{n-2}(s) \rangle e^{-nas} \right]. \quad (2.14)$$

The first moment ($n = 1$) evolves in time according to,

$$\langle x(t) \rangle = \langle x(0) \rangle e^{at}, \quad (2.15)$$

whereas the second moment ($n = 2$) satisfies

$$\langle x^2(t) \rangle = e^{2at} \left[\langle x^2(0) \rangle + \frac{K}{a} (1 - e^{-2at}) \right]. \quad (2.16)$$

For small time t , $\exp(-2at) \approx 1$, and Eq. (2.16) reduces to

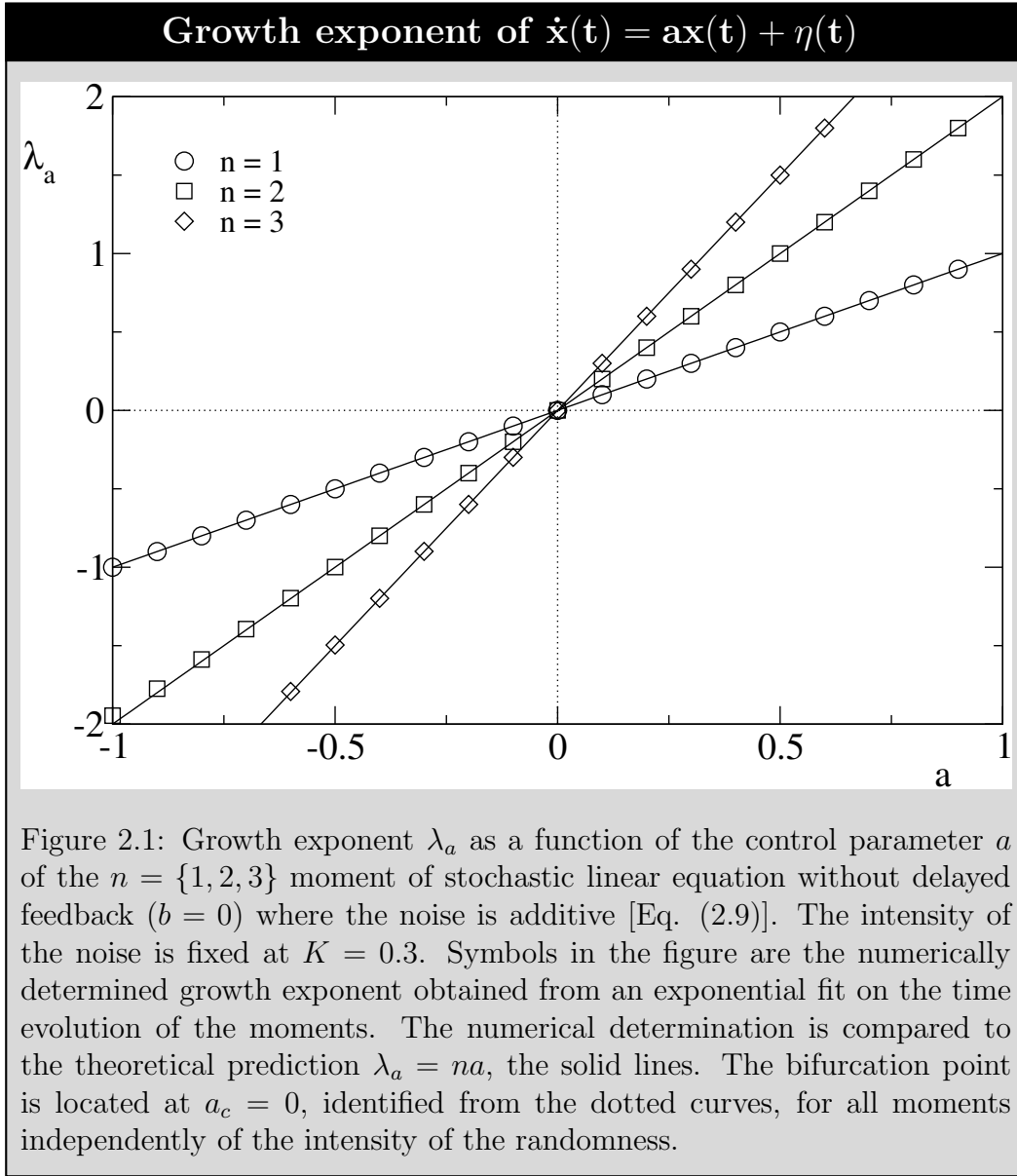
$$\langle x^2(t) \rangle = \langle x^2(0) \rangle e^{2at}. \quad (2.17)$$

The solution of the higher moments in the limit of small t can be found from Eqs. (2.14), (2.15), and (2.17). In the small t limit where $\exp(-nat) \approx 1$, the n^{th} moment satisfies

$$\langle x^n(t) \rangle = \langle x^n(0) \rangle e^{nat}. \quad (2.18)$$

Let $\lambda_a = na$ be the growth exponent of the moments. Hence, the bifurcation point is located at $\lambda_a = 0$ or $a_c = 0$, point separating exponentially growing from decaying solutions. The location of the bifurcation point thus agrees with the deterministic model and is independent of the intensity of the randomness.

We have verified our numerical algorithm with additive noise [Eq. (2.1)] by integrating Eq. (2.9) over 10^8 independent realizations of the noise. Trajectories are obtained by setting $b = 0$, $\gamma = 0$, and $K = 0.3$ in Eq. (2.1) and by



using a integration step of $\Delta t = 0.01$. The growth exponent λ_a is computed from an exponential fit performed on the time evolution of the moments in the time window $t = [0, 5]$. Results are shown in Fig. 2.1 and compared to the analytical prediction $\lambda_a = na$. The agreement between the two is excellent.

The phenomenology changes considerably if parametric noise is considered instead,

$$\dot{x}(t) = ax(t) + x(t)\xi(t) . \quad (2.19)$$

Equation (2.19) is to be interpreted under Stratonovich calculus. Parametric or multiplicative noise of the form of Eq. (2.19) is encountered in stochastic differential equations in which fluctuations in control parameters are considered, i.e. if $a \rightarrow a + \xi(t)$. The bifurcation threshold of Eq. (2.19) is also studied from its associated stationary probability distribution function and from the statistical moments. The Fokker-Planck associated with Eq. (2.19) is obtained by using Eq. (B.29) with $f(x) = ax$ and $g(x) = x$,

$$\frac{\partial}{\partial t} p(x, t) = -\frac{\partial}{\partial x} [(a + D)xp(x, t)] + D\frac{\partial^2}{\partial x^2} [x^2 p(x, t)] . \quad (2.20)$$

The stationary probability distribution function of Eq. (2.20) is found from Eq. (B.9) with $g(x) = x$ and yields,

$$p_s(x) = \begin{cases} \delta(x) \\ \mathcal{N}|x|^{\frac{a}{D}-1} \end{cases} , \quad (2.21)$$

where \mathcal{N} is a normalization constant found by conserving probabilities over all space,

$$1 = \int_{-\infty}^{\infty} p_s(x) dx = 2\mathcal{N} \int_0^{\infty} x^{\frac{a}{D}-1} dx = \frac{2D\mathcal{N}}{a} x^{\frac{a}{D}} \Big|_0^{\infty} . \quad (2.22)$$

On the one hand, the power law solution is not normalizable and hence it is not an admissible solution. On the other hand, trajectories are observed numerically to diverge above a certain threshold and the delta function is not stable in this region. The bifurcation threshold is hence not well defined since the solution does not exist everywhere.

Alternatively, one may wish to define the bifurcation from the stability of

the moments of Eq. (2.19). Substitute Eq. (2.20) into Eq. (2.12) and integrate by parts, by assuming that the probability distribution function vanishes at $x = \pm\infty$,

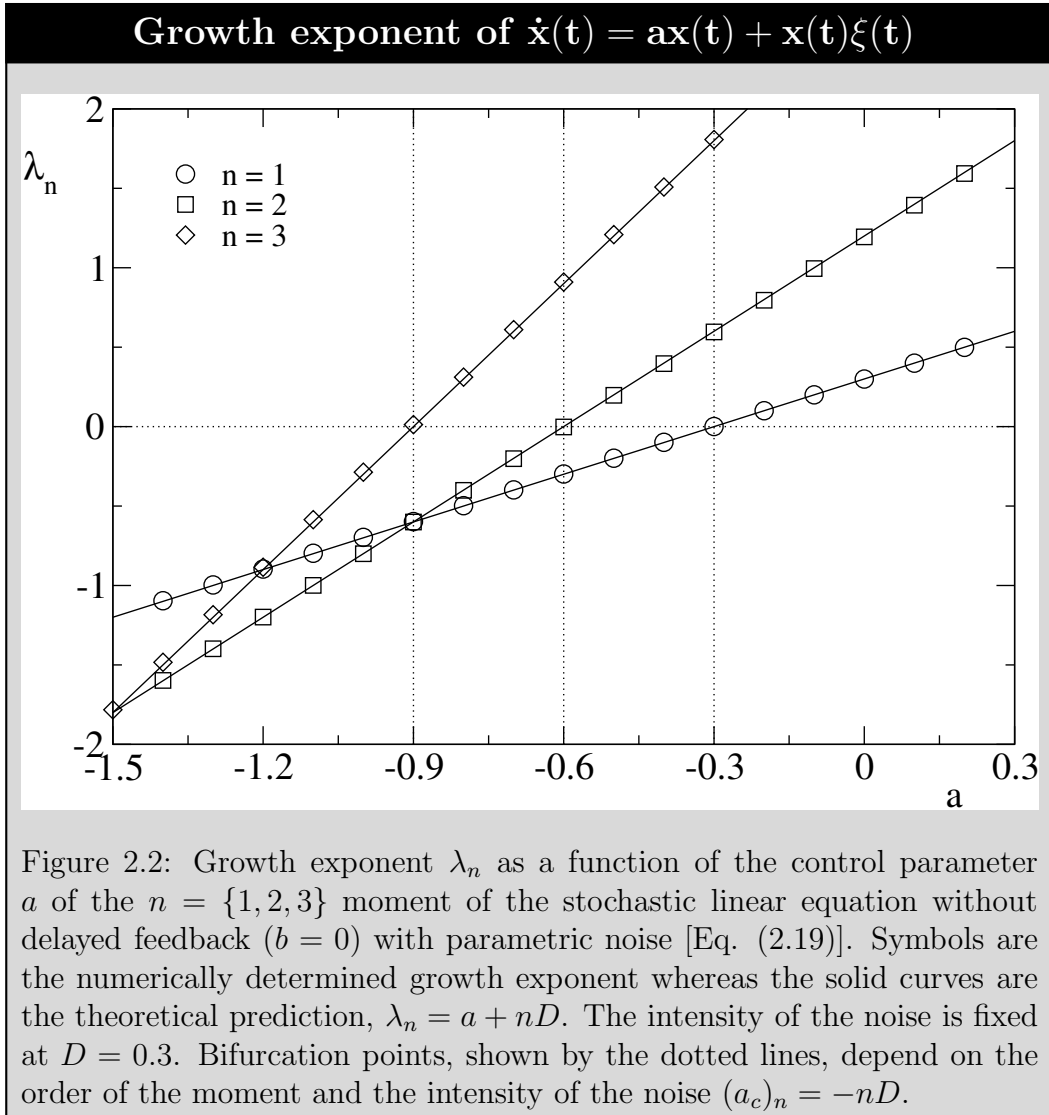
$$\frac{\partial}{\partial t} \langle x^n(t) \rangle = na \langle x^n(t) \rangle + Dn^2 \langle x^n(t) \rangle. \quad (2.23)$$

Assume a solution of the form $\langle x^n(t) \rangle = \mathcal{C} \exp(n\lambda_n t)$, where \mathcal{C} is a constant and λ_n the growth exponent. After substitution in Eq. (2.23), it leads to the characteristic equation,

$$\lambda_n = a + nD. \quad (2.24)$$

The bifurcation occurs at $\lambda_n = 0$, or $(a_c)_n = -nD$. Despite the lack of existence of a stationary distribution function above threshold, one seems to find a bifurcation that depends on the order of the moment n .

This apparent bifurcation point is well reproduced numerically. Equation (2.19) is integrated by using Eq. (2.2) with $b = 0$, $\gamma = 0$, and $D = 0.3$ in order to verify these results. Trajectories are generated in the time interval $t = [0, 20]$ by using an integration step of $\Delta t = 0.01$. Over 10^8 independent realizations of the noise are averaged to determine the time evolution of the moments. The growth exponent λ_n is computed from an exponential fit on the time evolution of each moment. Numerical results are shown in Fig. 2.2 and compared to Eq. (2.24). The two are in excellent agreement with each other. The bifurcation point thus appears to depend on the order n of the moment considered with parametric noise, which differs from the deterministic result $a_c = 0$. This is a peculiar property of power law distributions. It is known that this behavior can be traced to a significant probability of encountering extremely diverging trajectories. Those trajectories dominate the ensemble average becoming more and more significant for higher moment of x . This pathology can be resolved



by introducing a saturating nonlinearity on the model.

2.3 Normal form of a pitchfork bifurcation

Consider the deterministic ($K = D = 0$) but nonlinear ($\gamma = 1$) counterpart of Eq. (1.10) without delayed feedback ($b = 0$),

$$\dot{x}(t) = ax(t) - x^3(t). \quad (2.25)$$

Equation (2.25) is known as the Landau model [99, 100, 101]. This equation has one stable fixed point $x^* = 0$ if $a < 0$ and three fixed points as $a > 0$, $x^* = 0$, which is unstable, and two stable fixed points located at $x^* = \pm\sqrt{a}$. The bifurcation point is thus located at $a_c = 0$.

In order to investigate further the validity of our numerical integration method, we have computed the location of the bifurcation threshold of the stochastic counterpart of Eq. (2.25) with additive and multiplicative noise. Consider then Eq. (2.25) with additive noise,

$$\dot{x}(t) = ax(t) - x^3(t) + \eta(t) . \quad (2.26)$$

Take the ensemble average of Eq. (2.26) on both sides,

$$\partial_t \langle x(t) \rangle = a \langle x(t) \rangle - \langle x^3(t) \rangle , \quad (2.27)$$

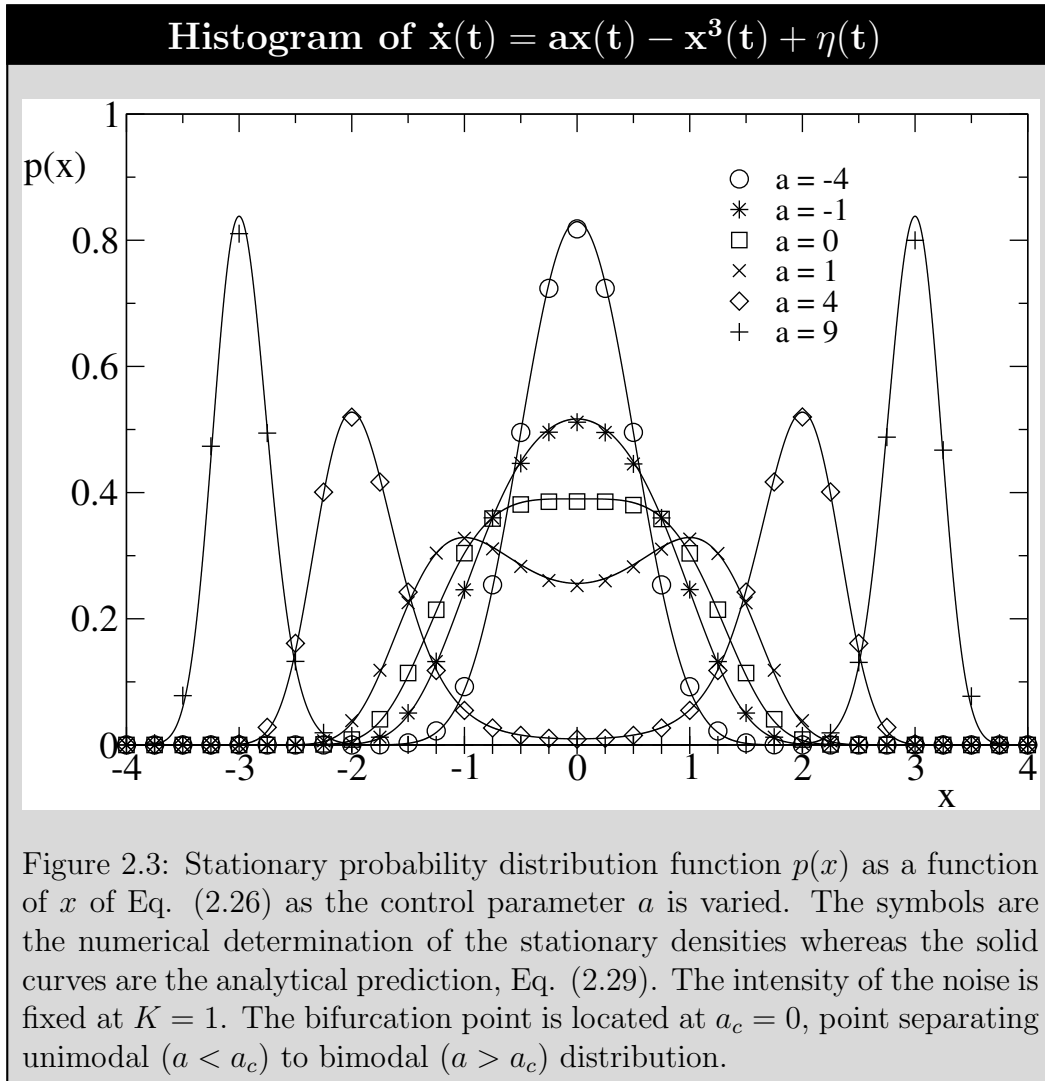
where we have used $\langle \eta(t) \rangle = 0$. The moments of Eq. (2.27) are not of the same order excluding an analytical determination of the solution of this equation. Nevertheless, the bifurcation threshold is found from its associated stationary probability distribution function.

Consider then the Fokker-Planck equation associated with Eq. (2.26). Given Eq. (B.32) with $f(x) = ax - x^3$, we have

$$\frac{\partial}{\partial t} p(x, t) = -\frac{\partial}{\partial x} [(ax - x^3) p(x, t)] + K \frac{\partial^2}{\partial x^2} p(x, t) . \quad (2.28)$$

The stationary solution of Eq. (2.28) is found by using Eq. (B.9) with $g(x) = 1$ and is

$$p_s(x) = \mathcal{N} \exp \left(a \frac{x^2}{2K} - \frac{x^4}{4K} \right) , \quad (2.29)$$



where \mathcal{N} is a normalization constant. This probability distribution function is shown in Fig. 2.3. The position of the maxima of the distribution are located at $x^* = \pm\sqrt{a}$ if $a > 0$ and at $x^* = 0$ if $a < 0$. Clearly the bifurcation occurs at $a_c = 0$, the point separating unimodal from bimodal densities. The bifurcation threshold thus agrees with the deterministic model.

We next turn our attention to the case where Eq. (2.25) includes parametric noise,

$$\dot{x}(t) = ax(t) - x^3(t) + x(t)\xi(t). \quad (2.30)$$

This equation has been studied in [82, 102, 98] and is commonly called the

Stratonovich model. Consider the first moment of Eq. (2.30) found by taking the ensemble average,

$$\partial_t \langle x(t) \rangle = a \langle x(t) \rangle - \langle x^3(t) \rangle + \langle x(t) \xi(t) \rangle . \quad (2.31)$$

The correlation of the state variable $x(t)$ and the noise $\xi(t)$ can be found by using the Furutsu-Novikov theorem [103, 104],

$$\langle x(t) \xi(t) \rangle = \langle x(t) \rangle \langle \xi(t) \rangle + \int_0^t \langle \xi(t) \xi(t') \rangle \left\langle \frac{\delta x(t)}{\delta \xi(t')} \right\rangle dt' , \quad (2.32)$$

where $\delta x(t)/\delta \xi(t')$ is the functional derivative of $x(t)$ with respect to $\xi(t')$. By using $\langle \xi(t) \rangle = 0$ and $\langle \xi(t) \xi(t') \rangle = 2D\delta(t - t')$ and performing the integration, Eq. (2.32) reduces to

$$\langle x(t) \xi(t) \rangle = D \left\langle \frac{\delta x(t)}{\delta \xi(t)} \right\rangle . \quad (2.33)$$

By using Eq. (B.25), we find

$$\langle x(t) \xi(t) \rangle = D \langle x(t) \rangle , \quad (2.34)$$

and Eq. (2.31) thus reduces to

$$\partial_t \langle x(t) \rangle = (a + D) \langle x(t) \rangle - \langle x^3(t) \rangle . \quad (2.35)$$

This equation is not closed and cannot be solved analytically. We note however that the effect of the correlation $\langle x(t) \xi(t) \rangle$ is to renormalize the control parameter a . Interestingly, this renormalization does not lead to a change in the location of the bifurcation point with respect to the deterministic equation, as we show next.

The bifurcation of the Stratonovich model is investigated from its stationary probability density. Given Eq. (B.29) with $f(x) = ax - x^3$ and $g(x) = x$, the Fokker-Planck equation associated with Eq. (2.30) is

$$\frac{\partial}{\partial t} p(x, t) = -\frac{\partial}{\partial x} \{[(a + D)x - x^3] p(x, t)\} + D \frac{\partial^2}{\partial x^2} [x^2 p(x, t)] . \quad (2.36)$$

The stationary probability distribution function of Eq. (2.36) is obtained by using Eq. (B.9) with $g(x) = x$ and is

$$p_0(x) = \begin{cases} \delta(x) & \text{if } \alpha \leq -1 \\ \mathcal{N} |x|^\alpha e^{-\frac{x^2}{2D}} & \text{if } \alpha > -1 \end{cases} , \quad (2.37)$$

where \mathcal{N} is a normalization constant and where $\alpha = a/D - 1$ is the exponent of the power law. The distribution is normalizable as long as $\alpha > -1$. In this limit, the normalization constant \mathcal{N} is found by imposing conservation of probability over all space,

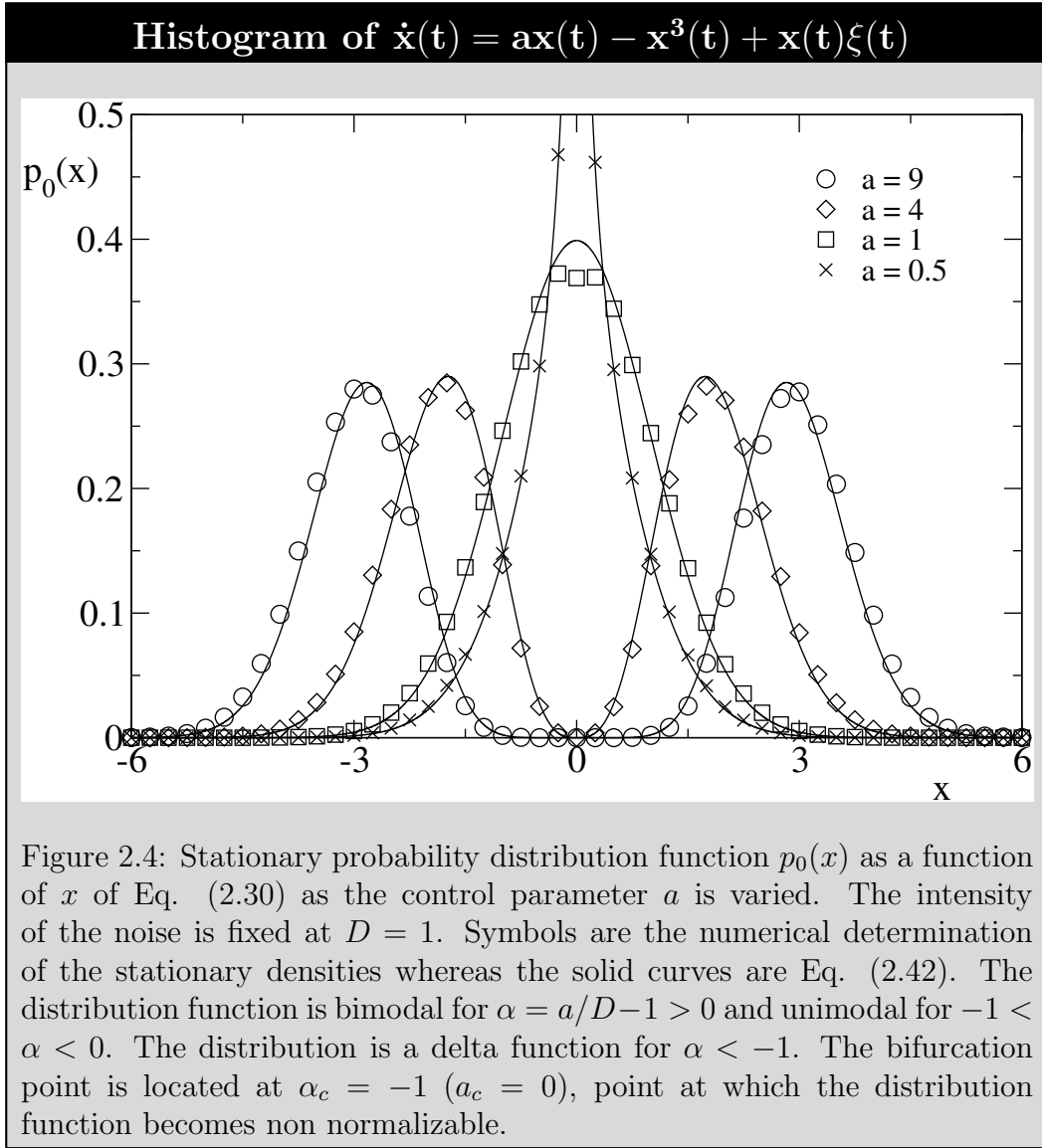
$$1 = \int_{-\infty}^{\infty} p_0(x) dx = 2\mathcal{N} \int_0^{\infty} |x|^\alpha e^{-\frac{x^2}{2D}} dx , \quad (2.38)$$

where we have used the fact that the stationary probability distribution function $p_0(x)$ is symmetric in x . Perform the change of variable $t = (2D)^{-1}x^2$. In those terms Eq. (2.38) is,

$$1 = 2(2D)\mathcal{N} \int_0^{\infty} (2Dt)^{\frac{\alpha-1}{2}} e^{-t} dt = 2\mathcal{N}(2D)^{\frac{\alpha+1}{2}} \Gamma\left(\frac{\alpha+1}{2}\right) , \quad (2.39)$$

where we have introduced the gamma function $\Gamma(z)$ defined by,

$$\Gamma(z) = \int_0^{\infty} t^{z-1} e^{-t} dt . \quad (2.40)$$



The normalization constant \mathcal{N} is thus

$$\mathcal{N} = \frac{1}{2}(2D)^{-\left(\frac{\alpha+1}{2}\right)}\Gamma^{-1}\left(\frac{\alpha+1}{2}\right), \quad (2.41)$$

and the stationary probability distribution function for $\alpha > -1$ is

$$p_0(x) = \frac{1}{2}(2D)^{-\left(\frac{\alpha+1}{2}\right)}\Gamma^{-1}\left(\frac{\alpha+1}{2}\right)|x|^\alpha e^{-\frac{x^2}{2D}}. \quad (2.42)$$

The stationary probability distribution function is not normalizable if $\alpha <$

–1. Hence, the bifurcation occurs at the point where $\alpha_c = -1$, or $a_c = 0$, independently of the intensity of the randomness. The bifurcation point is characterized as the point at which the stationary distribution function $p_0(x)$ changes from a delta function $\delta(x)$ to a power law with an exponential cut off at large x . Note that this is in contrast with the *linearized* counterpart of Eq. (2.30) where the bifurcation occurs at $(a_c)_n = -nD$, where n is the order of the moment considered. Note that the solution [Eq. (2.42)] is unimodal with a singularity at $x = 0$ for $\alpha \in [-1, 0]$, whereas it is bimodal for $\alpha > 0$.

The stationary distribution function of Eq. (2.30) has been computed numerically by setting $b = 0$, $\gamma = 1$, and $D = 1$ in Eq. (2.2). Histograms are calculated in the time interval $t = [480, 500]$ with $\Delta t = 0.01$, where the solution is believed to be stationary. Over 10^5 independent realization of the noise are considered in the ensemble average. Results are shown in Fig. 2.4. Note the excellent agreement between numerical results and the theoretical prediction.

The saturating nonlinearity in the model allows for a bound stationary probability distribution above threshold, and therefore a determination of the bifurcation. Interestingly, the bifurcation remains at $a_c = 0$, the same value as in the case without fluctuations. It is now believed that the divergence of the moment at $(a_c)_n = -nD$ is spurious, and related to large deviations allowed by the linear model. In short, one concludes from this analysis that a stochastic bifurcation requires the analysis of a nonlinear model, in contrast with conventional theory.

Chapter 3

Stochastic bifurcation of delayed equations

We address in this chapter the bifurcation diagram of a stochastic differential equation with delayed feedback. Recall (cf. Chapter 2) that the linear counterpart of Eq. (1.10) without delayed feedback does not have a stationary probability distribution function, and hence does not have a well defined bifurcation threshold. The solution of the linear counterpart of Eq. (1.10) with delayed feedback diverges also above threshold, and hence we will repeat the procedure of adding a nonlinear saturating term to the governing equation.

We study the bifurcation threshold through both the time evolution of the moments and from the stationary probability density. The analog of a Fokker-Planck equation is derived, except that time delay introduces a non-Markovian drift term in the equation, and hence it is not closed. We explore several approximate schemes to obtain the drift term when the delay time τ is small as compared to the other characteristic time scales in the system. We present two methods existing in the literature to expand this term based on the Ito interpretation and introduce a new procedure following the Stratonovich in-

terpretation of stochastic calculus. Unfortunately, expansions of the drift term results in an effective Markovian model which fails to capture any oscillatory behavior, the hallmark of a feedback loop as discussed next.

3.1 Delayed feedback induces oscillation

The bifurcation diagrams of both the deterministic and stochastic linear ($\gamma = 0$) counterpart of Eq. (1.10) with delayed feedback ($b \neq 0$) are known. We briefly review these results. Consider first the deterministic equation ($K = D = 0$). It corresponds to the equation introduced by Bratsun as a model of protein degradation [74],

$$\dot{x}(t) = ax(t) + bx(t - \tau) , \quad (3.1)$$

where a, b are constants, and where $\tau > 0$ is the delay time. The analytical solution to Eq. (3.1) is known [44, 105]. Assume a solution of the form $x(t) = \mathcal{C} \exp(\lambda t)$, where λ is a growth exponent and \mathcal{C} is a constant, and substitute into Eq. (3.1). This yields a characteristic equation,

$$\lambda = a + be^{-\lambda\tau} . \quad (3.2)$$

Split the growth exponent into a real and imaginary part $\lambda = \mu + i\omega$,

$$\mu = a + be^{-\mu\tau} \cos(\omega\tau) , \quad (3.3)$$

$$\omega = -be^{-\mu\tau} \sin(\omega\tau) . \quad (3.4)$$

A direct bifurcation occurs as $\mu = \omega = 0$, or

$$a_c = -b . \quad (3.5)$$

This branch separates exponentially decaying solutions ($a_c < -b$) from exponentially diverging solutions ($a_c > -b$). There is another bifurcation that is a direct consequence of the delay: a Hopf bifurcation at $\mu = 0$ but $\omega \neq 0$,

$$-\frac{a_c}{b} = \cos\left(\tau\sqrt{b^2 - a_c^2}\right). \quad (3.6)$$

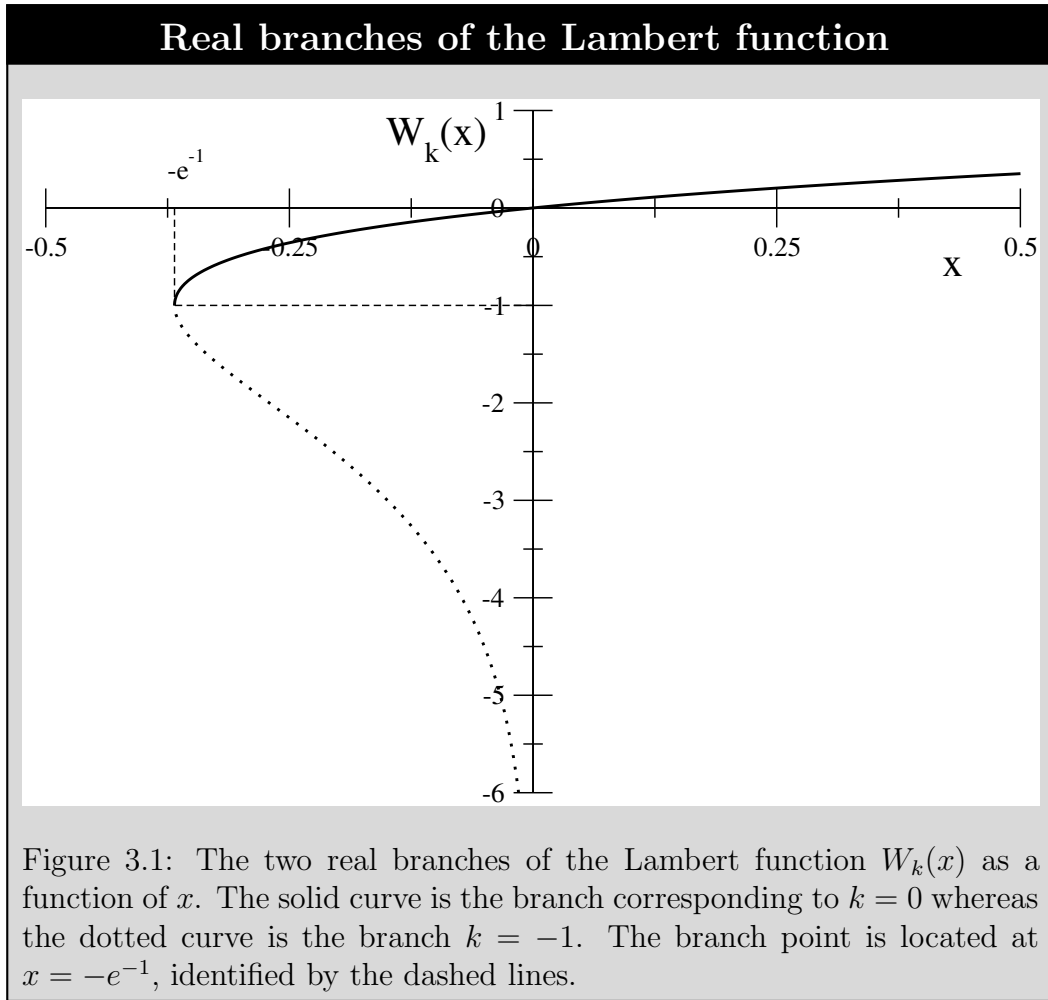
Oscillations ($\omega \neq 0$) are a direct consequence of the presence of time delay in Eq. (3.1). It is well known that oscillatory behavior requires at least a two dimensional system [80]. However, delay terms are considered as independent variables, and thus Eq. (3.1) has an infinite number of dimensions. It is instructive to express the eigenvalue equation [Eq. (3.2)] in terms of the Lambert function. The Lambert function, also known as the product-log function, is a well studied function in the field of delay differential equations [106, 50, 107]. By definition, the Lambert function $y = W_k(x)$ is the set of the k branches of the inverse of $x = y \exp(y)$. The characteristic equation [Eq. (3.2)] can be written as,

$$(\lambda - a)\tau e^{(\lambda - a)\tau} = b\tau e^{-a\tau}. \quad (3.7)$$

We can thus use the definition of the Lambert function to write the growth exponent λ_k as

$$\lambda_k = \frac{1}{\tau} W_k(b\tau e^{-a\tau}) + a. \quad (3.8)$$

Each branch $W_k(b\tau e^{-a\tau})$ corresponds to a different eigenvalue λ_k . Since there are an infinite number of branches, Eq. (3.1) has an infinite number of independent solutions. Again, this property might seem peculiar as one would expect a single independent solution to a first order differential equation. Since the initial condition is a function being defined in $[-\tau, 0]$, it implies an infinite numbers of variables to describe the dynamics of the system. The Lam-

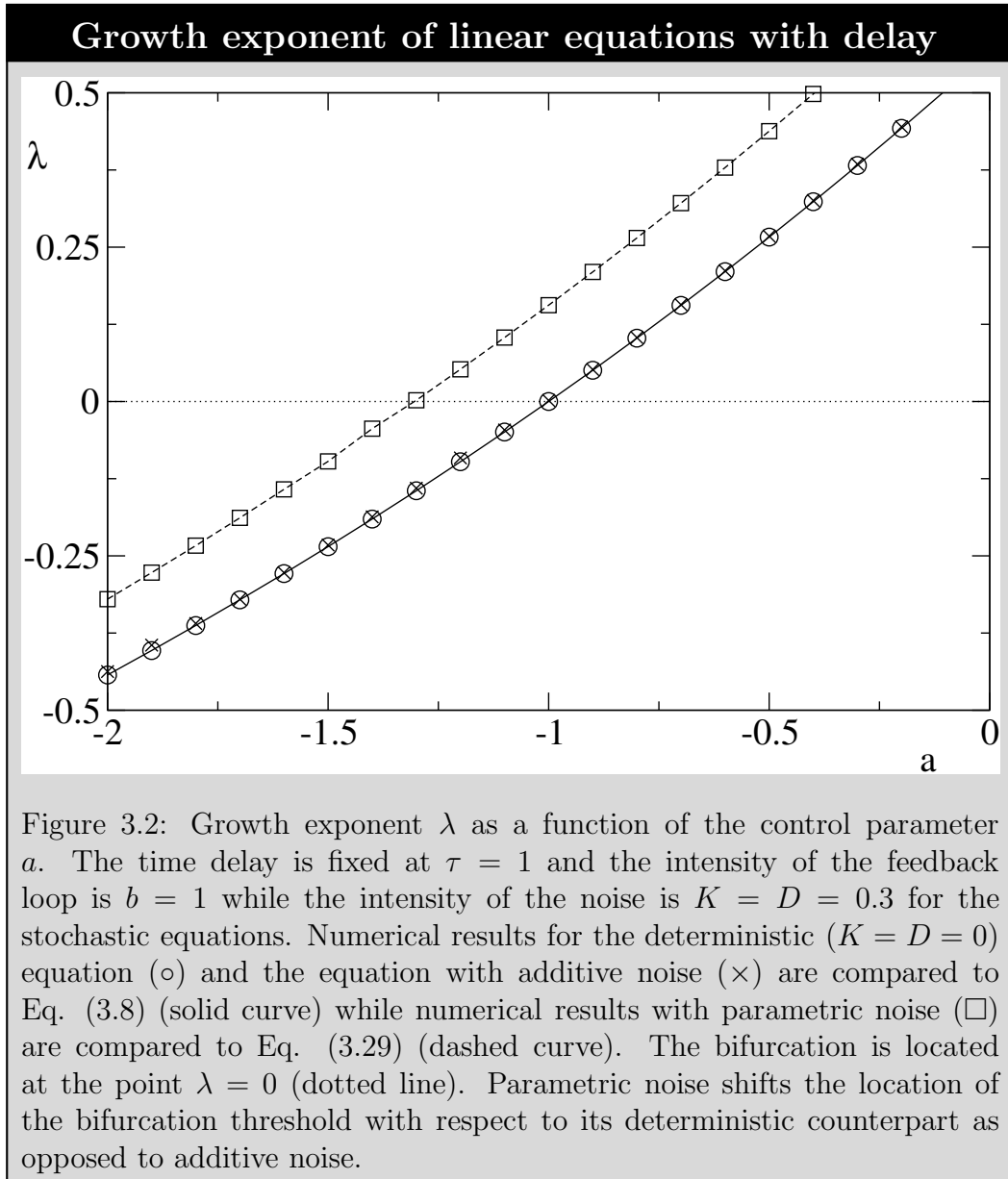


bert function has only two real valued branches in the domain $[-e^{-1}, \infty]$ and $[-e^{-1}, 0]$. The principal branch $W_0(x)$, shown in Fig. 3.1, is the only branch that contains any part of the positive real axis in its range. It has a second order branch point located at $x = -e^{-1}$, corresponding to $y = -1$. This point is also shared with the branch $k = 1$ and $k = -1$. All the other branches map the real line into the complex plane, providing complex values for λ , and thus oscillatory solutions for $x(t)$. This property contrasts with first order differential equations which can not provide oscillatory solutions [80]. In terms of the parameters of the model, the multicritical point is at $(a, b) = (1/\tau, -1/\tau)$. Furthermore, the eigenvalue is complex and hence the solution is oscillatory if

$b\tau \exp(-a\tau) < -\exp(-1)$. Note that in the special case of short delay $\tau \rightarrow 0$, the multicritical point moves to $(a, b) = (\infty, -\infty)$ and the Hopf branch [Eq. (3.6)] disappears.

The bifurcation diagram of Eq. (3.1) is also investigated numerically to verify the validity of our numerical method with delayed feedback, as well as the procedure to locate the bifurcation line. Equation (3.1) is integrated by using Eq. (2.1) with $\gamma = 0$ and $K = 0$. The initial condition over the time interval $[-\tau, 0]$ is a constant being drawn from a Gaussian distribution with mean 0 and variance 1. The bifurcation threshold is determined by averaging 10^6 trajectories with different initial conditions at fixed parameters a , b , and τ . The integration step is fixed at $\Delta t = 0.01$. The numerically determined growth exponent λ is computed from an exponential fit in the time window $t = [290, 300]$ to the averaged trajectories. The process is repeated for several values of a at fixed b and time delays τ . The bifurcation point is then identified as the point in the (a, b) plane for which the growth exponent is zero. The growth exponent is shown in Fig. 3.2 and compared to Eq. (3.8). The analysis is repeated for many intensities of the feedback loop b . The resulting bifurcation diagram is shown in Fig. 3.3 and compared to the theoretical predictions Eqs. (3.5) and (3.6). Both are in excellent agreement with each other. We showed in Chapter 2 that the bifurcation threshold of the stationary moments of the linear equation ($\gamma = 0$) without delayed feedback ($b = 0$) and parametric noise depend on the order of the moment considered while it is unchanged with additive noise. We verify if this is the case with delayed feedback.

Consider then the case of a differential delay equation with additive noise

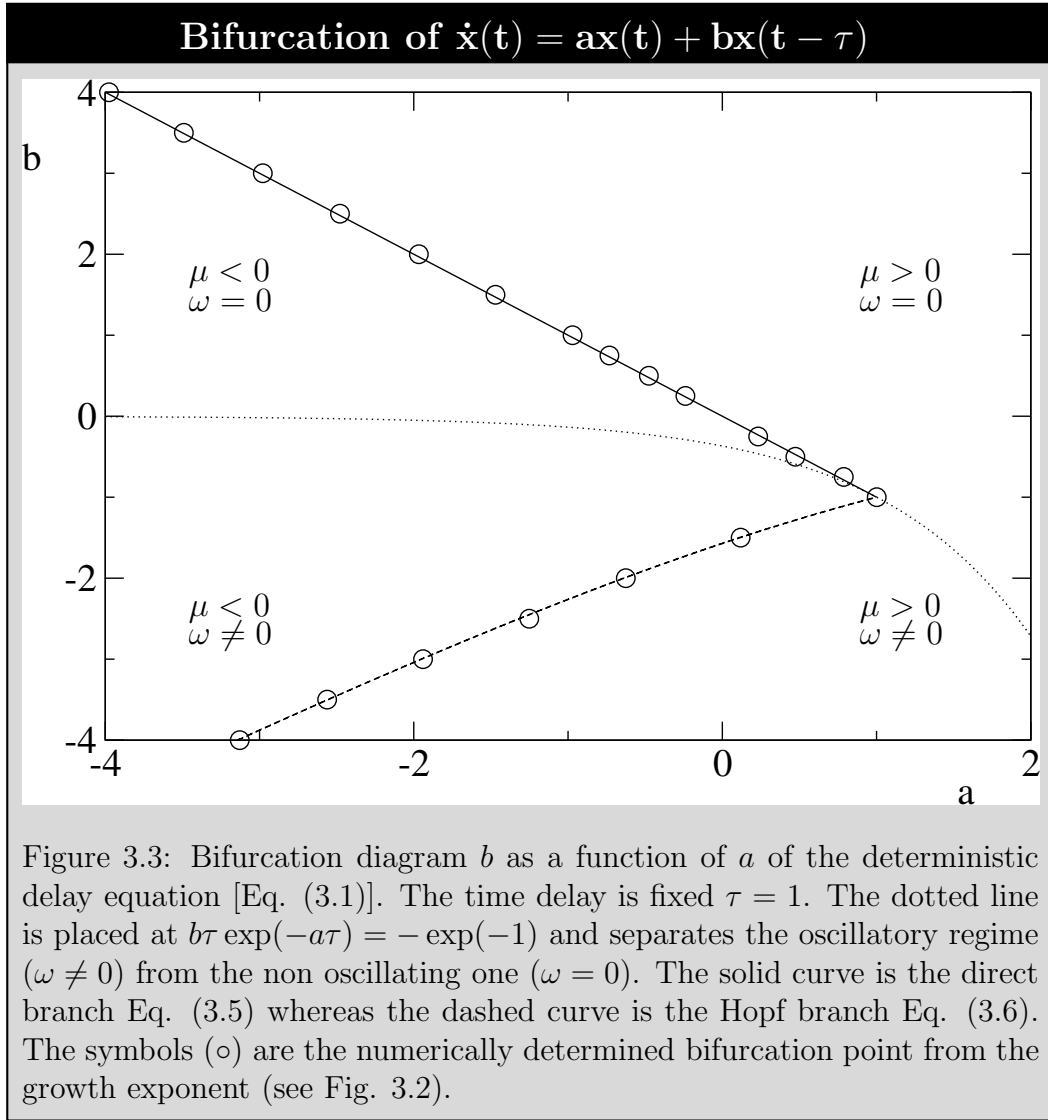


$$\dot{x}(t) = ax(t) + bx(t - \tau) + \eta(t) . \quad (3.9)$$

The location of the bifurcation threshold of the first moment of this equation is known [44]. Take the ensemble average on both sides,

$$\partial_t \langle x(t) \rangle = a \langle x(t) \rangle + b \langle x(t - \tau) \rangle , \quad (3.10)$$

where we have used $\langle \eta(t) \rangle = 0$. Assuming a solution of the form $\langle x(t) \rangle =$



$\mathcal{C} \exp(\lambda t)$, where λ is the growth exponent and \mathcal{C} is a constant, we obtain the same characteristic equation [Eq. (3.8)] and hence the same location of the bifurcation threshold than the deterministic and linear delayed equation [Eqs. (3.5) and (3.6)].

Associated with Eq. (3.9) is the equivalent of a Fokker-Planck equation from which the time evolution of the moments can be obtained. Derivation of the Fokker-Planck equation follows the lines of Appendix B. However, the derivation must be generalized to include delay. In fact, the drift coefficient is

now a function of a time delay term $f[x(t); x(t - \tau)]$. Moreover, the functional derivative of the solution $x(t)$ with respect to the noise might be modified by the time delay. In order to generalize the derivation of the Fokker-Planck equation, consider a general Langevin equation with a delayed drift coefficient,

$$\dot{x}(t) = f[x(t), x(t - \tau)] + g[x(t)]\xi(t), \quad (3.11)$$

where $\xi(t)$ is a Gaussian white noise with mean $\langle \xi(t) \rangle = 0$ and correlation $\langle \xi(t)\xi(t') \rangle = 2D\delta(t - t')$, where D is the intensity of the randomness. Consider then the definition of the one point probability distribution function $p(x, t) = \langle \delta[x(t) - x] \rangle$ as in Eq. (B.12). Take the time derivative on both sides, and substitute Eq. (3.11),

$$\begin{aligned} \frac{\partial}{\partial t} p(x, t) = & - \frac{\partial}{\partial x} \left\{ \langle \delta[x - x(t)] f(x, x_\tau) \rangle \right\} \\ & - \frac{\partial}{\partial x} \left\{ g(x) \langle \delta[x - x(t)] \xi(t) \rangle \right\}, \end{aligned} \quad (3.12)$$

where we have used the identity given in Eq. (B.15). Consider first the drift coefficient in Eq. (3.12),

$$\langle f(x, x_\tau) \delta[x - x(t)] \rangle = \iint f(x, x_\tau) \delta[x - x(t)] p(x; x_\tau) dx dx_\tau, \quad (3.13)$$

where $p(x; x_\tau) dx dx_\tau$ is the joint probability distribution function that $x \in [x, x + dx]$ at time t and $x_\tau \in [x_\tau, x_\tau + dx_\tau]$ at time $t - \tau$. Use the property, $p(x; x_\tau) = p(x_\tau|x)p(x)$, and substitute $f(x, x_\tau) = ax + bx_\tau$ in Eq. (3.13),

$$\begin{aligned} \langle (ax + bx_\tau) \delta[x - x(t)] \rangle &= \iint (ax + bx_\tau) \delta[x - x(t)] p(x_\tau|x) p(x) dx dx_\tau \\ &= p(x, t) \left[ax(t) + b \int x_\tau p(x_\tau|x) dx_\tau \right]. \end{aligned} \quad (3.14)$$

Equation (3.14) contains a non-Markovian term,

$$\langle x_\tau | x \rangle = \int x_\tau p(x_\tau | x) dx_\tau . \quad (3.15)$$

This integral is called the average conditional drift [87, 88]. There is no analytical solution to Eq. (3.15) to our knowledge. Nevertheless, the drift coefficient with delayed feedback associated with Eq. (3.9) is,

$$\langle f(x, x_\tau) \delta[x - x(t)] \rangle = [ax + b\langle x_\tau | x \rangle] p(x, t) . \quad (3.16)$$

Consider next the derivation of the diffusive term but corresponding to a Langevin equation with delayed feedback. Equations (B.17) to (B.19) are the same starting from Eq. (3.12) but the functional derivative involved in Eq. (B.19) is modified by the time delay. Integrate Eq. (B.11) with respect to time but with $f[x(t), x(t - \tau)] = ax(t) + bx(t - \tau)$,

$$x(t) = x(t') + \int_{t'}^t \{ax(s) + bx(s - \tau) + g[x(s)]\xi(s)\} ds . \quad (3.17)$$

Take then the functional derivative with respect to $\xi(t')$ on both sides,

$$\begin{aligned} \frac{\delta x(t)}{\delta \xi(t')} = \int_{t'}^t \left\{ a \frac{\delta x(s)}{\delta \xi(t')} + b \frac{\delta x(s - \tau)}{\delta \xi(t')} + \xi(s) \frac{\partial g}{\partial x} \frac{\delta x(s)}{\delta \xi(t')} \right. \\ \left. + g[x(s)] \frac{\delta \xi(s)}{\delta \xi(t')} \right\} ds . \end{aligned} \quad (3.18)$$

We introduce the change of variable $s = s - \tau$ in the second term of the integrand of Eq. (3.18) so that,

$$\int_{t'}^t \frac{\delta x(s - \tau)}{\delta \xi(t')} ds = \int_{t' - \tau}^{t - \tau} \frac{\delta x(s)}{\delta \xi(t')} ds . \quad (3.19)$$

Furthermore, the causality condition [Eq. (B.22)] implies that the functional derivative is zero for times earlier than t' ,

$$\int_{t'}^t \frac{\delta x(s - \tau)}{\delta \xi(t')} ds = \int_{t'}^{t-\tau} \frac{\delta x(s)}{\delta \xi(t')} ds. \quad (3.20)$$

Therefore, by using Eq. (B.23), Eq. (3.18) is

$$\begin{aligned} \frac{\delta x(t)}{\delta \xi(t')} = & H(t - t') \left\{ g[x(t')] + \int_{t'}^t \left[a \frac{\delta x(s)}{\delta \xi(t')} + \xi(s) \frac{\partial g}{\partial x} \frac{\delta x(s)}{\delta \xi(t')} \right. \right. \\ & \left. \left. + g[x(s)] \frac{\delta \xi(s)}{\delta \xi(t')} \right] ds \right\} + H(t - \tau - t') \left[b \int_{t'}^{t-\tau} \frac{\delta x(s - \tau)}{\delta \xi(t')} ds \right], \end{aligned} \quad (3.21)$$

where the causality condition has been taken into account by the introduction of the step function $H(t - t') = 1$ if $t > t'$ and $H(t - t') = 0$ otherwise, and $H(t - \tau - t') = 1$ if $t - \tau > t'$ and $H(t - \tau - t') = 0$ otherwise. If $t = t'$, the functional derivative is,

$$\frac{\delta x(t)}{\delta \xi(t)} = g[x(t)], \quad (3.22)$$

which is the same result than without delayed feedback. Time delay does not change the diffusion coefficient. We can hence apply these results to Eq. (3.9). For additive noise, $g[x(t)] = 1$, and the Fokker-Planck equation is found from Eq. (B.32) but with drift coefficient given by Eq. (3.13),

$$\frac{\partial}{\partial t} p(x, t) = -\frac{\partial}{\partial x} [(ax + b\langle x_\tau | x \rangle) p(x, t)] + K \frac{\partial^2}{\partial x^2} p(x, t). \quad (3.23)$$

The Fokker-Planck equation associated to Eq. (3.9) is non Markovian and hence not closed because of the presence of the average conditional drift $\langle x_\tau | x \rangle$. We cannot therefore solve for the stationary probability distribution function.

We investigate next the time evolution of the moments. Use the definition

of the ensemble average [Eq. (2.12)] and substitute Eq. (3.23),

$$\begin{aligned} \partial_t \langle x^n(t) \rangle = \iint x^n \left\{ - \frac{\partial}{\partial x} [(ax + b\langle x_\tau | x \rangle) p(x, t)] \right. \\ \left. + K \frac{\partial^2}{\partial x^2} p(x, t) \right\} dx dx_\tau . \end{aligned} \quad (3.24)$$

Integrate by parts and assume that the probability distribution function vanishes at $x = \pm\infty$,

$$\partial_t \langle x^n(t) \rangle = na \langle x^n(t) \rangle + nb \langle x^{n-1}(t)x(t-\tau) \rangle + Kn(n-1) \langle x^{n-2}(t) \rangle . \quad (3.25)$$

The time evolution of the n^{th} moment of x thus requires the determination of the correlation $\langle x^{n-1}(t)x(t-\tau) \rangle$. No analytical expression is known for this term, precluding the solution of Eq. (3.25). Only the bifurcation threshold of the first moment can thus be solved analytically. The numerical determination of the bifurcation threshold of the first moment is shown in Fig. 3.4 and compared to Eqs. (3.5) and (3.6). The two are in excellent agreement. The method used to determine the threshold is the same than the deterministic case. Equation (3.9) is integrated using Eq. (2.1) with $\gamma = 0$ and $K = 0.3$. The moment of x is estimated by averaging over 10^6 independent realizations of the noise. The growth exponent λ is found from an exponential fit to the time evolution of the moment and the bifurcation point is determined from the point at which the growth exponent is zero. The numerically determined growth exponent is shown in Fig. 3.2. We again conclude that additive noise does not change the location of the bifurcation threshold of the first moment of x relative to its deterministic counterpart even with delayed feedback.

This conclusion does not hold with parametric noise. For instance, consider

the linear counterpart of Eq. (1.10) with multiplicative noise only ($K = 0$),

$$\dot{x}(t) = ax(t) + bx(t - \tau) + x(t)\xi(t) . \quad (3.26)$$

An analytical expression for the location of the bifurcation threshold of the first moment of Eq. (3.26) is also known [44]. Taking again the ensemble average on both sides,

$$\partial_t \langle x(t) \rangle = a \langle x(t) \rangle + b \langle x(t - \tau) \rangle + \langle x(t)\xi(t) \rangle . \quad (3.27)$$

Since we showed that the functional derivative of $x(t)$ with respect to the noise $\xi(t)$ is not affected by time delay [Eq. (3.22)], we can use the Furutsu-Novikov theorem and the result of Eq. (2.34) to write

$$\partial_t \langle x(t) \rangle = (a + D) \langle x(t) \rangle + b \langle x(t - \tau) \rangle . \quad (3.28)$$

Equation (3.28) is identical to Eq. (3.10) except that $a \rightarrow a + D$. By using this observation, we conclude that the growth exponent satisfies,

$$\lambda_k = \frac{1}{\tau} W_k [b\tau e^{-(a+D)\tau}] + (a + D) . \quad (3.29)$$

The location of the direct bifurcation threshold of the first moment is found by setting $\mu = \omega = 0$, leading to

$$a_c = -(b + D) , \quad (3.30)$$

whereas the Hopf bifurcation is located at $\mu = 0$ and $\omega \neq 0$ yielding,

$$-\left(\frac{a_c + D}{b}\right) = \cos\left(\tau\sqrt{b^2 - (a_c + D)^2}\right). \quad (3.31)$$

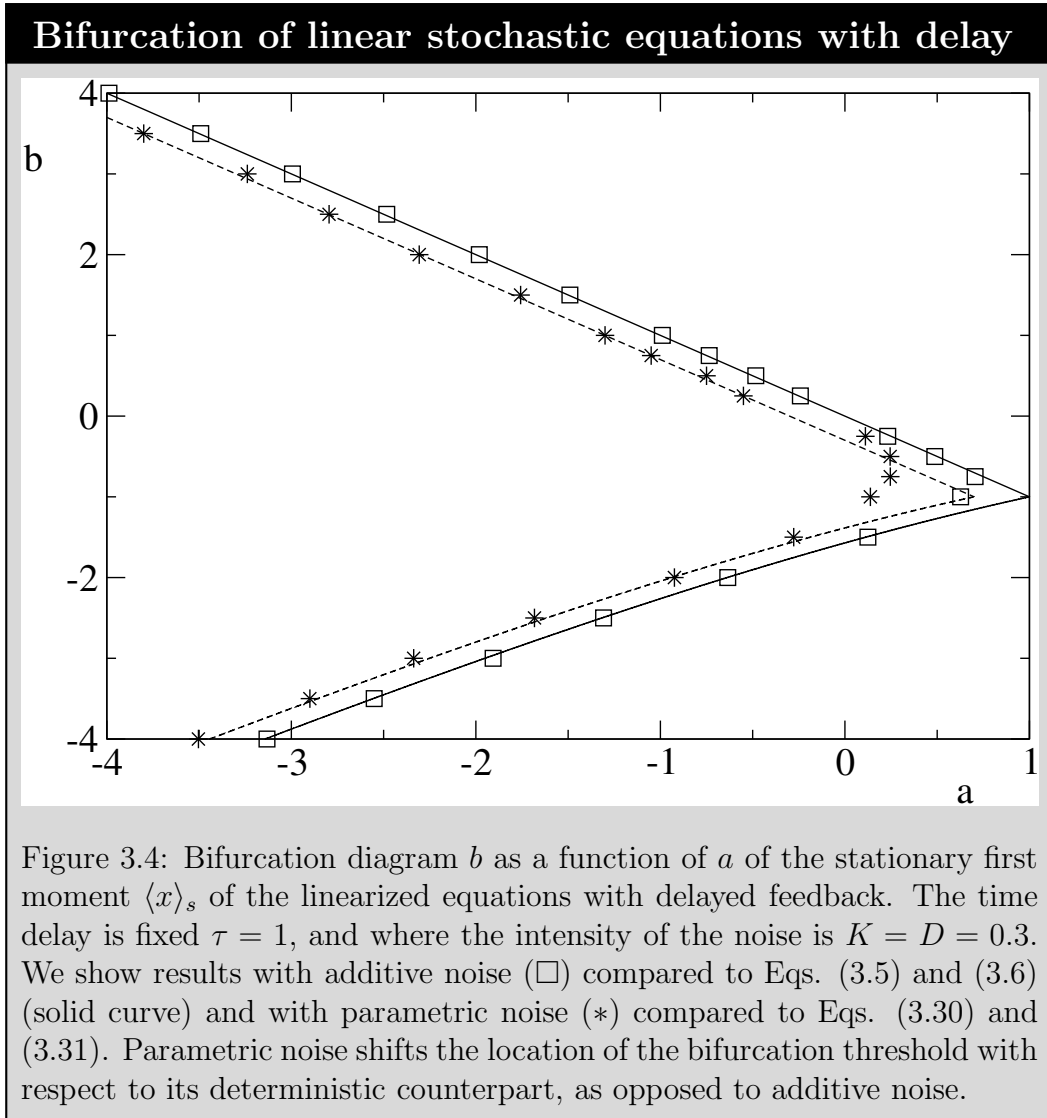
Therefore the location of the bifurcation threshold of the first moment is shifted by an amount that scales with the intensity of the randomness D . The bifurcation threshold might be further investigated by computing the stationary probability distribution function, and by the time evolution of higher order moments. Consider the Fokker-Planck equation associated to Eq. (3.26). The drift coefficient is the same as in the additive case, $f(x, x_\tau) = ax + bx_\tau$ but now $g(x) = x$. Combining the Fokker-Planck equation given by Eq. (B.29) but with delayed drift coefficient, Eq. (3.13), we find

$$\frac{\partial}{\partial t}p(x, t) = -\frac{\partial}{\partial x}\{[(a + D)x + b\langle x_\tau|x\rangle]p(x, t)\} + D\frac{\partial^2}{\partial x^2}[x^2p(x, t)]. \quad (3.32)$$

As with additive noise, the stationary probability density cannot be determined from Eq. (3.32) due to the presence of the average conditional drift $\langle x_\tau|x\rangle$. The time evolution of the moments can be given by substituting Eq. (3.32) into Eq. (2.12) and integrating by parts. If the surface terms are zero at $x = \pm\infty$, one finds

$$\partial_t\langle x^n(t)\rangle = n(a + nD)\langle x^n(t)\rangle + nb\langle x^{n-1}(t)x(t - \tau)\rangle, \quad (3.33)$$

and a hierarchy of equation results, except for $n = 1$. Again the correlation $\langle x^{n-1}(t)x(t - \tau)\rangle$ is not known and there is no analytical solution to Eq. (3.33). Numerical results for the first moment are shown in Fig. 3.4, and compared with the theoretical predictions, Eqs. (3.30) and (3.31). We have used the same



numerical procedure to determine location of the bifurcation as for additive noise, namely Eq. (3.26) is integrated using Eq. (2.2) with $\gamma = 0$ and $D = 0.3$. Over 10^6 independent realizations of the noise are considered in the ensemble average. The numerically determined growth exponent is shown in Fig. 3.2. As shown in Eqs. (3.30) and (3.31), the bifurcation threshold of the first moment is shifted relative to the deterministic threshold.

Recall that the solution of the linear equations considered with delayed feedback diverges above threshold, and the moments can only be computed numerically. In order to stabilize the solution in this region of the bifurcation

diagram, we have augmented the linear stochastic equations by a saturating nonlinearity. As it was shown in Chapter 2, nonlinear cubic term saturates the solution to a finite value above threshold without delayed feedback. This addition permits the calculation of the stationary probability distribution function above threshold.

3.2 Stationary density for small time delay

The theoretical methods introduced in section 3.1 can be combined to directly write the Fokker-Planck equation associated with Eq. (1.10) with multiplicative noise only ($K = 0$) and $\gamma = 1$. In fact, given the Fokker-Planck equation with parametric noise Eq. (B.29), combined with the result for the delayed drift coefficient, Eq. (3.13), but with $f(x, x_\tau) = ax + bx_\tau - x^3$ and $g(x) = x$, we find that the Fokker-Planck equation associated with Eq. (1.10) with $K = 0$ is

$$\begin{aligned} \frac{\partial}{\partial t} p(x, t) = & - \frac{\partial}{\partial x} \{ [(a + D)x - x^3 + b\langle x_\tau | x \rangle] p(x, t) \} \\ & + D \frac{\partial^2}{\partial x^2} [x^2 p(x, t)]. \end{aligned} \quad (3.34)$$

This equation is not closed due to the presence of the average conditional drift $\langle x_\tau | x \rangle$. The average conditional drift can be expanded by using a Taylor stochastic expansion under the assumption that the time delay is small [56, 57]. We first review two methods that exist in the literature, introduced by Guillouzic [87, 88] and by Frank [95, 86] to perform such an approximation. However, both require an Ito interpretation of the Langevin equation being expanded. The first method introduced by Guillouzic simply expands the stochastic process $dx(t, t - \tau)$ in small τ . We present here a simple description for a general Langevin equation with delayed feedback and parametric noise

under the Ito interpretation of stochastic calculus,

$$dx(t, t - \tau) = f(x, x_\tau)dt + g(x)dW(t) , \quad (3.35)$$

where $f(x, x_\tau)$ and $g(x)$ are respectively the drift and diffusion coefficient, and where $W(t)$ is a Wiener process as defined in Appendix A with mean $\langle W(t) \rangle = 0$ and variance $\langle W^2(t) \rangle = 2Dt$. The idea is to derive an expression for the approximate drift and diffusion coefficient by expanding the stochastic delay process $dx(t, t - \tau)$ and by assuming that the resulting process is Markovian. Let $dx^{(a)}(t)$ be the Markovian counterpart of Eq. (3.35) defined by

$$dx^{(a)}(t) = f^{(a)}(x)dt + g^{(a)}(x)dW(t) , \quad (3.36)$$

where $f^{(a)}(x)$ and $g^{(a)}(x)$ are respectively the approximate drift and diffusion coefficient.

Since the stochastic Taylor expansion follows the rules of ordinary calculus [108, 38] in the Ito interpretation, one can expand the stochastic process $dx(t, t - \tau)$ by assuming that the time delay τ is small,

$$\begin{aligned} dx(t, t - \tau) = & dx(t, t - \tau) \Big|_{x=x_\tau} \\ & + [x(t - \tau) - x(t)] \frac{\partial}{\partial x_\tau} dx(t, t - \tau) \Big|_{x=x_\tau} + \dots \end{aligned} \quad (3.37)$$

A stochastic Taylor expansion can also be performed on the delay term $x(t - \tau)$,

$$x(t - \tau) = x(t) - \tau \frac{dx(t, t - \tau)}{dt} \Big|_{t=t-\tau} + \dots \quad (3.38)$$

Since only the drift coefficient of Eq. (3.35) involves the delay term, we have

$$\frac{\partial}{\partial x_\tau} dx(t, t - \tau) \Big|_{x=x_\tau} = \frac{\partial}{\partial x_\tau} f(x, x_\tau) dt \Big|_{x=x_\tau}. \quad (3.39)$$

Substitution of Eqs. (3.38) and (3.39) into Eq. (3.37) yields,

$$\begin{aligned} dx(t, t - \tau) = dx(t, t - \tau) \Big|_{x=x_\tau} \\ - \tau \frac{dx(t, t - \tau)}{dt} \Big|_{t=t-\tau} \frac{\partial}{\partial x_\tau} f(x, x_\tau) dt \Big|_{x=x_\tau} + \mathcal{O}(\tau^2). \end{aligned} \quad (3.40)$$

After cancellation of the dt , we obtain the Markovian approximation up to first order in τ ,

$$dx(t, t - \tau) = dx(t, t - \tau) \Big|_{x=x_\tau} \left[1 - \tau \frac{\partial}{\partial x_\tau} f(x, x_\tau) \Big|_{x=x_\tau} \right] + \mathcal{O}(\tau^2). \quad (3.41)$$

In terms of the approximate drift $f^{(a)}(x)$ and diffusive coefficient $g^{(a)}(x)$, the Markovian process defined by Eq. (3.36) is,

$$f^{(a)}(x) = \left[1 - \tau \frac{\partial}{\partial x_\tau} f(x, x_\tau) \Big|_{x=x_\tau} \right] f(x, x_\tau) \Big|_{x=x_\tau}, \quad (3.42)$$

$$g^{(a)}(x) = \left[1 - \tau \frac{\partial}{\partial x_\tau} f(x, x_\tau) \Big|_{x=x_\tau} \right] g(x). \quad (3.43)$$

In order to apply this result to Eq. (1.10) with $K = 0$, it must first be written under the Ito interpretation of stochastic calculus. In order to do so, use Eq. (A.17) to find

$$dx(t, t - \tau) = [(a + D)x + bx_\tau - x^3]dt + x dW(t). \quad (3.44)$$

Using then Eqs. (3.42) and (3.43) with $f(x, x_\tau) = (a + D)x + bx_\tau - x^3$ and

$g(x) = x$, the approximate Markovian process for small time delay is

$$dx^{(a)}(t) = (1 - b\tau)\{[(a + b + D)x - x^3]dt + x dW(t)\} . \quad (3.45)$$

The Fokker-Planck equation associated to Eq. (3.45) is derived using the Ito interpretation of stochastic calculus. Use Eq. (B.8) with $f^{(a)}(x) = (1 - b\tau)[(a + b + D)x - x^3]$ and $g^{(a)}(x) = (1 - b\tau)x$,

$$\begin{aligned} \frac{\partial}{\partial t} p(x, t) = & - (1 - b\tau) \frac{\partial}{\partial x} \{[(a + b + D)x - x^3]p(x, t)\} \\ & + D(1 - b\tau)^2 \frac{\partial^2}{\partial x^2} [x^2 p(x, t)] . \end{aligned} \quad (3.46)$$

The stationary solution is found by using Eq. (B.9) and leads to the stationary probability distribution function,

$$p_s(x) = \begin{cases} \delta(x) & \text{if } \alpha \leq -1 \\ \mathcal{N}|x|^\alpha e^{-\frac{1}{(1-b\tau)}\frac{x^2}{2D}} & \text{if } \alpha > -1 \end{cases} , \quad (3.47)$$

where the exponent of the power law is

$$\alpha = \frac{(a + b + D)}{(1 - b\tau)D} - 2 . \quad (3.48)$$

The normalization constant \mathcal{N} is found by imposing conservation of probability over all space. To determine its value, use then Eq. (2.41) but with $2D \rightarrow 2D(1 - b\tau)$. The stationary probability distribution function is then

$$p_s(x) = \frac{1}{2} [2D(1 - b\tau)]^{-\left(\frac{\alpha+1}{2}\right)} \Gamma^{-1}\left(\frac{\alpha+1}{2}\right) |x|^\alpha e^{-\frac{1}{(1-b\tau)}\frac{x^2}{2D}} , \quad (3.49)$$

for $\alpha > -1$. The location of the pitchfork bifurcation threshold is located at

$\alpha_c = -1$ or

$$a_c = -b(1 + D\tau). \quad (3.50)$$

Equation (3.50) does not agree with our numerical simulations because we have use a fairly large value of the time delay τ , as it will be shown in Chapter 5. However, to first order in τ , $(1 - b\tau)^{-1} \approx (1 + b\tau)$. With this approximation, the stationary probability distribution function [Eq. (3.49)] is

$$p_s(x) = \begin{cases} \delta(x) & \text{if } \alpha \leq -1 \\ \mathcal{N}|x|^\alpha e^{-(1+b\tau)\frac{x^2}{2D}} & \text{if } \alpha > -1 \end{cases}, \quad (3.51)$$

where the exponent of the power law is

$$\alpha = \frac{(1 + b\tau)(a + b + D)}{D} - 2. \quad (3.52)$$

The normalization constant \mathcal{N} is found again by imposing conservation of probabilities over all space. Use again Eq. (2.41) but with $2D \rightarrow 2D/(1 + b\tau)$.

In those terms, the stationary probability distribution function is thus

$$p_s(x) = \frac{1}{2} \left[\frac{2D}{(1 + b\tau)} \right]^{-\left(\frac{\alpha+1}{2}\right)} \Gamma^{-1} \left(\frac{\alpha + 1}{2} \right) |x|^\alpha e^{-(1+b\tau)\frac{x^2}{2D}}, \quad (3.53)$$

if $\alpha > -1$. The pitchfork bifurcation threshold is located at $\alpha_c = -1$, or in terms of the parameter of the model at,

$$a_c = -\frac{b[1 + \tau(b + D)]}{1 + b\tau}. \quad (3.54)$$

This prediction agrees with our numerical results but only around the pitchfork branch ($b\tau > -1$) as it will be shown in Chapter 5. This is expected

as the approximation leads to a one dimensional Markovian equation [Eq. (3.46)] and oscillatory behavior can only originate in system having at least two dimensions.

A second method has been proposed by Frank [95, 86], and involves expanding the drift coefficient $f(x, x_\tau)$ for small time delay τ in Eq. (3.35). The idea is to perform a Taylor expansion directly on the conditional probability distribution function $p(x_\tau, t - \tau | x, t)$ and to assume that the resulting transition probabilities are normally distributed. The resulting Fokker-Planck equation,

$$\frac{\partial}{\partial t} p(x, t) = -\frac{\partial}{\partial x} [f^{(a)}(x)p(x, t)] + D \frac{\partial^2}{\partial x^2} [g^2(x)p(x, t)] , \quad (3.55)$$

is then closed and the stationary distribution function can be calculated. In fact, consider Eq. (3.35) describing a general Langevin equation under the Ito interpretation of stochastic calculus. Derivation of the Fokker-Planck equation introduced in Appendix B under the Ito interpretation must be modified to include delay. This generalization has been performed in [95, 86, 87]. Follow the steps shown in Appendix B, section B.1 but with $f[x(t)] \rightarrow f[x(t), x(t-\tau)]$ up to Eq. (B.6). Define then $p(x, t; x_\tau, t - \tau) dx dx_\tau$ as the joint probability that $x \in [x, x + dx]$ at time t and $x_\tau \in [x_\tau, x_\tau + dx_\tau]$ at time $t - \tau$. Equation (B.7) is then generalized to

$$\begin{aligned} \int_{-\infty}^{\infty} \int_{-\infty}^{\infty} G(x) \frac{\partial}{\partial t} p(x, t; x_\tau, t - \tau) dx_\tau dx = \\ \int_{-\infty}^{\infty} \int_{-\infty}^{\infty} G(x) \left\{ -\frac{\partial}{\partial x} [f(x, x_\tau)p(x, t; x_\tau, t - \tau)] \right. \\ \left. + D \frac{\partial^2}{\partial x^2} [g^2(x)p(x, t; x_\tau, t - \tau)] \right\} dx_\tau dx , \end{aligned} \quad (3.56)$$

where the right-hand side has been integrated by parts with respect to x , assuming that the surface terms at $x = \pm\infty$ vanish. Since $G(x)$ is arbitrary, then

$$\begin{aligned} \frac{\partial}{\partial t} p(x, t) = & - \frac{\partial}{\partial x} \left[p(x, t) \int_{-\infty}^{\infty} f(x, x_\tau) p(x_\tau, t - \tau | x, t) dx_\tau \right] \\ & + D \frac{\partial^2}{\partial x^2} [g^2(x) p(x, t)] , \end{aligned} \quad (3.57)$$

where we have used $p(x, t; x_\tau, t - \tau) = p(x_\tau, t - \tau | x, t) p(x, t)$. Assume that the process is in a stationary state. In this regime, the transition probabilities only depend on the time difference between two states and $p_s(x_{-\tau} | x) = p_s(x_\tau | x)$ [95, 86, 35] where $x_{-\tau} = x(t + \tau)$ and $x_\tau = x(t - \tau)$. Assume further that the time delay τ is small and expand the conditional probability distribution function up to order τ so that

$$p_s(x_{-\tau} | x) = p_s^{(0)}(x_{-\tau} | x) + \mathcal{O}(\tau) . \quad (3.58)$$

It has been shown that the zeroth order transition probability $p_s^{(0)}(x_{-\tau} | x)$ can be approximated by a Gaussian distribution in this limit [73]. This procedure has been used in [95, 86, 109, 110]. Under this approximation, the transition probabilities are

$$p_s^{(0)}(x_{-\tau} | x) = \sqrt{\frac{1}{2\pi\tau g^2(x)}} \exp \left\{ - \frac{[x_\tau - x - \tau f^{(0)}(x)]^2}{2\tau g^2(x)} \right\} , \quad (3.59)$$

where $f^{(0)}(x) = f(x, x_\tau)|_{x_\tau=x}$. To order τ , the Markovian drift coefficient

$f^{(a)}(x)$ is

$$\begin{aligned} f^{(a)}(x) &= \int_{-\infty}^{\infty} f(x, x_\tau) p_s^{(0)}(x_{-\tau}|x) dx_\tau \\ &= \sqrt{\frac{1}{2\pi\tau g^2(x)}} \int_{-\infty}^{\infty} f(x, x_\tau) e^{-\frac{[x_\tau - x - \tau f^{(0)}(x)]^2}{2\tau g^2(x)}} dx_\tau, \end{aligned} \quad (3.60)$$

and can be substituted into the Fokker-Planck equation [Eq. (3.55)]. The resulting equation is then Markovian. Let's apply these results to Eq. (1.10) with $K = 0$ but interpreted under Ito stochastic calculus rules, Eq. (3.44). In those terms, $f(x, x_\tau) = (a + D)x + bx_\tau - x^3 = \tilde{f}(x) + bx_\tau$, where we define $\tilde{f}(x) = (a + D)x - x^3$ so that $f^{(0)}(x) = (a + b + D)x - x^3$, and where $g(x) = x$. The Markovian drift coefficient is then

$$\begin{aligned} f^{(a)}(x) &= \tilde{f}(x) + b \sqrt{\frac{1}{2\pi\tau g^2(x)}} \int_{-\infty}^{\infty} x_\tau e^{-\frac{[x_\tau - x - \tau f^{(0)}(x)]^2}{2\tau g^2(x)}} dx_\tau \\ &= \tilde{f}(x) + b [x + \tau f^{(0)}(x)] = (1 + b\tau) f^{(0)}(x) \\ &= (1 + b\tau) [(a + b + D)x - x^3] . \end{aligned} \quad (3.61)$$

Substitute Eq. (3.61) into the Fokker-Planck equation Eq. (3.55),

$$\begin{aligned} \frac{\partial}{\partial t} p(x, t) &= - (1 + b\tau) \frac{\partial}{\partial x} \{ [(a + b + D)x - x^3] p(x, t) \} \\ &\quad + D \frac{\partial^2}{\partial x^2} [x^2 p(x, t)] . \end{aligned} \quad (3.62)$$

The stationary probability distribution function of Eq. (3.62) satisfies $\dot{p}_s(x) = 0$ and leading to

$$p_s(x) = \begin{cases} \delta(x) & \text{if } \alpha \leq -1 \\ \mathcal{N}|x|^\alpha e^{-(1+b\tau)\frac{x^2}{2D}} & \text{if } \alpha > -1 \end{cases}, \quad (3.63)$$

where the exponent of the power law is

$$\alpha = \frac{a + b [1 + \tau(a + b + D)]}{D} - 1 . \quad (3.64)$$

This probability density is identical to Eq. (3.51). The bifurcation threshold is thus located at $\alpha_c = -1$ or

$$a_c = -\frac{b [1 + \tau(b + D)]}{1 + b\tau} . \quad (3.65)$$

This prediction agrees with our numerical results and with Eq. (3.54).

3.3 Expansion under Stratonovich calculus

It is instructive to derive the approximations just introduced under a Stratonovich interpretation. Since both interpretations are equivalent, the same result is anticipated. However, the Stratonovich interpretation provides additional insight into the coupling between delay and correlations. Assume that the time delay is small and integrate Eq. (1.10) with multiplicative noise only ($K = 0$) over the time interval $[t, t - \tau]$,

$$x(t) = x(t - \tau) + \int_{t-\tau}^t [ax(t') - x^3(t') + bx(t' - \tau) + x(t')\xi(t')] dt' . \quad (3.66)$$

Consider the first integrand of Eq. (3.66) and integrate it again, but over $[t - \tau, t']$,

$$x(t') = x(t - \tau) + \int_{t-\tau}^{t'} [ax(t'') - x^3(t'') + bx(t'' - \tau) + x(t'')\xi(t'')] dt'' . \quad (3.67)$$

Approximate then the integrands of Eq. (3.67) by their value at the lower bound, $x(t'') \approx x(t - \tau)$, $x(t'' - \tau) \approx x(t - 2\tau)$, and $x^3(t'') \approx x^3(t - \tau)$, so that

$$\begin{aligned} x(t') &= x(t - \tau) + [ax(t - \tau) - x^3(t - \tau) + bx(t - 2\tau)] [t' - (t - \tau)] \\ &\quad + x(t - \tau) \int_{t-\tau}^{t'} \xi(t'') dt'' . \end{aligned} \quad (3.68)$$

The first integral of Eq. (3.66) is thus

$$\begin{aligned} \int_{t-\tau}^t x(t') dt' &= x(t - \tau)\tau + \frac{1}{2} [ax(t - \tau) - x^3(t - \tau) + bx(t - 2\tau)] \tau^2 \\ &\quad + x(t - \tau) \int_{t-\tau}^t \int_{t-\tau}^{t'} \xi(t'') dt'' dt' . \end{aligned} \quad (3.69)$$

Since the stochastic integral in Eq. (3.69) is of the order $\mathcal{O}(\Delta t^{3/2})$, only the first term in the right hand side of Eq. (3.69) contributes to the order of our approximation. The same procedure can be applied to the other integrals of Eq. (3.66) yielding,

$$\int_{t-\tau}^t x(t' - \tau) dt' \approx x(t - 2\tau)\tau , \quad (3.70)$$

$$\int_{t-\tau}^t x^3(t') dt' \approx x^3(t - \tau)\tau , \quad (3.71)$$

and

$$\int_{t-\tau}^t x(t') \xi(t') dt' \approx x(t - \tau) \int_{t-\tau}^t \int_{t-\tau}^{t'} \xi(t') \xi(t'') dt'' dt' . \quad (3.72)$$

Equation (3.72) is the only stochastic integral that is first order in τ . Substitute Eqs. (3.69)-(3.72) into Eq. (3.66)

$$\begin{aligned} x(t) &= x(t - \tau) + [ax(t - \tau) - x^3(t - \tau) + bx(t - 2\tau)] \tau \\ &\quad + x(t - \tau) \int_{t-\tau}^t \int_{t-\tau}^{t'} \xi(t') \xi(t'') dt'' dt' . \end{aligned} \quad (3.73)$$

Consider then Eq. (3.73) and let $t \rightarrow t - \tau$. Then $x(t - \tau) \approx x(t - 2\tau) + \mathcal{O}(\tau)$ and use this result in Eq. (3.73). Furthermore, take the ensemble average on both sides given the numerical value of $x(t - \tau)$,

$$\begin{aligned} \langle x(t)|x(t - \tau) \rangle &= x(t - \tau) + [ax(t - \tau) - x^3(t - \tau) + bx(t - \tau)] \tau \\ &\quad + x(t - \tau) \int_{t-\tau}^t \int_{t-\tau}^{t'} \langle \xi(t')\xi(t'') \rangle dt'' dt' , \end{aligned} \quad (3.74)$$

where we have used $\langle \xi(t')\xi(t'')|x(t - \tau) \rangle = \langle \xi(t')\xi(t'') \rangle$ since the quantity $x(t - \tau)$ is given. Use further $\langle \xi(t')\xi(t'') \rangle = 2D\delta(t' - t'')$ and integrate the delta function so that,

$$\langle x(t)|x(t - \tau) \rangle = x(t - \tau) + \tau[(a + b + D)x(t - \tau) - x^3(t - \tau)] . \quad (3.75)$$

We then make a step forward in time so that $t \rightarrow t + \tau$, leading to

$$\langle x(t + \tau)|x(t) \rangle = x(t) + \tau[(a + b + D)x(t) - x^3(t)] . \quad (3.76)$$

Note further that under stationary conditions, the conditional probability distribution function only depends on time differences [35], i.e τ in this case, so that we have

$$\langle x_{-\tau}|x \rangle = \langle x_{\tau}|x \rangle , \quad (3.77)$$

where $x_{-\tau} = x(t + \tau)$ and $x_{\tau} = x(t - \tau)$. We then obtain an expression for the average conditional drift for small time delay,

$$\langle x_{\tau}|x \rangle = x + \tau[(a + b + D)x - x^3] . \quad (3.78)$$

Substitute then Eq. (3.78) into Eq. (3.34),

$$\begin{aligned} \frac{\partial}{\partial t} p(x, t) = & - (1 + b\tau) \frac{\partial}{\partial x} \{ [(a + b + D)x - x^3] p(x, t) \} \\ & + D \frac{\partial^2}{\partial x^2} [x^2 p(x, t)] . \end{aligned} \quad (3.79)$$

The stationary solution of Eq. (3.79) satisfies $\dot{p}_s(x) = 0$ and leads to the stationary probability distribution function,

$$p_s(x) = \begin{cases} \delta(x) & \text{if } \alpha \leq -1 \\ \mathcal{N}|x|^\alpha e^{-(1+b\tau)\frac{x^2}{2D}} & \text{if } \alpha > -1 \end{cases} , \quad (3.80)$$

where the exponent of the power law is

$$\alpha = \frac{(1 + b\tau)(a + b + D)}{D} - 2 . \quad (3.81)$$

The distribution obtained, Eq. (3.80), is identical to Eqs. (3.51) and (3.63).

The expansion in small delay τ can also be performed on equations with additive noise only. For instance, consider the expansion applied on Eq. (1.10) but with $D = 0$. The only difference stands in the stochastic integrals, as none of them is of first order in τ . For this case, the average conditional drift is

$$\langle x_\tau | x \rangle = x + \tau [(a + b)x - x^3] . \quad (3.82)$$

The Fokker-Plack equation associated with Eq. (1.10) but with additive noise is thus,

$$\begin{aligned} \frac{\partial}{\partial t} p(x, t) = & - (1 + b\tau) \frac{\partial}{\partial x} \{ [(a + b)x - x^3] p(x, t) \} \\ & + K \frac{\partial^2}{\partial x^2} [x^2 p(x, t)] . \end{aligned} \quad (3.83)$$

The stationary distribution function associated to Eq. (3.83) is

$$p_s(x) = \mathcal{N} \exp \left\{ \frac{(1 + b\tau)}{K} \left[(a + b) \frac{x^2}{2} - \frac{x^4}{4} \right] \right\}. \quad (3.84)$$

which might be compared to Eq. (2.29) in the absence of delay. In this case, the bifurcation occurs at $a_c = -b$, the same as in the deterministic and linear equation. Note that $b\tau = -1$ is the point separating the pitchfork and the Hopf lines. Hence, additive noise does not change the location of the pitchfork bifurcation threshold.

In summary, delayed feedback and parametric stochasticity couple and shift the location of the bifurcation threshold as shown in Eq. (3.65). The bifurcation diagram of Eq. (1.10) has been determined numerically as shown in Chapter 5. The results are compared to the analytical results achieved in this chapter. Interestingly, we show that both are in agreement even when the time delay is not small. In fact, our numerical calculations were done by using a value of $\tau = 1$, well beyond the region of what one can consider small τ .

It is worth remarking that the moments of x of the stochastic *linear* equations with and without delay diverge above threshold. Even though an analysis of the stability of the linear equations provides some insight about the effect of time delay, nonlinearity must be introduced into the equation in order to have a well defined bifurcation threshold in all cases. This is in marked contrast with the case of deterministic systems in which linearization is sufficient to determine the location of the bifurcation threshold.

All the analyses described in this chapter fail around the Hopf bifurcation branch. Naively, all methods described are first order in the time delay and lead to an effective Markovian one dimensional differential equation, hence they cannot describe an oscillatory instability. One might consider a second

order expansion in τ instead. Unfortunately, it has been rigorously shown that such an expansion is not valid even in the deterministic limit [89, 56, 57]. Furthermore, the location of the multicritical point goes to infinity as $\tau \rightarrow 0$, and the Hopf branch completely disappears in this limit. A completely different procedure is thus needed to analytically determine the location of the Hopf branch. We have introduced a multiple time scale expansion method, which we describe in the next chapter.

Chapter 4

Multiple time scale expansion

Taylor expansion of delay terms as described in Chapter 3 fails to describe oscillatory instabilities. The fact that the multicritical point moves to infinity as the delay time goes to zero suggests that $\tau \rightarrow 0$ leads in effect to a singular perturbation. We generalize here the classical multiple time scale expansion to obtain asymptotic solutions of stochastic differential equations with delay near a bifurcation threshold. We exploit the separation of temporal scales between fast random variables, order one oscillation near the bifurcation threshold, and a divergent correlation time, as the threshold is approached. The method has been previously used in the stochastic processes literature on the linear counterpart of Eq. (1.10) [91, 92], and on studies of the van der Pol-Duffing oscillator with parametric noise [90, 93, 94].

We extend the method to obtain the Fokker-Planck equation describing the stochastic dynamics of the slowly varying amplitude or envelope variables. We then predict the location of the Hopf bifurcation threshold from normalization conditions imposed on the stationary probability density of the slow envelope. The method is general and can be applied in principle to any stochastic equation with delayed feedback that presents a similar separation of scales. In order

to verify the methodology, we apply it first to the stochastic van der Pol oscillator with added delayed feedback. The location of the bifurcation threshold without time delay is known for this model [102, 111], and we show that our general solution reduces to the known case when the feedback is removed. We also note that the van der Pol oscillator with delayed feedback is important in its own right in the theory of vibration. For example, there is a recent interest in this model to help reduce abnormal behavior of engineered structures caused by interaction with the environment. We use our method to derive an analytic expression for the location of the Hopf bifurcation threshold for the delayed oscillator. Interestingly, the procedure also yields an expression for the renormalized Hopf frequency. The analytical expression agrees with the location of the bifurcation threshold of the stochastic oscillator without delayed feedback. Furthermore, the theoretical prediction is compared with a numerical integration of the governing equation, and shown to be in excellent agreement. We then use the multiple time scale expansion method to obtain an asymptotic solution of Eq. (1.10), our model of interest.

4.1 Van der Pol oscillator with delayed feedback

The location of the Hopf bifurcation of the van der Pol oscillator driven by a parametric noise and under delayed feedback is derived in this section by using a multiple time scale expansion of the solution. In order to do so, consider the van der Pol (VDP) oscillator with delayed feedback driven by multiplicative noise,

$$\ddot{x}(t) + \omega_0^2 x(t) + \chi x(t - \tau) = \beta \dot{x}(t) + \kappa \dot{x}(t - \tau) + bx^2(t)\dot{x}(t) + x(t)\xi(t), \quad (4.1)$$

where ω_0^2 is the natural frequency of the oscillator, χ is the intensity of the feedback loop in the position of the oscillator and has units of frequency, β is the damping parameter, κ is the intensity of the feedback loop in the velocity of the oscillator and has units of damping coefficient, b is a positive constant, and $\xi(t)$ is a Gaussian white noise process with mean $\langle \xi(t) \rangle = 0$ and correlation $\langle \xi(t)\xi(t') \rangle = 2D\delta(t-t')$, where D is the intensity of the noise.

The deterministic van der Pol oscillator was introduced by Appleton and van der Pol to describe triode oscillations in electrical circuits [112]. Since then, the model has been used as a prototypical equation that describe self-excited stable oscillations. The deterministic ($D = 0$) oscillator without delayed feedback $\chi = \kappa = 0$ has a fixed point at $(x, \dot{x}) = (0, 0)$. In order to study the stability of this fixed point, consider the system of equations,

$$\dot{x}(t) = y(t), \quad (4.2)$$

$$\dot{y}(t) = -\omega_0^2 x(t) + \beta y(t) - bx^2(t)y(t), \quad (4.3)$$

obtained by setting $y(t) = \dot{x}(t)$. The Jacobian J_{VPD} associated to the system of equations (4.2) - (4.3) is,

$$J_{VPD} = \begin{bmatrix} 0 & 1 \\ -\omega_0^2 - 2bxy & \beta - bx^2 \end{bmatrix}. \quad (4.4)$$

The eigenvalues $\lambda_{1,2}$ around the fixed point $(x, y) = (0, 0)$ are

$$\lambda_{1,2} = \frac{\beta}{2} \left[1 \pm \sqrt{1 - \left(\frac{2\omega_0}{\beta} \right)^2} \right]. \quad (4.5)$$

If $\beta < 0$, the fixed point is stable. Otherwise, the fixed point is unstable and

the trajectory is a periodic orbit. The Hopf bifurcation is located at the point where the eigenvalue is zero, which occurs at $\beta_c = 0$.

The van der Pol model supplemented with delayed feedback plays an important role in the theory of nonlinear vibration. For example, complex response due to time delay such as bifurcation, high amplitude vibration, quasi-periodic motion, or chaotic behavior may cause the failure of an engineered structure subjected to vibration due to its environment. On the other hand, careful choices of parameters may enhance the control of oscillatory systems [113, 114, 115]. For instance, it has been shown in a periodically driven van der Pol oscillator with delay terms in position and velocity that feedback may control the amplitude of oscillation and even suppress quasi-periodic motion. A similar model but with a cubic nonlinearity has been investigated via a center manifold reduction together with an averaging method [116] to show that time delay can act as an effective switch, and control motion either from regular motion to a chaotic behavior or vice versa. The dynamics of a forced van der Pol-Duffing with both linear and nonlinear feedback control has also been studied [117, 118] as an example of a Neimark-Sacker bifurcation to quasi periodic motion.

The bifurcation diagram of the van der Pol oscillator without delayed feedback but parametrically driven by a stochastic source is well known. It has been obtained by either a perturbation analysis of the linear stability problem [111], or by adiabatic reduction [102]. It is found that the bifurcation point is shifted relative to the deterministic limit by an amount that is proportional to the intensity of the randomness. This model has also been investigated by using a multiple time scale expansion of the solution in order to derive the resulting slow amplitude or envelope equations near the bifurcation [93, 90, 94, 119].

The same multiple scale method has been used to analyze stochastic differential equations with delayed feedback in order to derive the stochastic time evolution of the envelope of the oscillation [91, 92] as well as to determine the location of the bifurcation threshold if the time delay is small [120].

Scant research has focused on stochastically driven oscillators with feedback as compared to its deterministic counterpart. The coherence and the frequency of the oscillator under delayed feedback is studied with additive Gaussian white noise in [121]. Moreover, a relationship between its coherence and reliability has been established [122]. Even less literature exists if the randomness is parametric. The stability and bifurcation of the van der Pol-Duffing oscillator is qualitatively studied in [123]. Moreover, the steady-state response as well as a stability analysis are investigated by means of the Lyapunov exponent in [124] where the oscillator is subjected to two time delays. Our focus here is an extension of this latter work, and focuses on a nonlinear oscillator with delayed feedback that is stochastically driven. We pay especial attention to the interplay between the delayed feedback and temporal correlations, and its effect on the stability of oscillation.

Consider then a multiple time scale expansion of the form [125],

$$x(t, \mathcal{T}) = \epsilon A(\mathcal{T}) \cos(\omega t) - \epsilon B(\mathcal{T}) \sin(\omega t), \quad (4.6)$$

$$\dot{x}(t, \mathcal{T}) = -\omega \epsilon A(\mathcal{T}) \sin(\omega t) - \omega \epsilon B(\mathcal{T}) \cos(\omega t), \quad (4.7)$$

where we have introduced a fast time scale t relative to a slow time scale $\mathcal{T} = \epsilon^2 t$, where $0 < \epsilon \ll 1$ is called a scaling parameter, and where ω is the frequency of the fast oscillation. We assume that the envelope of the oscillation $A(\mathcal{T})$ and $B(\mathcal{T})$ evolves over the slow time scale \mathcal{T} . We further assume that the dominant stochasticity near threshold is over the slow time scale. The envelope variables

are assumed to scale according to $\mathcal{O}(\epsilon)$ close to the bifurcation. The two time scales have to be understood as independent from each other even if we have defined the relation $\mathcal{T} = \epsilon^2 t$. We also assume that a linear combinations of the parameters of the model are small close to the bifurcation threshold and will be scaled accordingly in the expansion. Substitute Eqs. (4.6) and (4.7) into Eq. (4.1) and use the relation $\partial_t \rightarrow \partial_t + \epsilon^2 \partial_{\mathcal{T}}$,

$$\begin{aligned}
\epsilon^3 \partial_{\mathcal{T}} A(\mathcal{T}) \sin(\omega t) + \epsilon^3 \partial_{\mathcal{T}} B(\mathcal{T}) \cos(\omega t) = & -\frac{1}{\omega} \left\{ \right. \\
& (\omega^2 - \omega_0^2) [\epsilon \cos(\omega t) A(\mathcal{T}) - \epsilon \sin(\omega t) B(\mathcal{T})] \\
& - \chi \left\{ \epsilon \cos[\omega(t - \tau)] A(\mathcal{T} - \epsilon^2 \tau) \right. \\
& \quad \left. - \epsilon \sin[\omega(t - \tau)] B(\mathcal{T} - \epsilon^2 \tau) \right\} \\
& - \beta \omega [\epsilon \sin(\omega t) A(\mathcal{T}) + \epsilon \cos(\omega t) B(\mathcal{T})] \\
& - \kappa \omega \left\{ \epsilon \sin[\omega(t - \tau)] A(\mathcal{T} - \epsilon^2 \tau) \right. \\
& \quad \left. + \epsilon \cos[\omega(t - \tau)] B(\mathcal{T} - \epsilon^2 \tau) \right\} \\
& + b \omega [\epsilon \cos(\omega t) A(\mathcal{T}) - \epsilon \sin(\omega t) B(\mathcal{T})]^2 \times \\
& \quad [\epsilon \sin(\omega t) A(\mathcal{T}) + \epsilon \cos(\omega t) B(\mathcal{T})] \\
& \left. + [\epsilon \cos(\omega t) A(\mathcal{T}) - \epsilon \sin(\omega t) B(\mathcal{T})] \xi(t) \right\}.
\end{aligned} \tag{4.8}$$

For small ϵ and finite τ , we have $A(\mathcal{T} - \epsilon^2 \tau) \approx A(\mathcal{T})$ and $B(\mathcal{T} - \epsilon^2 \tau) \approx B(\mathcal{T})$. Define moreover the parameters $\mu = \beta \omega + \chi \sin(\omega \tau) + \omega \kappa \cos(\omega \tau)$ and $\nu = \omega^2 - \omega_0^2 - \chi \cos(\omega \tau) + \omega \kappa \sin(\omega \tau)$, for simplicity. We then eliminate the fast time scale by integrating Eq. (4.8) over a period of the oscillation. Multiply both sides of Eq. (4.8) by $L^{-1} \int_0^L dt \sin(\omega t)$, where $L = 2\pi/\omega$, and perform the integration. The method leads to a stochastic differential equation for the

envelope variable $A(\mathcal{T})$,

$$\begin{aligned} \epsilon^3 \partial_{\mathcal{T}} A(\mathcal{T}) = \frac{1}{\omega} \left\{ \mu \epsilon A(\mathcal{T}) + \nu \epsilon B(\mathcal{T}) - \frac{\epsilon^3}{4} b \omega A(\mathcal{T}) [A^2(\mathcal{T}) + B^2(\mathcal{T})] \right. \\ \left. + \epsilon \frac{B(\mathcal{T})}{L} \int_0^L \xi(t) dt - \epsilon \frac{B(\mathcal{T})}{L} \int_0^L \cos(2\omega t) \xi(t) dt \right. \\ \left. - \epsilon \frac{A(\mathcal{T})}{L} \int_0^L \sin(2\omega t) \xi(t) dt \right\}. \end{aligned} \quad (4.9)$$

We next determine the stochastic terms over the slow time scale. We first use the relation $\mathcal{T} = \epsilon^2 t$ to write

$$\xi(t) = \epsilon \xi_0(\mathcal{T}), \quad (4.10)$$

where $\xi_0(\mathcal{T})$ is a Gaussian random variable with mean $\langle \xi_0(\mathcal{T}) \rangle = 0$ and correlation $\langle \xi_0(\mathcal{T}) \xi_0(\mathcal{T}') \rangle = 2D \delta(\mathcal{T} - \mathcal{T}')$. This relation is further understood from the correlation of $\xi(t)$,

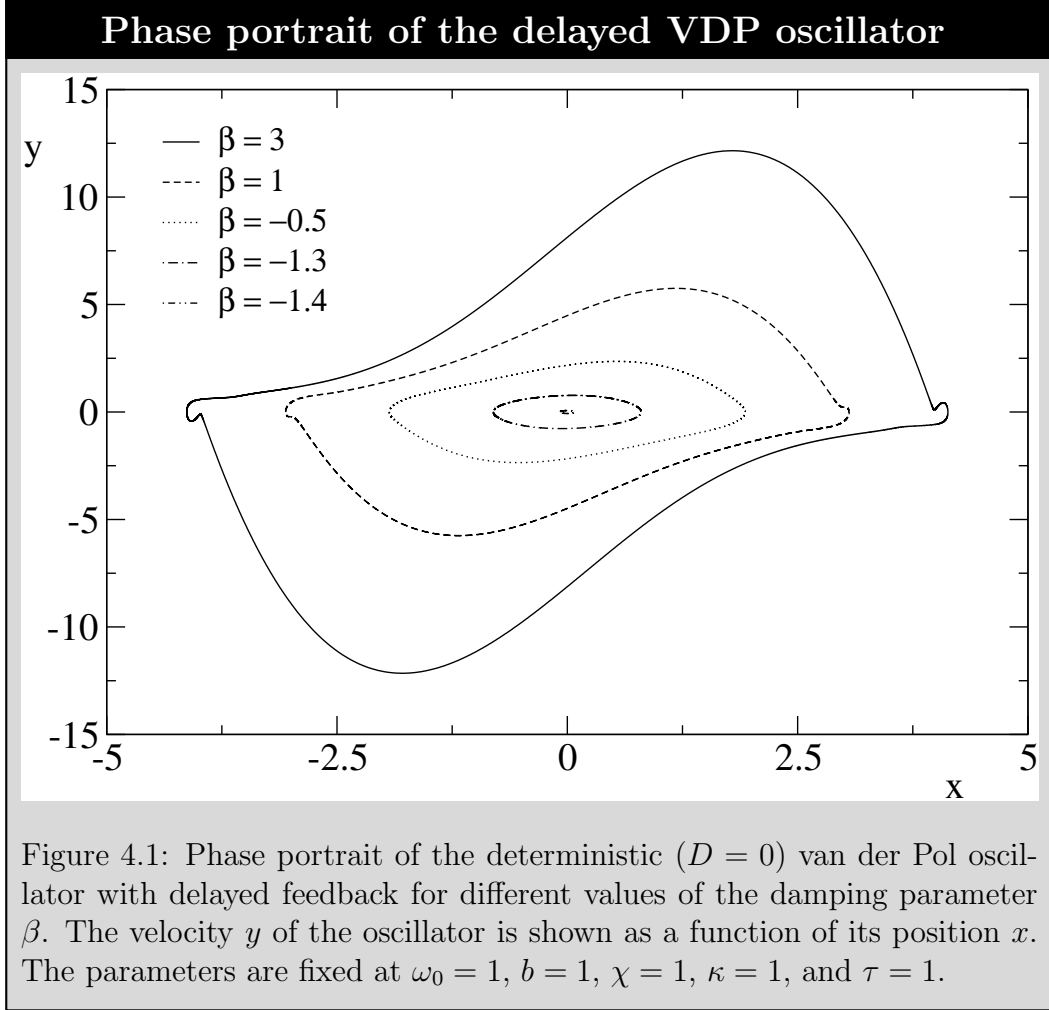
$$\begin{aligned} \langle \xi(t) \xi(t') \rangle &= 2D \delta(t - t') = 2D \delta \left[\frac{1}{\epsilon^2} (\mathcal{T} - \mathcal{T}') \right] = 2D \epsilon^2 \delta(\mathcal{T} - \mathcal{T}') \\ &= \epsilon^2 \langle \xi_0(\mathcal{T}) \xi_0(\mathcal{T}') \rangle, \end{aligned} \quad (4.11)$$

where we have used the identity for the delta function $\delta(\mathcal{C}x) = |\mathcal{C}|^{-1} \delta(x)$, where \mathcal{C} is a constant. In order to define the random sources $\cos(2\omega t) \xi(t)$ and $\sin(2\omega t) \xi(t)$ over the slow time scale, consider their correlations

$$\langle \cos(2\omega t) \xi(t) \cos(2\omega t') \xi(t') \rangle = \epsilon^2 \langle \cos^2(2\omega t) \rangle \langle \xi_1(\mathcal{T}) \xi_1(\mathcal{T}') \rangle, \quad (4.12)$$

$$\langle \sin(2\omega t) \xi(t) \sin(2\omega t') \xi(t') \rangle = \epsilon^2 \langle \sin^2(2\omega t) \rangle \langle \xi_2(\mathcal{T}) \xi_2(\mathcal{T}') \rangle, \quad (4.13)$$

where $\xi_1(\mathcal{T})$ and $\xi_2(\mathcal{T})$ are a Gaussian random variables with mean $\langle \xi_j(\mathcal{T}) \rangle = 0$



with $j = \{1, 2\}$ and correlation $\langle \xi_j(\mathcal{T}) \xi_k(\mathcal{T}') \rangle = 2D\delta(\mathcal{T} - \mathcal{T}')$ if $j = k$ and 0 otherwise. We replace the oscillating functions by their time averages. The random sources are then in the slow time scale

$$\cos(2\omega t)\xi(t) \rightarrow \frac{\epsilon}{\sqrt{2}}\xi_1(\mathcal{T}), \quad (4.14)$$

$$\sin(2\omega t)\xi(t) \rightarrow \frac{\epsilon}{\sqrt{2}}\xi_2(\mathcal{T}). \quad (4.15)$$

Substitute Eqs. (4.10), (4.14), and (4.15) into Eq. (4.9). We thus obtain a stochastic differential equation for the envelope variable $A(\mathcal{T})$ that is indepen-

dent of the fast time scale t ,

$$\begin{aligned} \epsilon^3 \partial_{\mathcal{T}} A(\mathcal{T}) = \frac{1}{\omega} \left\{ \mu \epsilon A(\mathcal{T}) + \nu \epsilon B(\mathcal{T}) - \frac{\epsilon^3}{4} b \omega A(\mathcal{T}) [A^2(\mathcal{T}) + B^2(\mathcal{T})] \right. \\ \left. + \epsilon^2 B(\mathcal{T}) \xi_0(\mathcal{T}) - \frac{\epsilon^2}{\sqrt{2}} B(\mathcal{T}) \xi_1(\mathcal{T}) - \frac{\epsilon^2}{\sqrt{2}} A(\mathcal{T}) \xi_2(\mathcal{T}) \right\}. \end{aligned} \quad (4.16)$$

The same method is applied to the envelope variable $B(\mathcal{T})$. Integrate then both sides of Eq. (4.8) by $L^{-1} \int_0^L dt \cos(\omega t)$, where $L = 2\pi/\omega$. Use further Eqs. (4.10), (4.14), and (4.15) to obtain the stochastic time evolution of the envelope variable $B(\mathcal{T})$,

$$\begin{aligned} \epsilon^3 \partial_{\mathcal{T}} B(\mathcal{T}) = \frac{1}{\omega} \left\{ -\nu \epsilon A(\mathcal{T}) + \mu \epsilon B(\mathcal{T}) - \frac{\epsilon^3}{4} b \omega B(\mathcal{T}) [A^2(\mathcal{T}) + B^2(\mathcal{T})] \right. \\ \left. - \epsilon^2 A(\mathcal{T}) \xi_0(\mathcal{T}) - \frac{\epsilon^2}{\sqrt{2}} A(\mathcal{T}) \xi_1(\mathcal{T}) + \frac{\epsilon^2}{\sqrt{2}} B(\mathcal{T}) \xi_2(\mathcal{T}) \right\}, \end{aligned} \quad (4.17)$$

where we have defined the stochastic term over the slow time scale. Assume that the parameters scale as $\mu = \epsilon^2 \tilde{\mu}$ and $\nu = \epsilon^2 \tilde{\nu}$ close to the bifurcation. In matrix form, the Langevin equations are,

$$\begin{aligned} \frac{d}{d\mathcal{T}} \begin{bmatrix} A \\ B \end{bmatrix} = \frac{1}{\omega} \begin{bmatrix} \tilde{\mu} & \tilde{\nu} \\ -\tilde{\nu} & \tilde{\mu} \end{bmatrix} \begin{bmatrix} A \\ B \end{bmatrix} - \frac{b}{4} \begin{bmatrix} A(A^2 + B^2) \\ B(A^2 + B^2) \end{bmatrix} \\ + \frac{1}{\epsilon \omega} \begin{bmatrix} 0 & 1 \\ -1 & 0 \end{bmatrix} \begin{bmatrix} A \\ B \end{bmatrix} \xi_0(\mathcal{T}) + \frac{1}{\sqrt{2} \epsilon \omega} \begin{bmatrix} 0 & -1 \\ -1 & 0 \end{bmatrix} \begin{bmatrix} A \\ B \end{bmatrix} \xi_1(\mathcal{T}) \\ + \frac{1}{\sqrt{2} \epsilon \omega} \begin{bmatrix} -1 & 0 \\ 0 & 1 \end{bmatrix} \begin{bmatrix} A \\ B \end{bmatrix} \xi_2(\mathcal{T}). \end{aligned} \quad (4.18)$$

We can then write the Fokker-Planck equation associated to Eq. (4.18). In order to do so, note that the Fokker-Planck equation associated to the system

of equations,

$$\frac{d}{dt} \begin{bmatrix} u \\ v \end{bmatrix} = \begin{bmatrix} a_{11} & a_{12} \\ a_{21} & a_{22} \end{bmatrix} \begin{bmatrix} u \\ v \end{bmatrix} + \begin{bmatrix} k_{11} & k_{12} \\ k_{21} & k_{22} \end{bmatrix} \begin{bmatrix} u \\ v \end{bmatrix} \xi(t), \quad (4.19)$$

where $\xi(t)$ is a Gaussian white noise process with mean $\langle \xi(t) \rangle = 0$ and correlation $\langle \xi(t)\xi(t') \rangle = 2D\delta(t - t')$, is [22, 126]

$$\begin{aligned} \frac{\partial}{\partial t} p(u, v, t) &= - \frac{\partial}{\partial u} [(a_{11}u + a_{12}v)p(u, v, t)] \\ &\quad - \frac{\partial}{\partial v} [(a_{21}u + a_{22}v)p(u, v, t)] \\ &\quad + D \left\{ \frac{\partial}{\partial u} \left[(k_{11}u + k_{12}v) \left\{ \frac{\partial}{\partial u} [(k_{11}u + k_{12}v)p(u, v, t)] \right. \right. \right. \\ &\quad \left. \left. \left. + \frac{\partial}{\partial v} [(k_{21}u + k_{22}v)p(u, v, t)] \right\} \right] \right. \\ &\quad \left. + \frac{\partial}{\partial v} \left[(k_{21}u + k_{22}v) \left\{ \frac{\partial}{\partial u} [(k_{11}u + k_{12}v)p(u, v, t)] \right. \right. \right. \\ &\quad \left. \left. \left. + \frac{\partial}{\partial v} [(k_{21}u + k_{22}v)p(u, v, t)] \right\} \right] \right\}. \end{aligned} \quad (4.20)$$

We use this result to write the Fokker-Planck equation corresponding to Eq.

(4.18),

$$\begin{aligned}
\frac{\partial}{\partial \mathcal{T}} p(A, B, \mathcal{T}) = & -\frac{1}{\omega} \frac{\partial}{\partial A} \left\{ \left[\tilde{\mu}A + \tilde{\nu}B - \frac{1}{4}b\omega A(A^2 + B^2) \right] p(A, B, \mathcal{T}) \right\} \\
& -\frac{1}{\omega} \frac{\partial}{\partial B} \left\{ \left[-\tilde{\nu}A + \tilde{\mu}B - \frac{1}{4}b\omega B(A^2 + B^2) \right] p(A, B, \mathcal{T}) \right\} \\
& + \frac{D}{\omega^2 \epsilon^2} \left\{ A^2 \frac{\partial^2}{\partial B^2} - 2AB \frac{\partial^2}{\partial A \partial B} + B^2 \frac{\partial^2}{\partial A^2} \right. \\
& \quad \left. - \left(A \frac{\partial}{\partial A} + B \frac{\partial}{\partial B} \right) \right\} p(A, B, \mathcal{T}) \\
& + \frac{D}{2\omega^2 \epsilon^2} \left\{ A^2 \frac{\partial^2}{\partial B^2} + 2AB \frac{\partial^2}{\partial A \partial B} + B^2 \frac{\partial^2}{\partial A^2} \right. \\
& \quad \left. + \left(A \frac{\partial}{\partial A} + B \frac{\partial}{\partial B} \right) \right\} p(A, B, \mathcal{T}) \\
& + \frac{D}{2\omega^2 \epsilon^2} \left\{ A^2 \frac{\partial^2}{\partial A^2} - 2AB \frac{\partial^2}{\partial A \partial B} + B^2 \frac{\partial^2}{\partial B^2} \right. \\
& \quad \left. + \left(A \frac{\partial}{\partial A} + B \frac{\partial}{\partial B} \right) \right\} p(A, B, \mathcal{T}),
\end{aligned} \tag{4.21}$$

Assume also that the intensity of the noise scales as $D = \epsilon^2 \tilde{D}$ close to the bifurcation. The bifurcation threshold is now obtained from the Fokker-Planck equation expressed in polar coordinates. Let $A = r \cos(\theta)$ and $B = r \sin(\theta)$. Under this change of variable, the probability distribution function transforms as $\tilde{p}(r, \theta, \mathcal{T}) = r p(A, B, \mathcal{T})$, where r is the Jacobian of the transformation. Furthermore, the diffusive terms of the Fokker-Planck equation Eq. (4.21) that are factors of $\tilde{D}/(2\omega^2)$ are

$$(A^2 + B^2) \left(\frac{\partial^2}{\partial A^2} + \frac{\partial^2}{\partial B^2} \right) + 2 \left(A \frac{\partial}{\partial A} + B \frac{\partial}{\partial B} \right) = r^2 \frac{\partial^2}{\partial r^2} + 3r \frac{\partial}{\partial r} + \frac{\partial^2}{\partial \theta^2}, \tag{4.22}$$

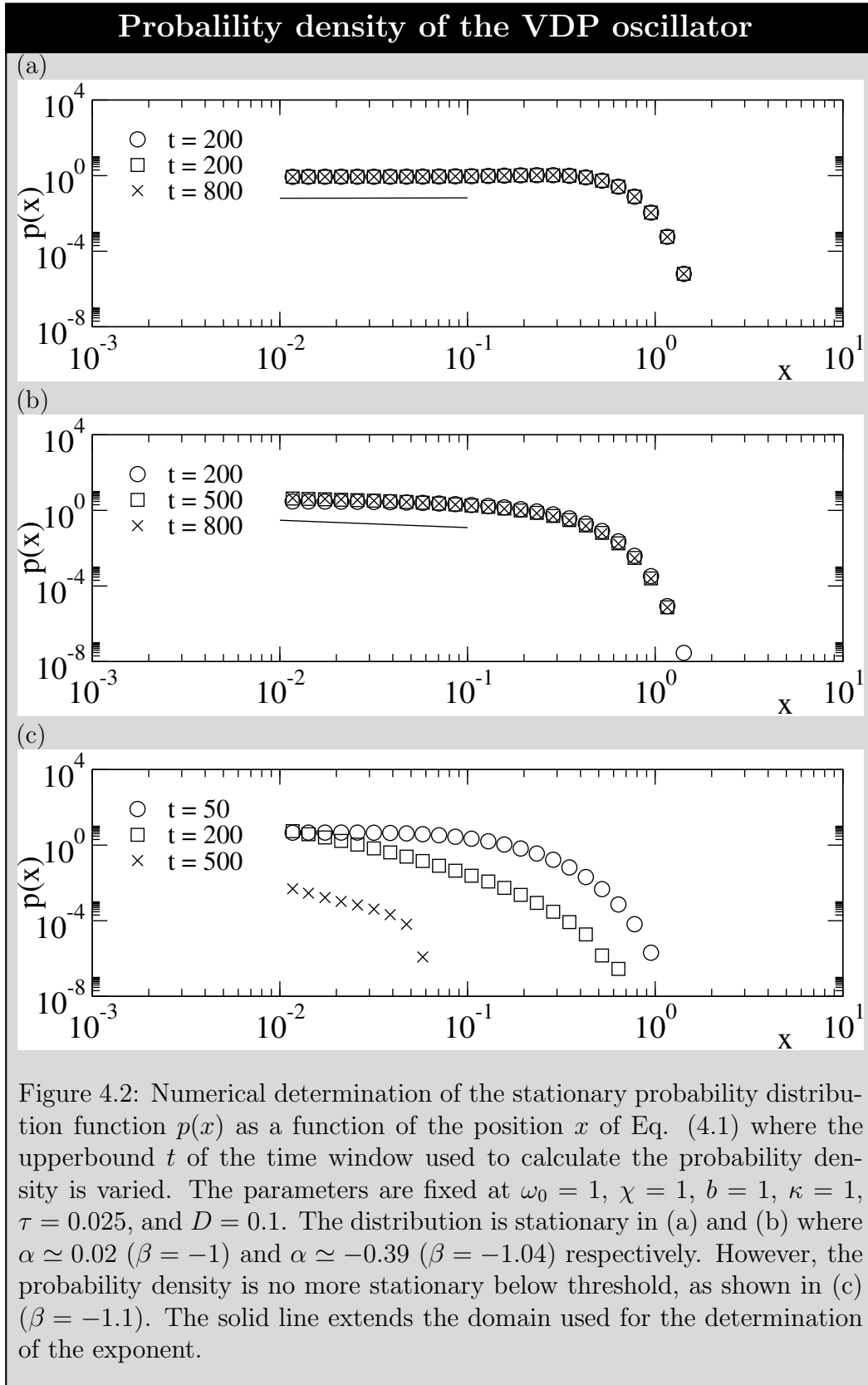


Figure 4.2: Numerical determination of the stationary probability distribution function $p(x)$ as a function of the position x of Eq. (4.1) where the upperbound t of the time window used to calculate the probability density is varied. The parameters are fixed at $\omega_0 = 1$, $\chi = 1$, $b = 1$, $\kappa = 1$, $\tau = 0.025$, and $D = 0.1$. The distribution is stationary in (a) and (b) where $\alpha \approx 0.02$ ($\beta = -1$) and $\alpha \approx -0.39$ ($\beta = -1.04$) respectively. However, the probability density is no more stationary below threshold, as shown in (c) ($\beta = -1.1$). The solid line extends the domain used for the determination of the exponent.

whereas terms that are proportional to \tilde{D}/ω^2 transform as

$$A^2 \frac{\partial^2}{\partial B^2} - 2AB \frac{\partial^2}{\partial A \partial B} + B^2 \frac{\partial^2}{\partial A^2} - \left(A \frac{\partial}{\partial A} + B \frac{\partial}{\partial B} \right) = \frac{\partial^2}{\partial \theta^2}. \quad (4.23)$$

Furthermore, we use the following expressions to write the drift terms in Eq. (4.21) in polar coordinates,

$$\frac{\partial}{\partial A} [Ap(A, B, \mathcal{T})] + \frac{\partial}{\partial B} [Bp(A, B, \mathcal{T})] = \frac{1}{r} \frac{\partial}{\partial r} [r\tilde{p}(r, \theta, \mathcal{T})], \quad (4.24)$$

$$\frac{\partial}{\partial A} [Bp(A, B, \mathcal{T})] - \frac{\partial}{\partial B} [Ap(A, B, \mathcal{T})] = -\frac{1}{r} \frac{\partial}{\partial \theta} [\tilde{p}(r, \theta, \mathcal{T})], \quad (4.25)$$

$$\begin{aligned} \frac{\partial}{\partial A} \{ [A(A^2 + B^2)] p(A, B, \mathcal{T}) \} + \frac{\partial}{\partial B} \{ [B(A^2 + B^2)] p(A, B, \mathcal{T}) \} = \\ \frac{1}{r} \frac{\partial}{\partial r} [r^3 \tilde{p}(r, \theta, \mathcal{T})]. \end{aligned} \quad (4.26)$$

Use also the following identity,

$$\begin{aligned} \left(r^2 \frac{\partial^2}{\partial r^2} + 3r \frac{\partial}{\partial r} \right) \frac{\tilde{p}(r, \theta, \mathcal{T})}{r} = \\ \frac{1}{r} \left\{ \frac{\partial^2}{\partial r^2} [r^2 \tilde{p}(r, \theta, \mathcal{T})] - 3 \frac{\partial}{\partial r} [r \tilde{p}(r, \theta, \mathcal{T})] \right\}. \end{aligned} \quad (4.27)$$

The Fokker-Planck equation Eq. (4.21) in polar coordinates is then,

$$\begin{aligned} \frac{\partial}{\partial \mathcal{T}} \tilde{p}(r, \theta, \mathcal{T}) = & \frac{\tilde{\nu}}{\omega} \frac{\partial}{\partial \theta} \tilde{p}(r, \theta, \mathcal{T}) + \frac{3\tilde{D}}{2\omega^2} \frac{\partial^2}{\partial \theta^2} \tilde{p}(r, \theta, \mathcal{T}) \\ & - \frac{1}{\omega} \frac{\partial}{\partial r} \left[\left(\tilde{\mu}r - \frac{b\omega}{4} r^3 \right) \tilde{p}(r, \theta, \mathcal{T}) \right] \\ & + \frac{\tilde{D}}{2\omega^2} \left\{ \frac{\partial^2}{\partial r^2} [r^2 \tilde{p}(r, \theta, \mathcal{T})] - 3 \frac{\partial}{\partial r} [r \tilde{p}(r, \theta, \mathcal{T})] \right\}. \end{aligned} \quad (4.28)$$

The radial and angular components of the Fokker-Planck equation [Eq. (4.28)] are uncoupled. The stationary probability distribution function can then be

solved independently from each other. Let $\tilde{p}(r, \theta) = p_s(r)p_s(\theta)$. Then

$$0 = \frac{\tilde{\nu}}{\omega} p_s(\theta) + \frac{3\tilde{D}}{2\omega^2} \frac{\partial}{\partial \theta} p_s(\theta). \quad (4.29)$$

The stationary solution of the angular component is,

$$p_s(\theta) = \mathcal{N}_\theta e^{-\frac{2\omega}{3\tilde{D}} \tilde{\nu} \theta}, \quad (4.30)$$

where \mathcal{N}_θ is a normalization constant. Furthermore, the stationary probability density of the radial component satisfies,

$$0 = -\frac{1}{\omega} \left(\tilde{\mu} r - \frac{b\omega}{4} r^3 \right) p_s(r) + \frac{\tilde{D}}{2\omega^2} \left\{ \frac{\partial}{\partial r} [r^2 p_s(r)] - 3[r p_s(r)] \right\}, \quad (4.31)$$

leading to

$$p_s(r) = \mathcal{N}_r |r|^{\frac{2\omega\tilde{\mu}}{\tilde{D}} + 1} e^{-\frac{b\omega^2}{4\tilde{D}} r^2}, \quad (4.32)$$

where \mathcal{N}_r is a normalization constant. The probability distribution function is normalized so that

$$1 = \int_0^{2\pi} \int_0^\infty p(r, \theta) dr d\theta = \left[\int_0^{2\pi} p_s(\theta) d\theta \right] \left[\int_0^\infty p_s(r) dr \right], \quad (4.33)$$

and we choose to normalize both terms in square brackets of Eq. (4.33) to 1. The normalization constant of the stationary probability distribution function of the angular component is

$$\mathcal{N}_\theta = \left(\frac{\tilde{\nu}\omega}{3\tilde{D}} \right) \frac{e^{\frac{2\pi\tilde{\nu}\omega}{3\tilde{D}}}}{\sinh\left(\frac{2\pi\tilde{\nu}\omega}{3\tilde{D}}\right)}. \quad (4.34)$$

The stationary probability distribution function of the angular component, Eq. (4.30), has to be invariant under the exchange of A and B . Choosing

$A = r \sin(\theta)$ and $B = r \cos(\theta)$ only changes the sign of the left hand side of Eq. (4.25), yielding a stationary distribution function $p_s(\theta) = \mathcal{N} \exp(\mathcal{C}\theta)$, where $\mathcal{C} = 2\omega\tilde{\nu}/(3\tilde{D})$. Interchanging A and B thus changes the sign of the argument of the exponential, suggesting that the exponential solution is not an admissible solution (unless $\mathcal{C} = 0$). If $\tilde{D} \rightarrow 0$, the solution of Eq. (4.28) is $\lim_{\tilde{D} \rightarrow 0} p(\theta) = \delta(\theta + \omega t)$ [127]. For $\tilde{D} \neq 0$ the density approaches a stationary state in the long time limit. Therefore, one can take the limit $t \rightarrow \infty$ prior the limit $\tilde{D} \rightarrow 0$ to obtain $\lim_{\tilde{D} \rightarrow 0} \lim_{t \rightarrow \infty} p(\theta) = \lim_{\tilde{D} \rightarrow 0} p_s(\theta) = 1/(2\pi)$. Given that $p_s(\theta) = 1/(2\pi)$, Eq. (4.29) must also be satisfied. This leads to $\tilde{\nu} = 0$, our condition for the location of the bifurcation threshold.

Furthermore, the normalization constant of the stationary probability distribution function of the radial component is

$$\mathcal{N}_r = 2 \left(\frac{4\tilde{D}}{b\omega^2} \right)^{-\left(\frac{\alpha+1}{2}\right)} \Gamma^{-1} \left(\frac{\alpha+1}{2} \right), \quad (4.35)$$

where

$$\alpha = \frac{2\omega\tilde{\mu}}{\tilde{D}} + 1. \quad (4.36)$$

If $\alpha < -1$, the probability distribution function is not normalizable. We then define the location of the threshold at the point where the exponent of the power law of the stationary distribution function is -1. We obtain two conditions at threshold,

$$\beta\omega^2 + \chi\omega \sin(\omega\tau) + \omega^2\kappa \cos(\omega\tau) + D = 0, \quad (4.37)$$

$$\omega^2 - \omega_0^2 - \chi \cos(\omega\tau) + \omega\kappa \sin(\omega\tau) = 0. \quad (4.38)$$

These conditions can be further reduced by expanding Eqs. (4.37) and (4.38)

up to order τ . One obtains from Eq. (4.38) the Hopf frequency,

$$\omega = \sqrt{\frac{\omega_0^2 + \chi}{1 + \kappa\tau}}. \quad (4.39)$$

By using this result, the exponent of the power law of the stationary probability distribution function of the radial component is

$$\alpha = \frac{2}{D} \left(\frac{\omega_0^2 + \chi}{1 + \kappa\tau} \right) (\beta + \chi\tau + \kappa) + 1. \quad (4.40)$$

We define the location of the bifurcation threshold as $\alpha_c = -1$, or

$$(\omega_0^2 + \chi)(\beta + \chi\tau + \kappa) = -D(1 + \kappa\tau). \quad (4.41)$$

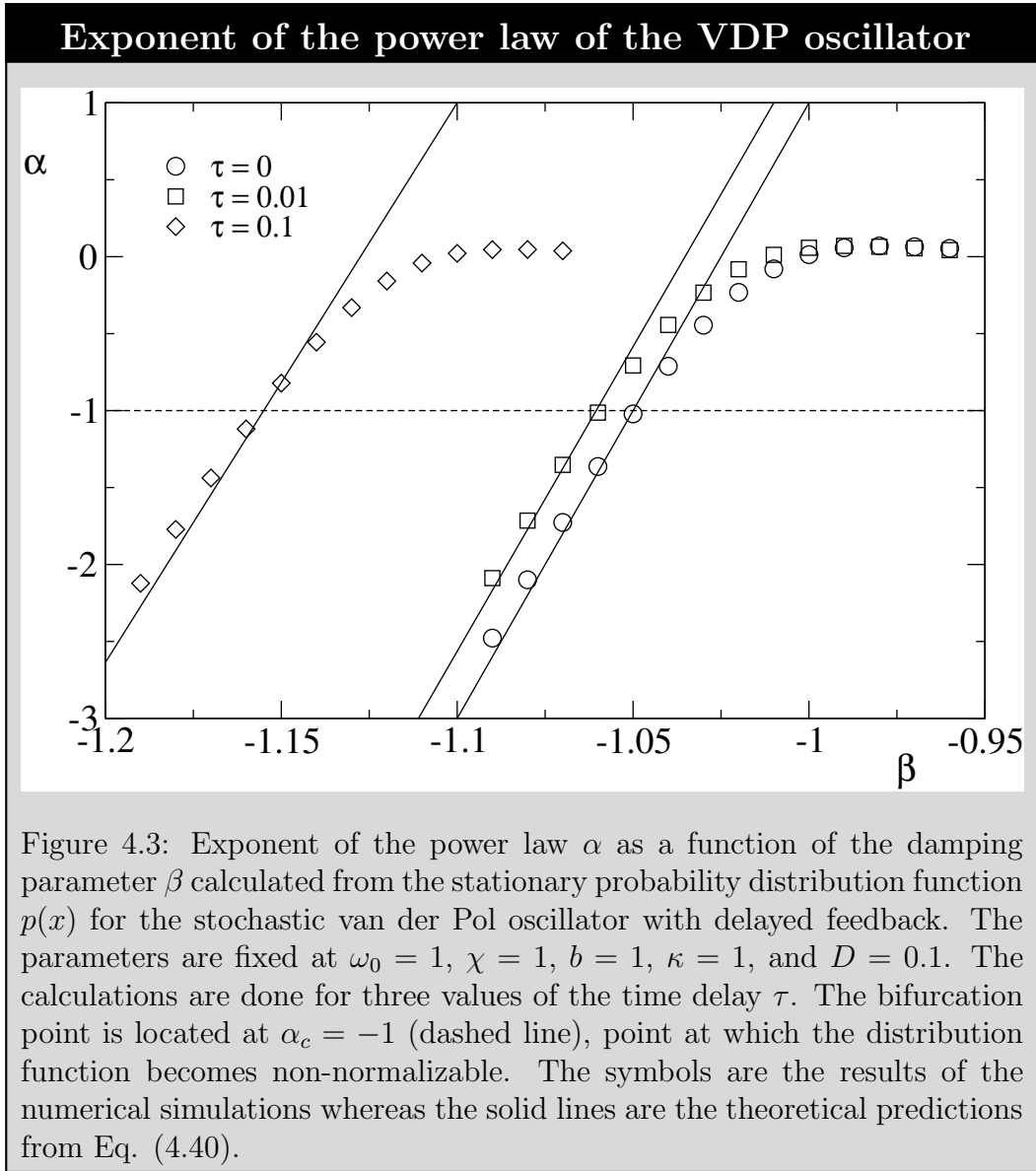
This is our central result. The bifurcation threshold Eq. (4.41) in the limit of no time delay, $\tau = 0$, is in agreement with Drolet [102] and Lücke [111]. However, it disagrees with Toral [119] by a numerical factor, and with earlier results of Knobloch and Wiesenfeld [126], and Seshadri, West, and Lindenberg [128].

Predictions of Eqs. (4.39), (4.40), and (4.41) have been verified numerically for $\tau > 0$. In order to do so, we have used a first order numerical method to integrate Eq. (4.1) [129]. Define $y(t) = \dot{x}(t)$. The algorithm with delay is

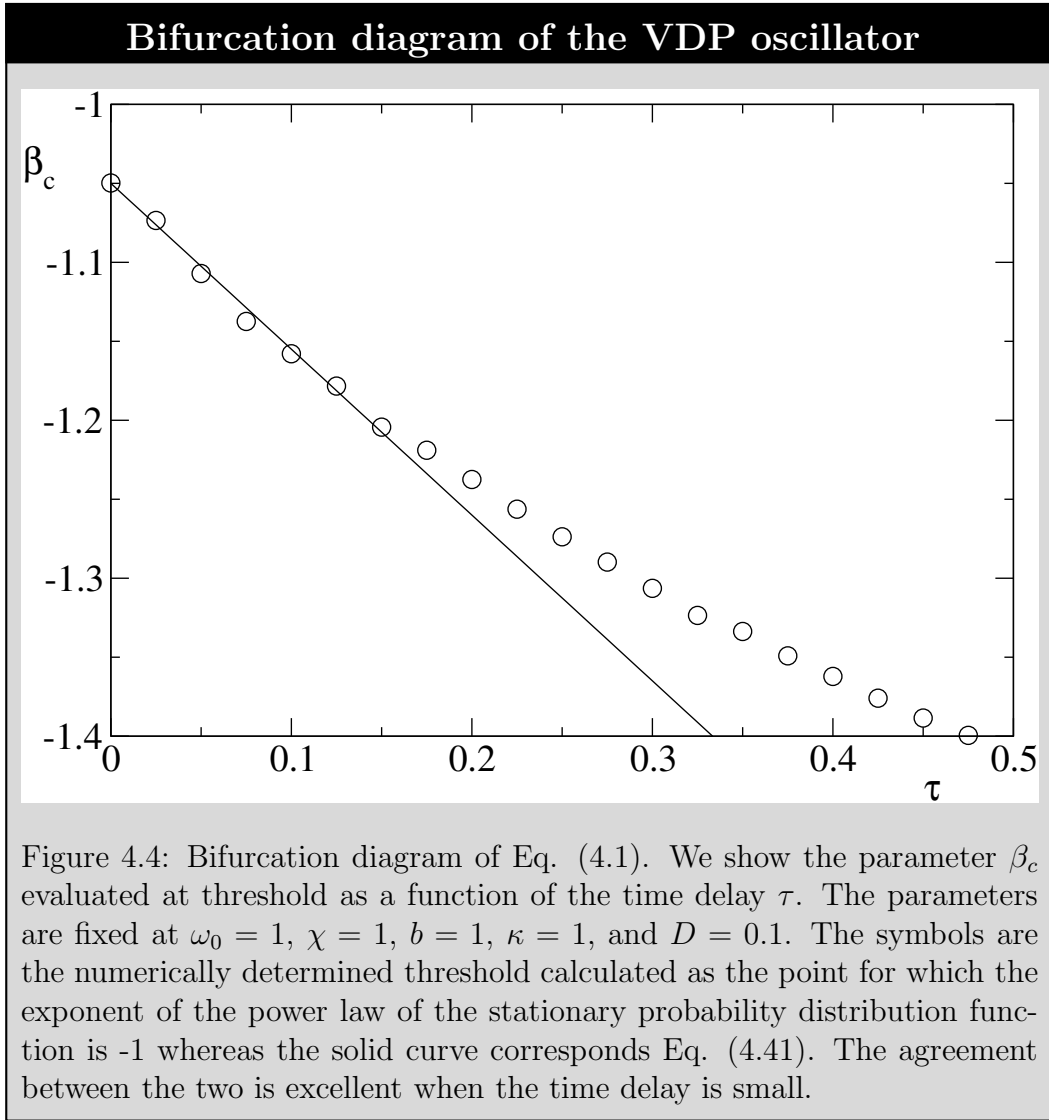
$$x(t + \Delta t) = x(t) + y(t)\Delta t, \quad (4.42)$$

$$y(t + \Delta t) = y(t) + [-\omega_0^2 x(t) - \chi x(t - \tau) + \beta y(t) + \kappa y(t - \tau) - bx^2(t)y(t)] \Delta t + x(t)\xi(t), \quad (4.43)$$

where $\xi(t) = \sqrt{2D\Delta t}\psi_1(t)$, where $\psi_1(t)$ is a random variable normally dis-

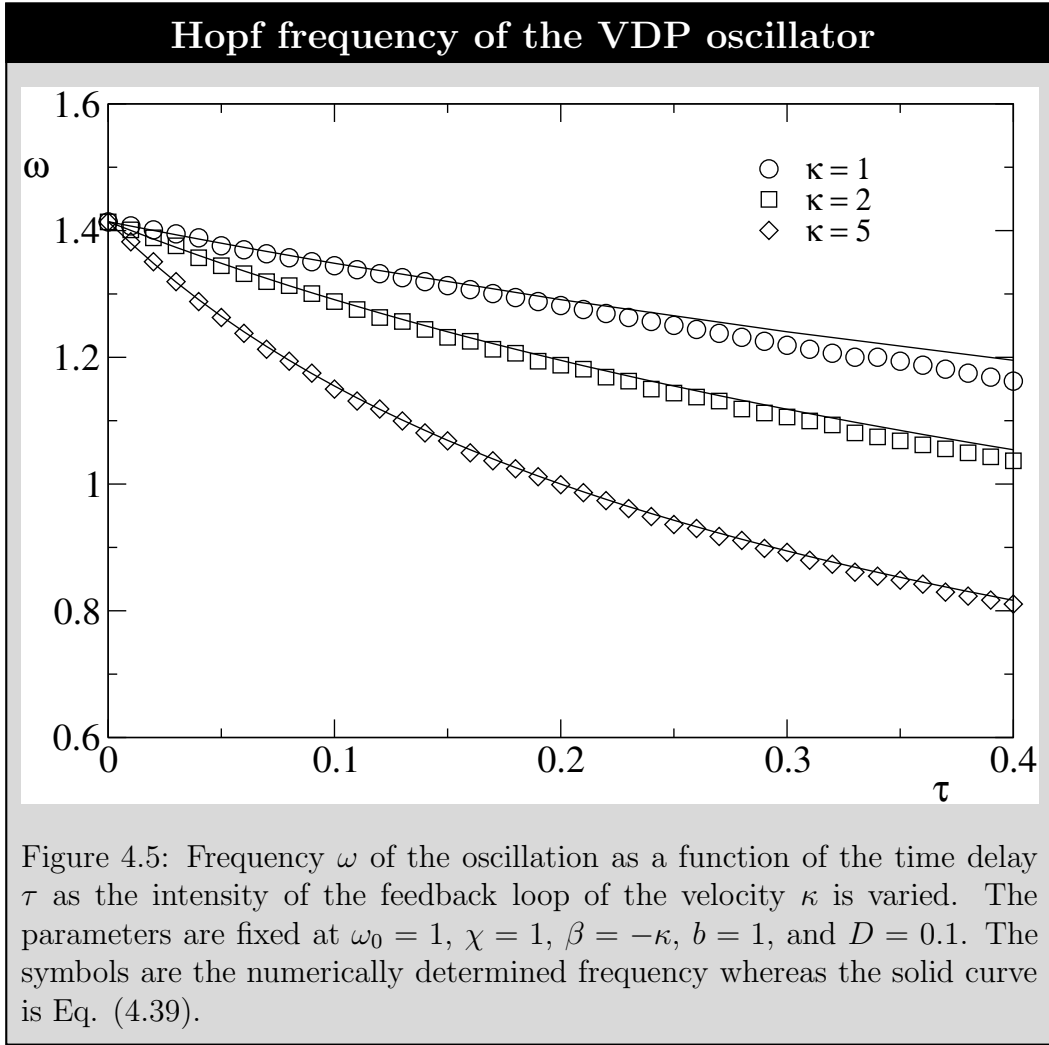


tributed with mean 0 and variance 1. The initial condition in $[-\tau, 0]$ is a constant drawn from a Gaussian distribution with mean 0 and variance 1. The equations are typically integrated up to $t_{max} = 500$, where the solution is believed to have reached a stationary state, by using an integration step of $\Delta t = 0.001$. The stationary probability density $p(x)$ of the position x of the oscillator is then constructed in the time interval $[t_{max} - 10, t_{max}]$. The overall process is repeated in order to generate an ensemble average of 10^6 indepen-



dent trajectories. A phase portrait showing the velocity y and the position x of the deterministic delayed oscillator is shown in Fig. 4.1 for different values of the damping parameter β .

Our results for the stationary probability density are shown in Fig. 4.2. Below the bifurcation threshold ($\beta < \beta_c$), the stationary distribution is given by $p(x) = \delta(x)$. As expected ([130]), we observe instead a very long transient with $p(x)$ approximately a power law distribution with an apparent exponent $\alpha < -1$ at small x . This is a non-normalizable distribution and hence unphysical. It only appears as a long-lived transient. The probability amplitude at



$x = 0$ (not shown in the figure) grows with time, signalling the build up of a delta function distribution. Because of normalization, the growth at $x = 0$ implies a decaying amplitude for $x > 0$ as shown in the figure. For $\beta > \beta_c$, we do obtain a time-independent power law distribution function with exponent $-1 < \alpha < 0$. This probability distribution function is normalizable and is the stationary distribution above threshold. We finally show $p(x)$ in the range of β values where it is bimodal.

The exponent α is estimated in the interval $x = \{0.01, 0.1\}$. Figure 4.3 shows the value of the exponent α obtained from a power law fit to $p(x)$ as a function of β . Predictions from Eq. (4.40) are also included for comparison.

We observe a smooth variation of α with β , allowing a convenient determination of β_c , the value for which $\alpha = -1$. That method was used to determine the threshold results shown in Fig. 4.4. For sufficiently small values of the time delay τ ($\tau < 0.15$ for the set of parameters shown in the figure), the numerical results are found to be in excellent agreement with predictions from Eq. (4.41).

Finally, we have numerically computed the Hopf frequency close to the bifurcation threshold of the oscillator. The Hopf frequency corresponds to the frequency at which the amplitude of the Fourier transform of the trajectories is maximum. Our numerical results are shown in Fig. 4.5 as a function of the time delay, and compared to the analytic result Eq. (4.39). Once again, excellent agreement between the two sets of data is found provided the time delay is sufficiently small.

4.2 Multiple time scale expansion of a SDDE

Multiple time scale expansion of the solution is then applied to the deterministic ($K = D = 0$) counterpart of Eq. (1.10),

$$\dot{x}(t) = ax(t) + bx(t - \tau) - x^3(t) , \quad (4.44)$$

where $\gamma = 1$. In order to separate the time scales of Eq. (4.44), we assume a solution of the form,

$$x(t, \mathcal{T}) = \epsilon A(\mathcal{T}) \cos(\omega t) + \epsilon B(\mathcal{T}) \sin(\omega t) , \quad (4.45)$$

where $A(\mathcal{T})$ and $B(\mathcal{T})$ are the envelopes of the oscillation evolving over the slow time scale $\mathcal{T} = \epsilon^2 t$ as compared to the fast time scale t of the oscillations,

where $0 < \epsilon \ll 1$ is small and is called the scaling parameter, and where ω is the frequency of the fast oscillations. Note that the envelope variable $A(\mathcal{T})$ and $B(\mathcal{T})$ are assumed to scale according to $\mathcal{O}(\epsilon)$ close to the bifurcation. We assume that some linear combinations of the parameters of the model are small close to threshold and will be scaled accordingly in the expansion. Substitute Eq. (4.45) into Eq. (4.44),

$$\begin{aligned}
& \epsilon^3 \partial_{\mathcal{T}} A(\mathcal{T}) \cos(\omega t) + \epsilon^3 \partial_{\mathcal{T}} B(\mathcal{T}) \sin(\omega t) = \\
& \quad \omega [\epsilon A(\mathcal{T}) \sin(\omega t) - \epsilon B(\mathcal{T}) \cos(\omega t)] \\
& \quad + a [\epsilon A(\mathcal{T}) \cos(\omega t) + \epsilon B(\mathcal{T}) \sin(\omega t)] \\
& \quad + b [\epsilon A(\mathcal{T} - \epsilon^2 \tau) \cos[\omega(t - \tau)] + \epsilon B(\mathcal{T} - \epsilon^2 \tau) \sin[\omega(t - \tau)]] \\
& \quad - [\epsilon A(\mathcal{T}) \cos(\omega t) + \epsilon B(\mathcal{T}) \sin(\omega t)]^3 .
\end{aligned} \tag{4.46}$$

We have thus used the relation $\partial_t \rightarrow \partial_t + \epsilon^2 \partial_{\mathcal{T}}$ to write Eq. (4.46) as before. Since the scaling parameter ϵ is small, we approximate $A(\mathcal{T} - \epsilon^2 \tau) \approx A(\mathcal{T})$ and $B(\mathcal{T} - \epsilon^2 \tau) \approx B(\mathcal{T})$. In those terms and after few steps of algebra, rewrite Eq. (4.46) as,

$$\begin{aligned}
& \epsilon^3 \partial_{\mathcal{T}} A(\mathcal{T}) \cos(\omega t) + \epsilon^3 \partial_{\mathcal{T}} B(\mathcal{T}) \sin(\omega t) = \\
& \quad \cos(\omega t) [-\epsilon \omega B(\mathcal{T}) + \epsilon a A(\mathcal{T}) + \epsilon b \cos(\omega \tau) A(\mathcal{T}) - \epsilon b \sin(\omega \tau) B(\mathcal{T}) \\
& \quad \quad - \epsilon^3 A^3(\mathcal{T}) \cos^2(\omega t) - 3\epsilon^3 A(\mathcal{T}) B^2(\mathcal{T}) \sin^2(\omega t)] \\
& \quad + \sin(\omega t) [\epsilon \omega A(\mathcal{T}) + \epsilon a B(\mathcal{T}) + \epsilon b \sin(\omega \tau) A(\mathcal{T}) + \epsilon b \cos(\omega \tau) B(\mathcal{T}) \\
& \quad \quad - \epsilon^3 B^3(\mathcal{T}) \sin^2(\omega t) - 3\epsilon^3 A^2(\mathcal{T}) B(\mathcal{T}) \cos^2(\omega t)] .
\end{aligned} \tag{4.47}$$

We next eliminate the dependence on the fast scale t . In order to do so, we use the orthogonality of the trigonometric functions. Multiply both sides of Eq. (4.47) by $(\omega/2\pi) \int_0^{2\pi/\omega} dt \cos(\omega t)$, where $2\pi/\omega$ is a period of the oscillation,

and perform the integration. Repeat the operation but multiply instead both sides by $(\omega/2\pi) \int_0^{\frac{2\pi}{\omega}} dt \sin(\omega t)$ and perform again the integration. We obtain two coupled deterministic differential equations,

$$\partial_{\mathcal{T}} A(\mathcal{T}) = \tilde{\mu} A(\mathcal{T}) - \tilde{\nu} B(\mathcal{T}) - \frac{3}{4} A(\mathcal{T}) [A^2(\mathcal{T}) + B^2(\mathcal{T})] , \quad (4.48)$$

$$\partial_{\mathcal{T}} B(\mathcal{T}) = \tilde{\nu} A(\mathcal{T}) + \tilde{\mu} B(\mathcal{T}) - \frac{3}{4} B(\mathcal{T}) [A^2(\mathcal{T}) + B^2(\mathcal{T})] , \quad (4.49)$$

where we have defined $\mu = a + b \cos(\omega\tau)$ and $\nu = \omega + b \sin(\omega\tau)$ for simplicity. These parameters have units of frequency. Assume furthermore that these parameters scale as $\mu = \epsilon^2 \tilde{\mu}$ and $\nu = \epsilon^2 \tilde{\nu}$ close to the bifurcation. Equations (4.48) and (4.49) can also be written in matrix form,

$$\frac{d}{d\mathcal{T}} \begin{bmatrix} A \\ B \end{bmatrix} = \begin{bmatrix} \tilde{\mu} & -\tilde{\nu} \\ \tilde{\nu} & \tilde{\mu} \end{bmatrix} \begin{bmatrix} A \\ B \end{bmatrix} - \frac{3}{4} \begin{bmatrix} A(A^2 + B^2) \\ B(A^2 + B^2) \end{bmatrix} . \quad (4.50)$$

The location of the bifurcation threshold is found in polar coordinates. Let $A = r \cos(\theta)$ and $B = r \sin(\theta)$. Under those variables, Eqs. (4.48) and (4.49) are

$$\dot{r}(\mathcal{T}) = \tilde{\mu} r(\mathcal{T}) - \frac{3}{4} r^3(\mathcal{T}) , \quad (4.51)$$

$$\dot{\theta}(\mathcal{T}) = \tilde{\nu} . \quad (4.52)$$

The bifurcation threshold is located at $\tilde{\nu}_c = 0$, the fixed point of Eq. (4.52), and at $\tilde{\mu}_c = 0$, point separating to two branches of the pitchfork bifurcation

of the radial component. Hence

$$a + b \cos(\omega\tau) = 0, \quad (4.53)$$

$$\omega + b \sin(\omega\tau) = 0. \quad (4.54)$$

Substitute further Eq. (4.53) into Eq. (4.54). It predicts that the Hopf frequency is

$$\omega = \sqrt{b^2 - a^2}. \quad (4.55)$$

Moreover, it predicts that the location of the Hopf bifurcation is

$$-\frac{a_c}{b} = \cos\left(\tau\sqrt{b^2 - a_c^2}\right). \quad (4.56)$$

This expression is identical to Eq. (3.6) predicting the location of the Hopf bifurcation of the deterministic linear counterpart of Eq. (1.10).

We next apply the method to the stochastic counterpart of Eq. (4.44). Consider first the case for which the noise enters additively. Assume again that there are two relevant time scales in the system and substitute Eq. (4.45) into the differential equation. Moreover, split the Gaussian white noise $\eta(t)$ into two independent white noises $\eta_A(t)$ and $\eta_B(t)$ with mean $\langle\eta_A(t)\rangle = \langle\eta_B(t)\rangle = 0$ and correlation $\langle\eta_A(t)\eta_A(t')\rangle = \langle\eta_B(t)\eta_B(t')\rangle = 2K\delta(t - t')$ so that

$$\eta(t) = \cos(\omega t)\eta_A(t) + \sin(\omega t)\eta_B(t). \quad (4.57)$$

The time evolution of the envelope variable $A(\mathcal{T})$ and $B(\mathcal{T})$ is then,

$$\begin{aligned}
& \epsilon^3 \partial_{\mathcal{T}} A(\mathcal{T}) \cos(\omega t) + \epsilon^3 \partial_{\mathcal{T}} B(\mathcal{T}) \sin(\omega t) = \\
& \quad \omega [\epsilon A(\mathcal{T}) \sin(\omega t) - \epsilon B(\mathcal{T}) \cos(\omega t)] \\
& \quad + a [\epsilon A(\mathcal{T}) \cos(\omega t) + \epsilon B(\mathcal{T}) \sin(\omega t)] \\
& \quad + b [\epsilon A(\mathcal{T} - \epsilon^2 \tau) \cos[\omega(t - \tau)] + \epsilon B(\mathcal{T} - \epsilon^2 \tau) \sin[\omega(t - \tau)]] \\
& \quad - [\epsilon A(\mathcal{T}) \cos(\omega t) + \epsilon B(\mathcal{T}) \sin(\omega t)]^3 \\
& \quad + \cos(\omega t) \eta_A(t) + \sin(\omega t) \eta_B(t) .
\end{aligned} \tag{4.58}$$

We again approximate $A(\mathcal{T} - \epsilon^2 \tau) \approx A(\mathcal{T})$ and $B(\mathcal{T} - \epsilon^2 \tau) \approx B(\mathcal{T})$. In those terms and after few steps of algebra, rewrite Eq. (4.58) as

$$\begin{aligned}
& \epsilon^3 \partial_{\mathcal{T}} A(\mathcal{T}) \cos(\omega t) + \epsilon^3 \partial_{\mathcal{T}} B(\mathcal{T}) \sin(\omega t) = \\
& \quad \cos(\omega t) [-\epsilon \omega B(\mathcal{T}) + \epsilon a A(\mathcal{T}) + \epsilon b \cos(\omega \tau) A(\mathcal{T}) - \epsilon b \sin(\omega \tau) B(\mathcal{T}) \\
& \quad \quad - \epsilon^3 A^3(\mathcal{T}) \cos^2(\omega t) - 3\epsilon^3 A(\mathcal{T}) B^2(\mathcal{T}) \sin^2(\omega t) + \eta_A(t)] \\
& \quad + \sin(\omega t) [\epsilon \omega A(\mathcal{T}) + \epsilon a B(\mathcal{T}) + \epsilon b \sin(\omega \tau) A(\mathcal{T}) + \epsilon b \cos(\omega \tau) B(\mathcal{T}) \\
& \quad \quad - \epsilon^3 B^3(\mathcal{T}) \sin^2(\omega t) - 3\epsilon^3 A^2(\mathcal{T}) B(\mathcal{T}) \cos^2(\omega t) + \eta_B(t)] .
\end{aligned} \tag{4.59}$$

We next eliminate the dependence on the fast scale t . Multiply both sides of the resulting equation by $L^{-1} \int_0^L dt \cos(\omega t)$, where $L = 2\pi/\omega$, and perform the integration. Repeat the same procedure but with $L^{-1} \int_0^L dt \sin(\omega t)$. We then have two coupled differential equations describing the time evolution of

the envelope variables of the oscillation,

$$\begin{aligned}
\epsilon^3 \partial_{\mathcal{T}} A(\mathcal{T}) &= \epsilon \mu A(\mathcal{T}) - \epsilon \nu B(\mathcal{T}) - \frac{3}{4} \epsilon^3 A(\mathcal{T}) [A^2(\mathcal{T}) + B^2(\mathcal{T})] \\
&\quad + \epsilon \eta_A(\mathcal{T}) , \\
\epsilon^3 \partial_{\mathcal{T}} B(\mathcal{T}) &= \epsilon \nu A(\mathcal{T}) + \epsilon \mu B(\mathcal{T}) - \frac{3}{4} \epsilon^3 B(\mathcal{T}) [A^2(\mathcal{T}) + B^2(\mathcal{T})] \\
&\quad + \epsilon \eta_B(\mathcal{T}) ,
\end{aligned} \tag{4.60}$$

where we have defined again $\mu = a + b \cos(\omega\tau)$ and $\nu = \omega + b \sin(\omega\tau)$. We have also used the relation $\mathcal{T} = \epsilon^2 t$ to define the noises over the slow time scale $\eta_A(t) = \epsilon \eta_A(\mathcal{T})$ and $\eta_B(t) = \epsilon \eta_B(\mathcal{T})$. The Fokker-Planck equation associated with Eq. (4.60) is found by using Eq. (4.20),

$$\begin{aligned}
\frac{\partial}{\partial \mathcal{T}} p(A, B, \mathcal{T}) &= - \frac{\partial}{\partial A} \left\{ \left[\tilde{\mu} A - \tilde{\nu} B - \frac{3}{4} A(A^2 + B^2) \right] p(A, B, \mathcal{T}) \right\} \\
&\quad - \frac{\partial}{\partial B} \left\{ \left[\tilde{\nu} A + \tilde{\mu} B - \frac{3}{4} B(A^2 + B^2) \right] p(A, B, \mathcal{T}) \right\} \\
&\quad + \tilde{K} \left\{ \frac{\partial^2}{\partial A^2} + \frac{\partial^2}{\partial B^2} \right\} p(A, B, \mathcal{T}) ,
\end{aligned} \tag{4.61}$$

where we have scaled the parameters so that $\tilde{\mu} = \epsilon^{-2} \mu$, $\tilde{\nu} = \epsilon^{-2} \nu$, and $\tilde{K} = \epsilon^{-4} K$. We again try to write the Fokker-Planck equation in polar coordinates. Set $A = r \cos(\theta)$ and $B = r \sin(\theta)$. The drift terms of Eq. (4.61) are,

$$\frac{1}{r} \frac{\partial}{\partial \mathcal{T}} \tilde{p}(r, \theta, \mathcal{T}) \sim - \frac{1}{r} \frac{\partial}{\partial r} \left[\left(\tilde{\mu} r - \frac{3}{4} r^3 \right) \tilde{p}(r, \theta, \mathcal{T}) \right] - \frac{1}{r} \frac{\partial}{\partial \theta} [\tilde{\nu} \tilde{p}(r, \theta, \mathcal{T})] . \tag{4.62}$$

Furthermore, the diffusion coefficient transforms as,

$$\left\{ \frac{\partial^2}{\partial A^2} + \frac{\partial^2}{\partial B^2} \right\} p(A, B, \mathcal{T}) = \left\{ \frac{\partial^2}{\partial r^2} + \frac{1}{r} \frac{\partial}{\partial r} + \frac{1}{r^2} \frac{\partial^2}{\partial \theta^2} \right\} \frac{\tilde{p}(r, \theta, \mathcal{T})}{r} . \tag{4.63}$$

Combine Eq. (4.62) and Eq. (4.63) so that the Fokker-Planck equation is,

$$\begin{aligned} \frac{\partial}{\partial \mathcal{T}} \tilde{p}(r, \theta, \mathcal{T}) = & - \frac{\partial}{\partial r} \left\{ \left[\tilde{\mu} r - \frac{3}{4} r^3 \right] \tilde{p}(r, \theta, \mathcal{T}) \right\} \\ & - \tilde{K} \frac{\partial}{\partial r} \left[\frac{1}{r} \tilde{p}(r, \theta, \mathcal{T}) \right] + \tilde{K} \frac{\partial^2}{\partial r^2} \tilde{p}(r, \theta, \mathcal{T}) \\ & - \frac{\partial}{\partial \theta} [\tilde{\nu} \tilde{p}(r, \theta, \mathcal{T})] + \tilde{K} \frac{1}{r^2} \frac{\partial^2}{\partial \theta^2} \tilde{p}(r, \theta, \mathcal{T}) . \end{aligned} \quad (4.64)$$

The radial and angular dependencies do not separate because of the presence of the radial variable in the last term of Eq. (4.64). Furthermore, the drift and the diffusion coefficients of Eq. (4.64) do not scale the same in the same way with ϵ . Since $\tilde{\mu} = \epsilon^{-2}\mu$, $\tilde{\nu} = \epsilon^{-2}\nu$, and $\tilde{K} = \epsilon^{-4}K$, the drift terms dominate as $\epsilon \rightarrow 0$, i.e. close to threshold. In this limit, we can ignore the diffusive terms of Eq. (4.64). The resulting equations are then identical to the deterministic limit. This result is in agreement with the location of the bifurcation threshold of the first moment derived in [44].

We consider next the model defined in Eq. (1.10) with multiplicative noise only ($K = 0$). Substitute Eq. (4.45) in Eq. (1.10),

$$\begin{aligned} \epsilon^3 \partial_{\mathcal{T}} A(\mathcal{T}) \cos(\omega t) + \epsilon^3 \partial_{\mathcal{T}} B(\mathcal{T}) \sin(\omega t) = \\ \omega [\epsilon A(\mathcal{T}) \sin(\omega t) - \epsilon B(\mathcal{T}) \cos(\omega t)] \\ + a [\epsilon A(\mathcal{T}) \cos(\omega t) + \epsilon B(\mathcal{T}) \sin(\omega t)] \\ + b [\epsilon A(\mathcal{T} - \epsilon^2 \tau) \cos[\omega(t - \tau)] + \epsilon B(\mathcal{T} - \epsilon^2 \tau) \sin[\omega(t - \tau)]] \\ - [\epsilon A(\mathcal{T}) \cos(\omega t) + \epsilon B(\mathcal{T}) \sin(\omega t)]^3 \\ + [\epsilon A(\mathcal{T}) \cos(\omega t) + \epsilon B(\mathcal{T}) \sin(\omega t)] \xi(t) . \end{aligned} \quad (4.65)$$

where we have used the relation $\partial_t \rightarrow \partial_t + \epsilon^2 \partial_{\mathcal{T}}$ in Eq. (4.65) as before. We further approximate $A(\mathcal{T} - \epsilon^2 \tau) \approx A(\mathcal{T})$ and $B(\mathcal{T} - \epsilon^2 \tau) \approx B(\mathcal{T})$ since the

scaling parameter ϵ is small to rewrite Eq. (4.65) as,

$$\begin{aligned}
& \epsilon^3 \partial_{\mathcal{T}} A(\mathcal{T}) \cos(\omega t) + \epsilon^3 \partial_{\mathcal{T}} B(\mathcal{T}) \sin(\omega t) = \\
& \cos(\omega t) [-\epsilon \omega B(\mathcal{T}) + \epsilon a A(\mathcal{T}) + \epsilon b \cos(\omega \tau) A(\mathcal{T}) - \epsilon b \sin(\omega \tau) B(\mathcal{T}) \\
& \quad - \epsilon^3 A^3(\mathcal{T}) \cos^2(\omega t) - 3\epsilon^3 A(\mathcal{T}) B^2(\mathcal{T}) \sin^2(\omega t) + \epsilon A(\mathcal{T}) \xi(t)] \quad (4.66) \\
& + \sin(\omega t) [\epsilon \omega A(\mathcal{T}) + \epsilon a B(\mathcal{T}) + \epsilon b \sin(\omega \tau) A(\mathcal{T}) + \epsilon b \cos(\omega \tau) B(\mathcal{T}) \\
& \quad - \epsilon^3 B^3(\mathcal{T}) \sin^2(\omega t) - 3\epsilon^3 A^2(\mathcal{T}) B(\mathcal{T}) \cos^2(\omega t) + \epsilon B(\mathcal{T}) \xi(t)].
\end{aligned}$$

We next eliminate the dependence on the fast scale t in the same way than we did for the deterministic equation. Multiply both sides of Eq. (4.66) by $(\omega/2\pi) \int_0^{2\pi/\omega} dt \cos(\omega t)$ and perform the integration. Repeat the operation but multiply instead by $(\omega/2\pi) \int_0^{2\pi/\omega} dt \sin(\omega t)$ and perform the integration. We thus obtain two coupled stochastic differential equations,

$$\begin{aligned}
\epsilon^3 \partial_{\mathcal{T}} A(\mathcal{T}) &= \epsilon \mu A(\mathcal{T}) - \epsilon \nu B(\mathcal{T}) - \frac{3}{4} \epsilon^3 A(\mathcal{T}) [A^2(\mathcal{T}) + B^2(\mathcal{T})] \\
&+ \epsilon A(\mathcal{T}) \frac{\omega}{2\pi} \int_0^{2\pi/\omega} \xi(t) dt + \epsilon A(\mathcal{T}) \frac{\omega}{2\pi} \int_0^{2\pi/\omega} \cos(2\omega t) \xi(t) dt \\
&+ \epsilon B(\mathcal{T}) \frac{\omega}{2\pi} \int_0^{2\pi/\omega} \sin(2\omega t) \xi(t) dt, \\
\epsilon^3 \partial_{\mathcal{T}} B(\mathcal{T}) &= \epsilon \nu A(\mathcal{T}) + \epsilon \mu B(\mathcal{T}) - \frac{3}{4} \epsilon^3 B(\mathcal{T}) [A^2(\mathcal{T}) + B^2(\mathcal{T})] \\
&+ \epsilon B(\mathcal{T}) \frac{\omega}{2\pi} \int_0^{2\pi/\omega} \xi(t) dt - \epsilon B(\mathcal{T}) \frac{\omega}{2\pi} \int_0^{2\pi/\omega} \cos(2\omega t) \xi(t) dt \\
&+ \epsilon A(\mathcal{T}) \frac{\omega}{2\pi} \int_0^{2\pi/\omega} \sin(2\omega t) \xi(t) dt,
\end{aligned} \tag{4.67}$$

where we have defined $\mu = a + b \cos(\omega \tau)$ and $\nu = \omega + b \sin(\omega \tau)$ for simplicity.

We assume furthermore that these parameters scale as $\mu = \epsilon^2 \tilde{\mu}$ and $\nu = \epsilon^2 \tilde{\nu}$ close to the bifurcation. We next define the stochasticity over the slow time

scale. One can take the advantage of the relation $\mathcal{T} = \epsilon^2 t$ to write

$$\xi(t) = \epsilon \xi_0(\mathcal{T}) , \quad (4.68)$$

where $\xi_0(\mathcal{T})$ is a Gaussian random variable with mean $\langle \xi_0(\mathcal{T}) \rangle = 0$ and correlation $\langle \xi_0(\mathcal{T}) \xi_0(\mathcal{T}') \rangle = 2D\delta(\mathcal{T} - \mathcal{T}')$. We exploit the same idea to define $\cos(2\omega t)\xi(t)$ and $\sin(2\omega t)\xi(t)$ over the slow time scale \mathcal{T} . In order to do so, consider their correlations,

$$\langle \cos(2\omega t)\xi(t) \cos(2\omega t')\xi(t') \rangle = \epsilon^2 \langle \cos^2(2\omega t) \rangle \langle \xi_1(\mathcal{T}) \xi_1(\mathcal{T}') \rangle , \quad (4.69)$$

$$\langle \sin(2\omega t)\xi(t) \sin(2\omega t')\xi(t') \rangle = \epsilon^2 \langle \sin^2(2\omega t) \rangle \langle \xi_2(\mathcal{T}) \xi_2(\mathcal{T}') \rangle , \quad (4.70)$$

where $\xi_1(\mathcal{T})$ and $\xi_2(\mathcal{T})$ are independent Gaussian white noise with mean $\langle \xi_j(\mathcal{T}) \rangle = 0$ and correlation $\langle \xi_j(\mathcal{T}) \xi_k(\mathcal{T}') \rangle = 2D\delta(\mathcal{T} - \mathcal{T}')$ if $j = k$ and zero otherwise with $(j, k) = \{1, 2\}$. We then replace the squared trigonometric function by their averages over a period, $\langle \cos^2(2\omega t) \rangle = \langle \sin^2(2\omega t) \rangle = 1/2$. We thus define over the slow time scale,

$$\cos(2\omega t)\xi(t) \rightarrow \frac{\epsilon}{\sqrt{2}} \xi_1(\mathcal{T}) , \quad (4.71)$$

$$\sin(2\omega t)\xi(t) \rightarrow \frac{\epsilon}{\sqrt{2}} \xi_2(\mathcal{T}) . \quad (4.72)$$

We then have two coupled stochastic differential equations in the slow time

scale,

$$\begin{aligned}
\epsilon^3 \partial_{\mathcal{T}} A(\mathcal{T}) &= \epsilon \mu A(\mathcal{T}) - \epsilon \nu B(\mathcal{T}) - \frac{3}{4} \epsilon^3 A(\mathcal{T}) [A^2(\mathcal{T}) + B^2(\mathcal{T})] \\
&\quad + \epsilon^2 A(\mathcal{T}) \xi_0(\mathcal{T}) + \frac{\epsilon^2}{\sqrt{2}} A(\mathcal{T}) \xi_1(\mathcal{T}) + \frac{\epsilon^2}{\sqrt{2}} B(\mathcal{T}) \xi_2(\mathcal{T}), \\
\epsilon^3 \partial_{\mathcal{T}} B(\mathcal{T}) &= \epsilon \nu A(\mathcal{T}) + \epsilon \mu B(\mathcal{T}) - \frac{3}{4} \epsilon^3 B(\mathcal{T}) [A^2(\mathcal{T}) + B^2(\mathcal{T})] \\
&\quad + \epsilon^2 B(\mathcal{T}) \xi_0(\mathcal{T}) - \frac{\epsilon^2}{\sqrt{2}} B(\mathcal{T}) \xi_1(\mathcal{T}) + \frac{\epsilon^2}{\sqrt{2}} A(\mathcal{T}) \xi_2(\mathcal{T}).
\end{aligned} \tag{4.73}$$

The system of equations (4.73) can then be written in matrix form,

$$\begin{aligned}
\frac{d}{d\mathcal{T}} \begin{bmatrix} A \\ B \end{bmatrix} &= \begin{bmatrix} \tilde{\mu} & -\tilde{\nu} \\ \tilde{\nu} & \tilde{\mu} \end{bmatrix} \begin{bmatrix} A \\ B \end{bmatrix} - \frac{3}{4} \begin{bmatrix} A(A^2 + B^2) \\ B(A^2 + B^2) \end{bmatrix} \\
&\quad + \frac{1}{\epsilon} \begin{bmatrix} 1 & 0 \\ 0 & 1 \end{bmatrix} \begin{bmatrix} A \\ B \end{bmatrix} \xi_0(\mathcal{T}) + \frac{1}{\epsilon \sqrt{2}} \begin{bmatrix} 1 & 0 \\ 0 & -1 \end{bmatrix} \begin{bmatrix} A \\ B \end{bmatrix} \xi_1(\mathcal{T}) \\
&\quad + \frac{1}{\epsilon \sqrt{2}} \begin{bmatrix} 0 & 1 \\ 1 & 0 \end{bmatrix} \begin{bmatrix} A \\ B \end{bmatrix} \xi_2(\mathcal{T}).
\end{aligned} \tag{4.74}$$

We can then write the Fokker-Planck equation associated with Eq. (4.74) by

using Eq. (4.20),

$$\begin{aligned}
\frac{\partial}{\partial \mathcal{T}} p(A, B, \mathcal{T}) = & -\frac{\partial}{\partial A} \left\{ \left[\tilde{\mu}A - \tilde{\nu}B - \frac{3}{4}A(A^2 + B^2) \right] p(A, B, \mathcal{T}) \right\} \\
& -\frac{\partial}{\partial B} \left\{ \left[\tilde{\nu}A + \tilde{\mu}B - \frac{3}{4}B(A^2 + B^2) \right] p(A, B, \mathcal{T}) \right\} \\
& + \frac{D}{\epsilon^2} \left\{ A^2 \frac{\partial^2}{\partial A^2} + 2AB \frac{\partial^2}{\partial A \partial B} + B^2 \frac{\partial^2}{\partial B^2} \right. \\
& \quad \left. + 5 \left(A \frac{\partial}{\partial A} + B \frac{\partial}{\partial B} \right) + 4 \right\} p(A, B, \mathcal{T}) \\
& + \frac{D}{2\epsilon^2} \left\{ A^2 \frac{\partial^2}{\partial A^2} - 2AB \frac{\partial^2}{\partial A \partial B} + B^2 \frac{\partial^2}{\partial B^2} \right. \\
& \quad \left. + \left(A \frac{\partial}{\partial A} + B \frac{\partial}{\partial B} \right) \right\} p(A, B, \mathcal{T}) \\
& + \frac{D}{2\epsilon^2} \left\{ B^2 \frac{\partial^2}{\partial A^2} + 2AB \frac{\partial^2}{\partial A \partial B} + A^2 \frac{\partial^2}{\partial B^2} \right. \\
& \quad \left. + \left(A \frac{\partial}{\partial A} + B \frac{\partial}{\partial B} \right) \right\} p(A, B, \mathcal{T}) .
\end{aligned} \tag{4.75}$$

The intensity of the noise scales as $D = \epsilon^2 \tilde{D}$, and all terms of Eq. (4.75) are of the same order in ϵ . In order to find the stationary solution of this Fokker-Planck equation, we introduce polar coordinates. Let $A = r \cos(\theta)$ and $B = r \sin(\theta)$. Under this change of variables, the probability distribution function transforms as $\tilde{p}(r, \theta, \mathcal{T}) = rp(A, B, \mathcal{T})$, where r is the Jacobian of the transformation. On the one hand, the drift coefficients of Eq. (4.75) are identical to Eq. (4.62). On the other hand, terms in brackets proportional to \tilde{D} in Eq. (4.75) transform as,

$$\begin{aligned}
& \left\{ A^2 \frac{\partial^2}{\partial A^2} + 2AB \frac{\partial^2}{\partial A \partial B} + B^2 \frac{\partial^2}{\partial B^2} + 5 \left(A \frac{\partial}{\partial A} + B \frac{\partial}{\partial B} \right) \right. \\
& \quad \left. + 4 \right\} p(A, B, \mathcal{T}) = \left\{ r^2 \frac{\partial^2}{\partial r^2} + 5r \frac{\partial}{\partial r} + 4 \right\} \frac{\tilde{p}(r, \theta, \mathcal{T})}{r} ,
\end{aligned} \tag{4.76}$$

whereas the sum of the terms in brackets proportional to $\tilde{D}/2$ in Eq. (4.75) transform as

$$\begin{aligned} & \left\{ (A^2 + B^2) \left[\frac{\partial^2}{\partial A^2} + \frac{\partial^2}{\partial B^2} \right] + 2 \left(A \frac{\partial}{\partial A} + B \frac{\partial}{\partial B} \right) \right\} p(A, B, \mathcal{T}) \\ &= \left\{ r^2 \frac{\partial^2}{\partial r^2} + 3r \frac{\partial}{\partial r} + \frac{\partial^2}{\partial \theta^2} \right\} \frac{\tilde{p}(r, \theta, \mathcal{T})}{r}. \end{aligned} \quad (4.77)$$

Combining Eqs. (4.62), (4.76), and (4.77), the Fokker-Planck equation in polar coordinates is

$$\begin{aligned} \frac{1}{r} \frac{\partial}{\partial \mathcal{T}} \tilde{p}(r, \theta, \mathcal{T}) &= -\frac{1}{r} \frac{\partial}{\partial r} \left[\left(\tilde{\mu} r - \frac{3}{4} r^3 \right) \tilde{p}(r, \theta, \mathcal{T}) \right] - \frac{1}{r} \frac{\partial}{\partial \theta} [\tilde{\nu} \tilde{p}(r, \theta, \mathcal{T})] \\ &+ \frac{\tilde{D}}{2} \left(3r^2 \frac{\partial^2}{\partial r^2} + 13r \frac{\partial}{\partial r} + 8 + \frac{\partial^2}{\partial \theta^2} \right) \frac{\tilde{p}(r, \theta, \mathcal{T})}{r}. \end{aligned} \quad (4.78)$$

We now make use of the identities,

$$\frac{1}{r} \frac{\partial^2}{\partial r^2} \left[r^3 \frac{\tilde{p}(r, \theta, \mathcal{T})}{r} \right] = \left(r^2 \frac{\partial^2}{\partial r^2} + 6r \frac{\partial}{\partial r} + 6 \right) \frac{\tilde{p}(r, \theta, \mathcal{T})}{r}, \quad (4.79)$$

$$\frac{2}{r} \frac{\partial}{\partial r} \left[r^3 \frac{\partial \tilde{p}(r, \theta, \mathcal{T})}{\partial r} \frac{1}{r} \right] = \left(2r^2 \frac{\partial^2}{\partial r^2} + 6r \frac{\partial}{\partial r} \right) \frac{\tilde{p}(r, \theta, \mathcal{T})}{r}, \quad (4.80)$$

$$\frac{1}{r} \frac{\partial}{\partial r} \left[r^2 \frac{\tilde{p}(r, \theta, \mathcal{T})}{r} \right] = \left(r \frac{\partial}{\partial r} + 2 \right) \frac{\tilde{p}(r, \theta, \mathcal{T})}{r}, \quad (4.81)$$

to rewrite the Fokker-Planck equation as,

$$\begin{aligned} \frac{\partial}{\partial \mathcal{T}} \tilde{p}(r, \theta, \mathcal{T}) &= -\frac{\partial}{\partial r} \left\{ \left[\left(\tilde{\mu} + \frac{5\tilde{D}}{2} \right) r - \frac{3}{4} r^3 \right] \tilde{p}(r, \theta, \mathcal{T}) \right\} \\ &+ \frac{3\tilde{D}}{2} \frac{\partial^2}{\partial r^2} [r^2 \tilde{p}(r, \theta, \mathcal{T})] - \frac{\partial}{\partial \theta} [\tilde{\nu} \tilde{p}(r, \theta, \mathcal{T})] + \frac{\tilde{D}}{2} \frac{\partial^2}{\partial \theta^2} \tilde{p}(r, \theta, \mathcal{T}). \end{aligned} \quad (4.82)$$

The Fokker-Planck equation can now be solved by separation of variables in the stationary regime. Let $\tilde{p}_s(r, \theta) = p_s(r)p_s(\theta)$. The stationary solution of

the angular component, $\dot{p}_s(\theta) = 0$, satisfies,

$$0 = -\frac{\partial}{\partial\theta} [\tilde{\nu}p_s(\theta)] + \frac{\tilde{D}}{2} \frac{\partial^2}{\partial\theta^2} p_s(\theta) , \quad (4.83)$$

which leads to

$$p_s(\theta) = \mathcal{N}_\theta \exp\left(\frac{2\tilde{\nu}}{\tilde{D}}\theta\right) , \quad (4.84)$$

where \mathcal{N}_θ is a normalization constant. The stationary solution of the radial component, $\dot{p}_s(r) = 0$, satisfies

$$0 = -\frac{\partial}{\partial r} \left\{ \left[\left(\tilde{\mu} + \frac{5\tilde{D}}{2} \right) r - \frac{3}{4}r^3 \right] p(r) \right\} + \frac{3\tilde{D}}{2} \frac{\partial^2}{\partial r^2} [r^2 p(r)] , \quad (4.85)$$

which leads to,

$$p_s(r) = \mathcal{N}_r |r|^{\alpha'} \exp\left(-\frac{r^2}{4\tilde{D}}\right) , \quad (4.86)$$

where \mathcal{N}_r is another normalization constant. We have defined,

$$\alpha' = \frac{1}{3} \left(\frac{2\tilde{\mu}}{\tilde{D}} - 1 \right) . \quad (4.87)$$

The stationary probability distribution functions are normalized according to,

$$1 = \int_0^{2\pi} \int_0^\infty \tilde{p}_s(r, \theta) dr d\theta = \left[\int_0^{2\pi} p_s(\theta) d\theta \right] \left[\int_0^\infty p_s(r) dr \right] , \quad (4.88)$$

and we choose to normalize both components in the square bracket to one.

Normalization of the radial component leads to,

$$N_r = 2(4\tilde{D})^{-\left(\frac{\alpha'+1}{2}\right)} \Gamma^{-1} \left(\frac{\alpha'+1}{2} \right) . \quad (4.89)$$

If $\alpha' < -1$, the probability distribution function of the radial component is

not normalizable. The bifurcation threshold is therefore located at $\alpha' = -1$.

This leads to the condition,

$$\tilde{\mu} + \tilde{D} = 0 . \quad (4.90)$$

Normalization of the angular component yields,

$$N_\theta = \left(\frac{\tilde{\nu}}{\tilde{D}} \right) \frac{\exp\left(-\frac{2\pi\tilde{\nu}}{\tilde{D}}\right)}{\sinh\left(\frac{2\pi\tilde{\nu}}{\tilde{D}}\right)} . \quad (4.91)$$

The dynamics in the deterministic limit is a limit cycle at threshold. Here, we choose the probability distribution function of the angular component to be uniform at threshold ($\alpha' = -1$) [127]. This occurs at $\tilde{\nu} = 0$ for all θ and the stationary probability distribution function of the angular component is $p_s(\theta) = 1/(2\pi)$. By combining both conditions we find,

$$a_c + D + b \cos(\omega\tau) = 0 , \quad (4.92)$$

$$\omega + b \sin(\omega\tau) = 0 . \quad (4.93)$$

By substituting Eq. (4.93) into Eq. (4.92), we find our final result for the Hopf bifurcation line,

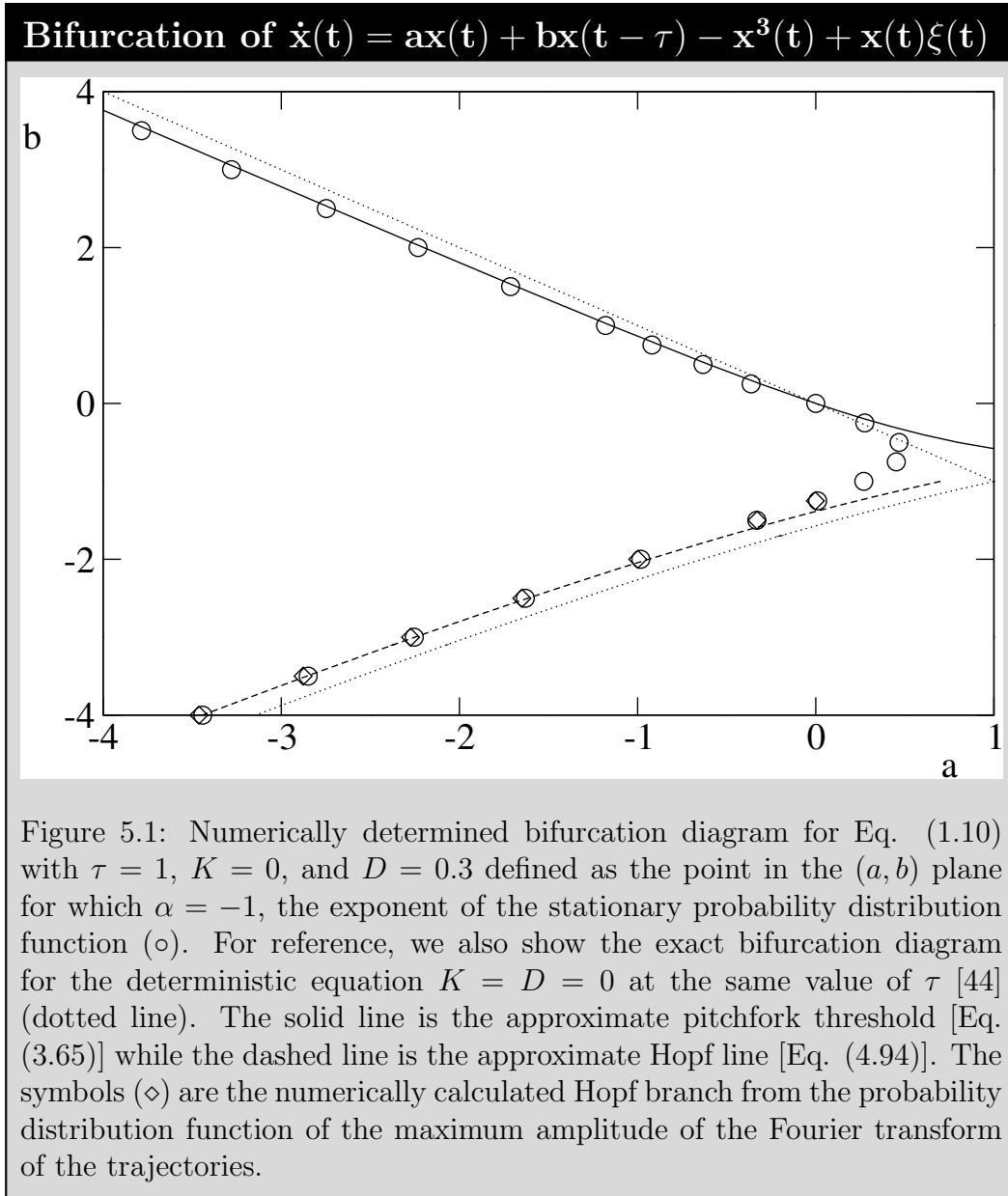
$$-\left(\frac{a_c + D}{b}\right) = \cos\left[\tau\sqrt{b^2 - (a_c + D)^2}\right] , \quad (4.94)$$

Interestingly, this condition agrees with the bifurcation threshold of the first moment $\langle x \rangle$ from the linearization of Eq. (1.10) with multiplicative noise only ($K = 0$) derived in Chapter 3 [Eq. (3.31)].

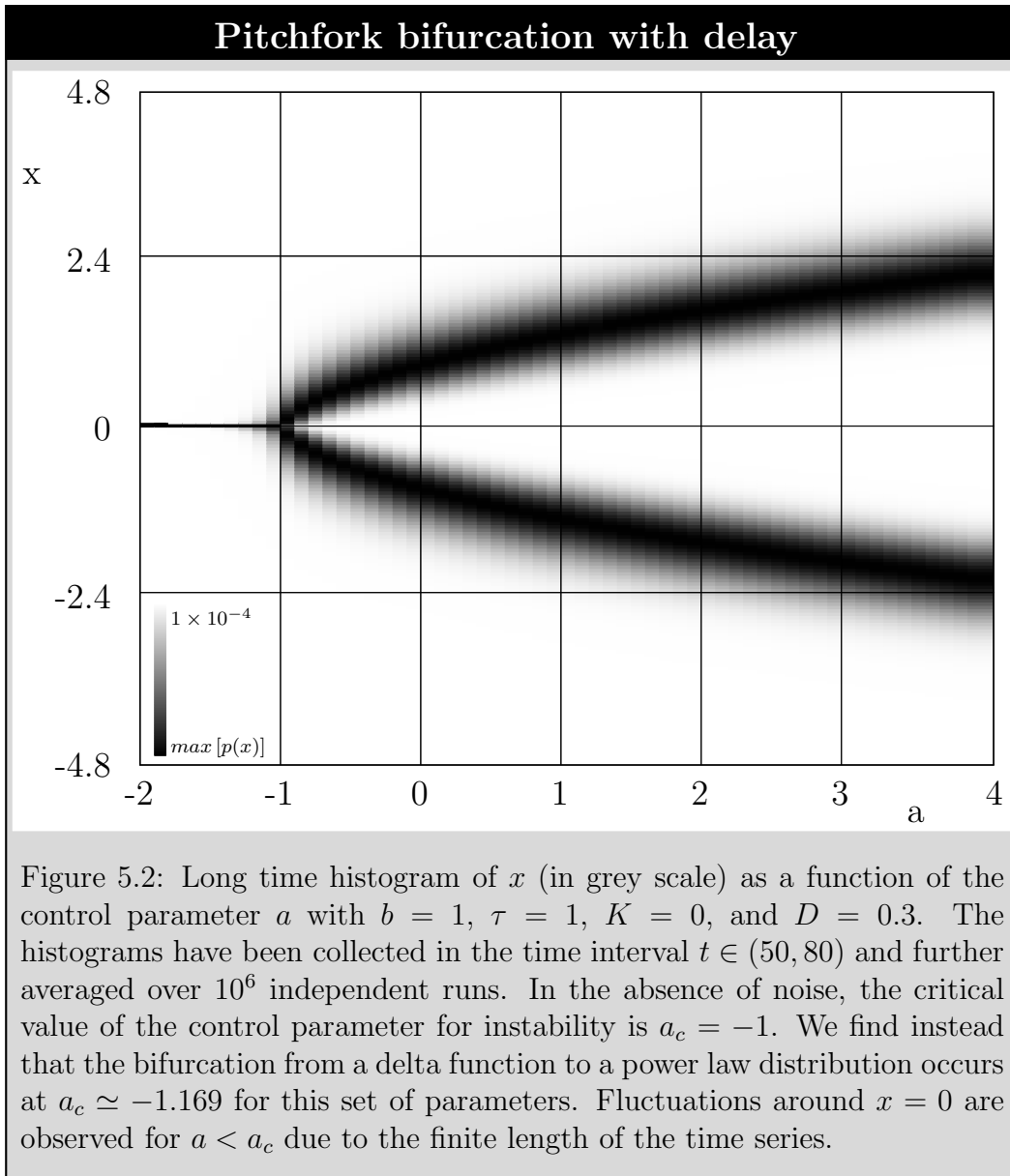
Chapter 5

Numerical stability analysis

We present in this chapter a numerical verification of several approximations described earlier, and a determination of the bifurcation thresholds of Eq. (1.10) with multiplicative noise only ($K = 0$) as we have shown that additive noise does not change the location of the bifurcation threshold. We employ the second order algorithm that we have developed [Eq. (2.2)], described in Appendix C. The bifurcation diagram of Eq. (1.10) with multiplicative noise only ($K = 0$) as numerically determined is shown in Fig. 5.1. The bifurcation threshold has been computed from the stationary probability distribution function $p(x)$ of the state variable x . The distribution function is dominated by a power law at small x and to exponential decay at large x . The bifurcation threshold is defined to be located at the set of parameter for which the exponent of the power law is -1 for normalizability reason. Equation (1.10) with $K = 0$ has been integrated over a finite time window $[0, t_{max}]$ by using Eq. (2.2) with $\gamma = 1$ and $D = 0.3$. The integration step is $\Delta t = 0.01$. The value of the upperbound t_{max} is chosen to ensure that trajectories have reached a stationary state above threshold. The stationary distribution probability distribution function is computed over a time domain $[t_{min}, t_{max}]$, typically with

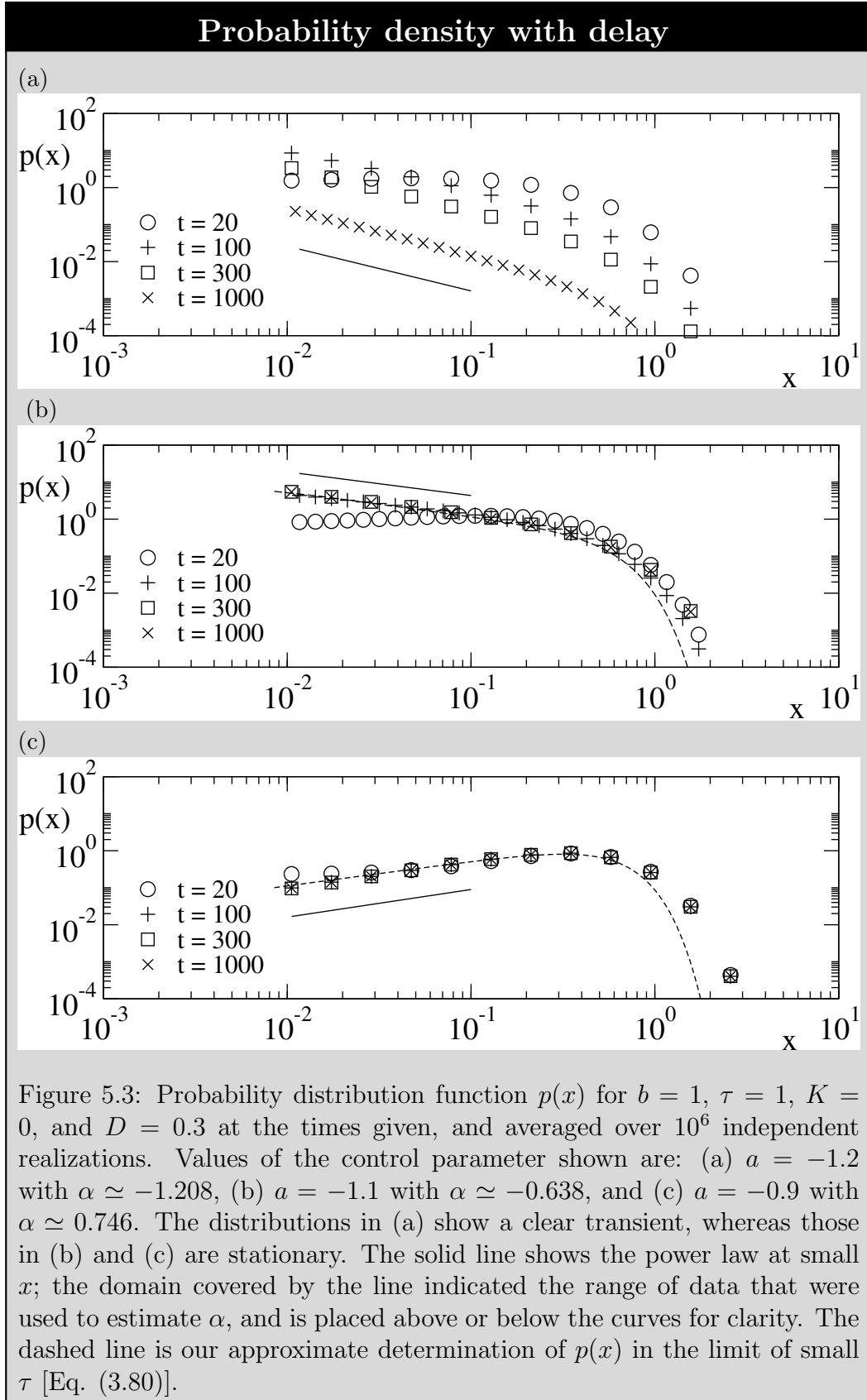


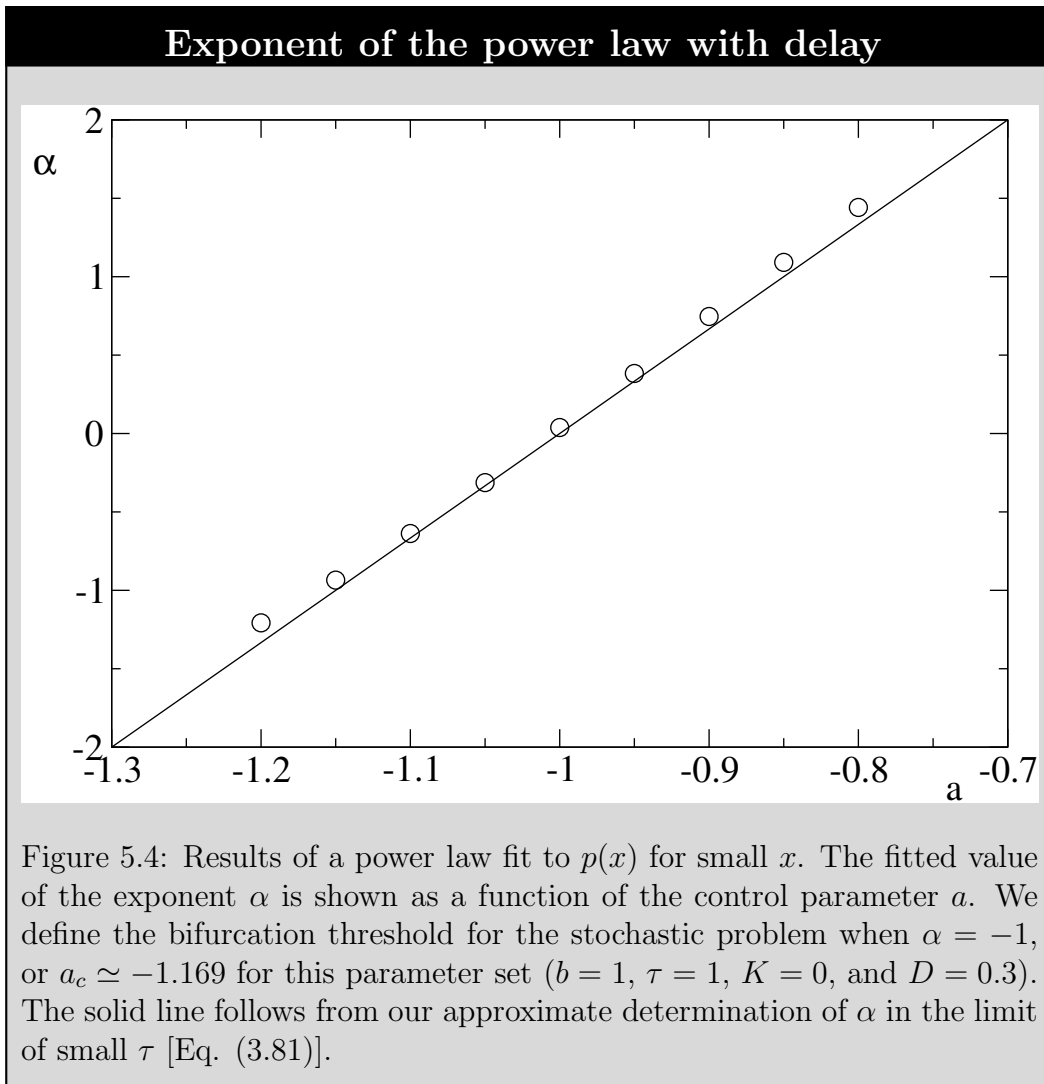
$t_{min} = t_{max} - 10$, in which the solution is believed to have reached the steady state. The calculation is repeated over several realizations over the random process $\xi(t)$. We usually consider an ensemble average of the order of 10^6 independent trajectories.



5.1 Pitchfork bifurcation

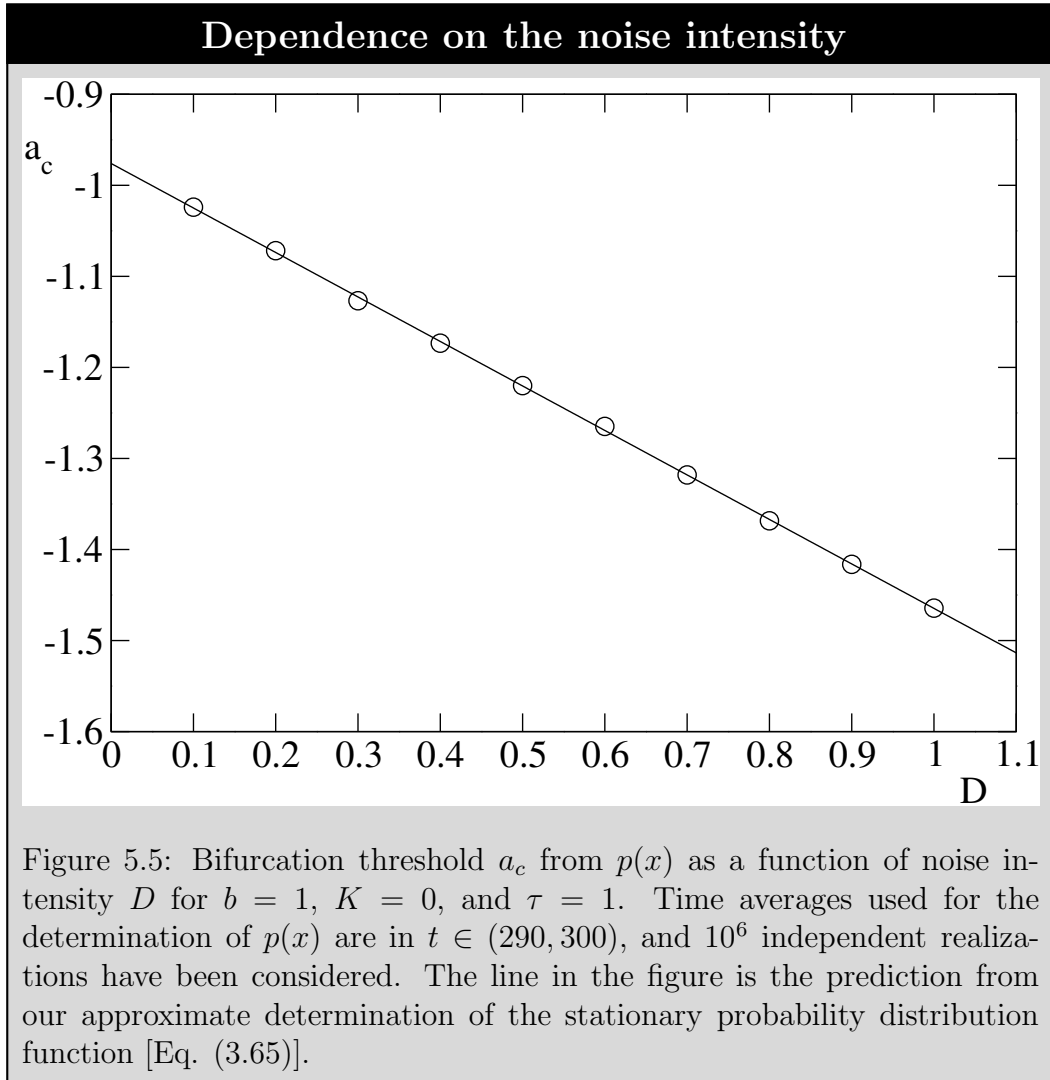
A qualitative depiction of the bifurcation of Eq. (1.10) with $K = 0$ is presented in Fig. 5.2. It shows in grey scale the stationary distribution function of x as a function of a . For $a \leq a_c \approx -1.17$, the histogram is sharply peaked at $x = 0$. At the critical value a_c , the bifurcation point, a broad distribution emerges, although the most likely value remains $x = 0$. Beyond a larger value of a , the histogram is a bimodal distribution. Note that a qualitatively similar





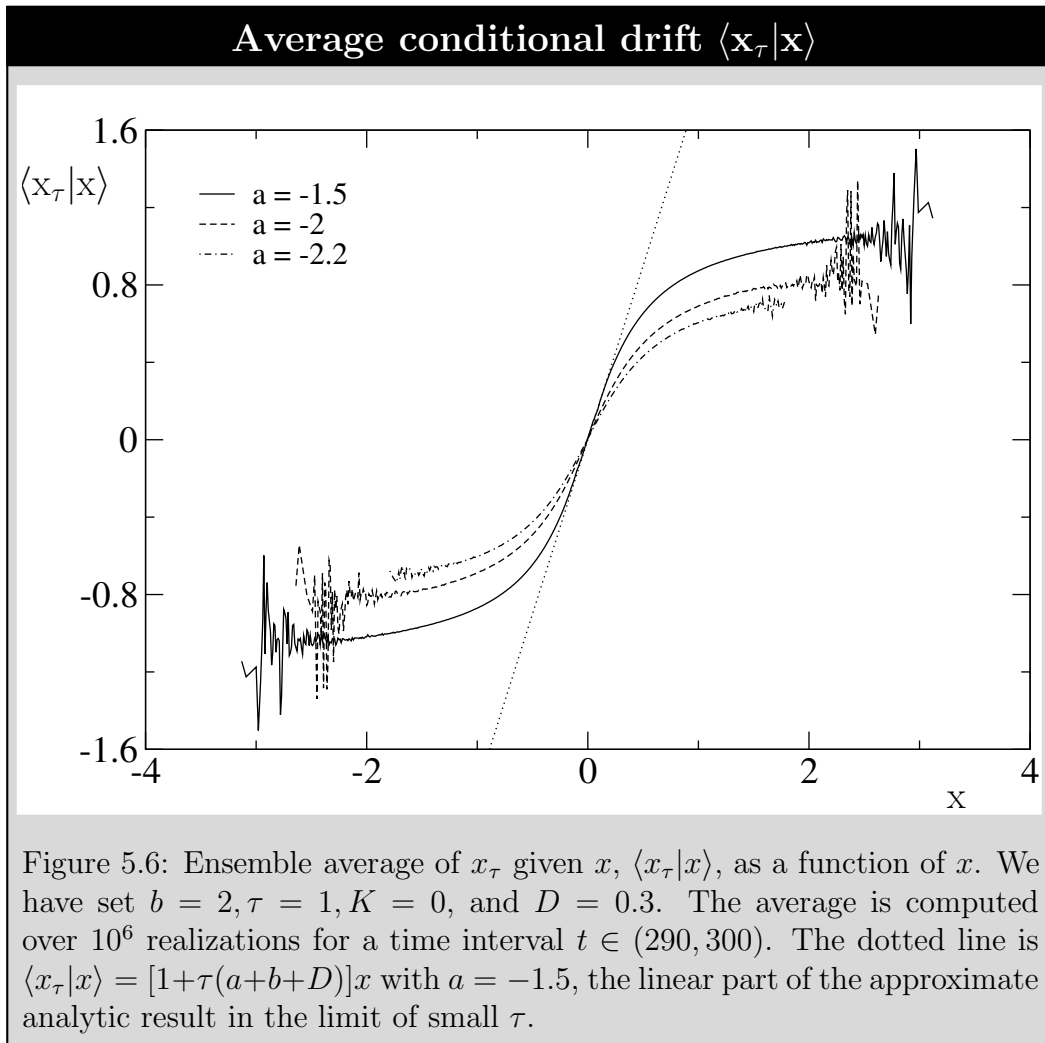
graph is obtained around the Hopf bifurcation (not shown).

The location of the bifurcation threshold is determined from the probability distribution function $p(x)$. Our results are summarized in Fig. 5.3 for three different values of a , and as the upper bound t_{max} of the time window used to compute the distribution function is varied. First (top), the probability distribution is not stationary as $a < a_c$. In fact, we would expect $p(x) = \delta(x)$ to the asymptotic stationary distribution, but instead we observe very long transients with $p(x)$ approximately characterized by a power law distribution, with an effective exponent $\alpha < -1$ (and hence non normalizable). The ampli-



tude of the point at $x = 0$ does grow with time, signalling the build up of the delta function around the origin. Because the overall normalization, growth at $x = 0$ implies a decaying amplitude for finite x , as shown in the figure. For $a > a_c$ the distribution quickly reaches a stationary power law form (middle), or a bimodal distribution ($a \gg a_c$) (bottom).

The location of the bifurcation point is determined from a power law fit to the distribution function at small x . A result of such a fit is shown in Fig. 5.4. We observe a smooth variation of the exponent α with respect to a that allows the determination of a_c , the value for which $\alpha = -1$. The fit has



been performed on several intervals of x for which the power law is observed, and no significant difference in a_c was observed. This is the method that has been used to determine numerically the bifurcation diagram of Eq. (1.10) with $K = 0$.

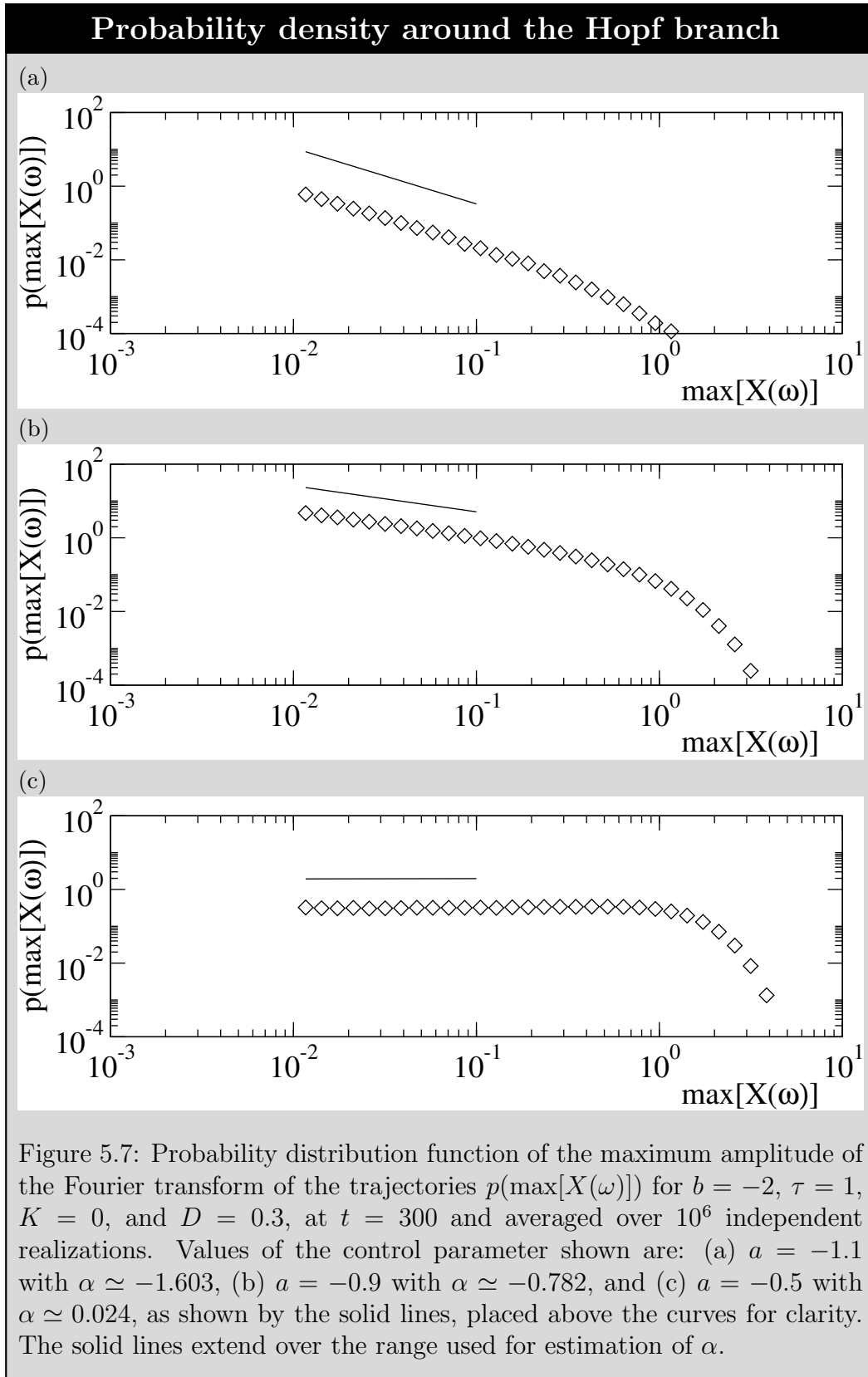
It is observed from the bifurcation diagram (Fig. 5.1) that the bifurcation threshold is shifted relative to its deterministic counterpart. The bifurcation threshold a_c determined from $p(x)$ in the vicinity of the pitchfork bifurcation is shown in Fig. 5.5 as the intensity of the noise is varied. The shift scales linearly with the intensity of the noise, as predicted by Eq. (3.65). In fact, time delay and parametric randomness couple, resulting in a shift on the location

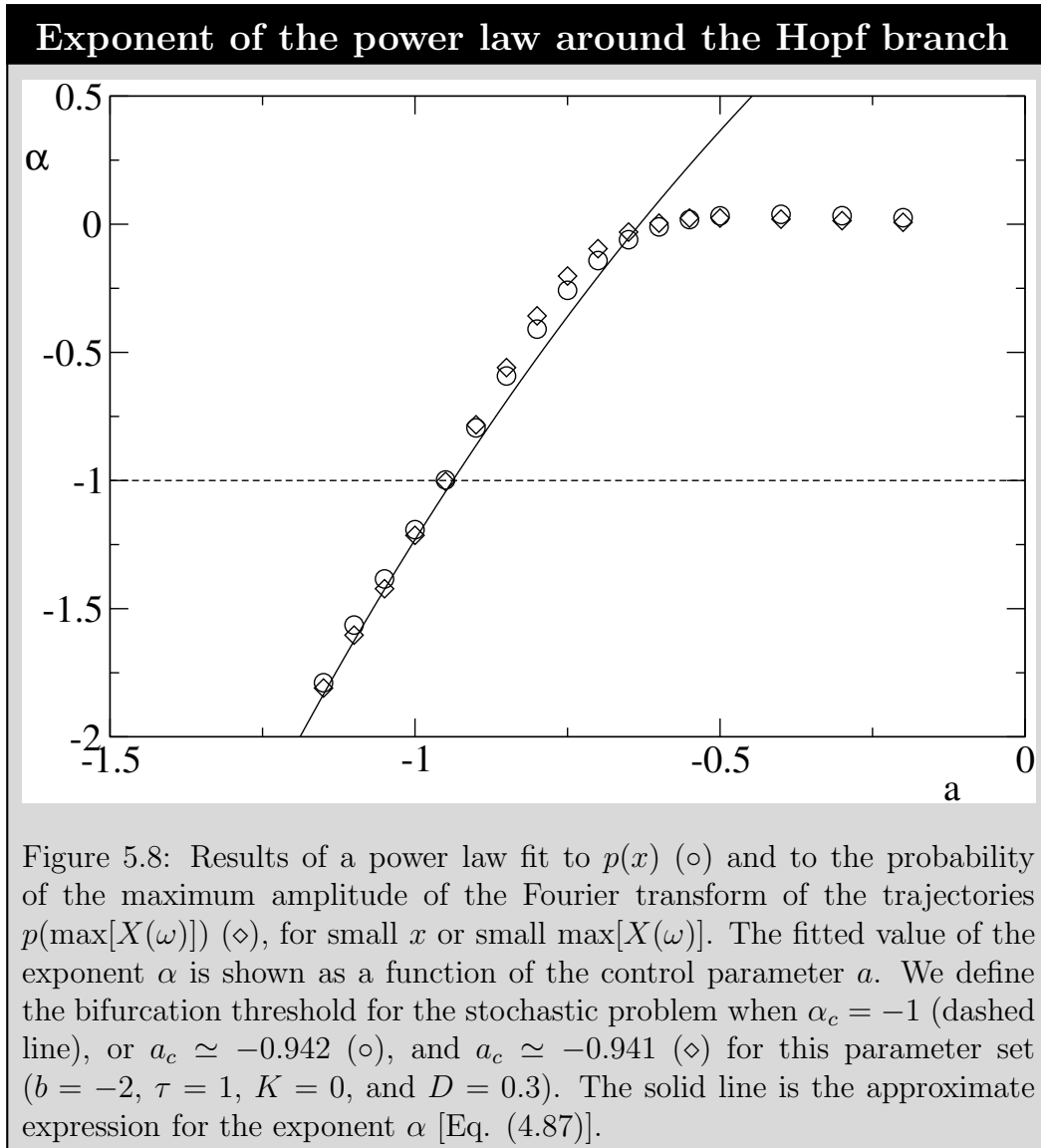
of the threshold. This coupling is captured by the average conditional drift $\langle x_\tau | x \rangle$. Note that the shift disappears when $b = 0$ (no delay).

Given that no analytical expression is known for the average conditional drift [Eq. (3.15)], we have computed this quantity numerically, with the results shown in Fig. 5.6. The figure shows a histogram of x_τ at time $t - \tau$ given its value at time t , as the trajectory has reached a stationary state. This term is directly responsible for the non-Markovian nature of the Fokker-Planck equation associated with the delay differential equation.

5.2 Hopf bifurcation

The same method has been used to determine the Hopf bifurcation line. In the deterministic case, the bifurcation is associated to oscillations. When fluctuations are added, oscillation amplitudes fluctuate as well. The location of the Hopf branch has been determined by calculating the Fourier transform of the trajectories because they oscillate close to the Hopf branch at approximately the Hopf frequency. The calculation of the stationary distribution function can thus be repeated but by using the maximum amplitude of the Fourier transform of the trajectories rather than the state variable x as order of parameter. This calculation is shown in Fig. 5.7. Technically, the Fourier transform of a trajectory is performed over a time interval for which the solution is believed to be stationary. We have used the same interval than in the determination of the probability distribution function of x . We then construct a histogram $p(\max[X(\omega)])$ of the maximum amplitude of the Fourier transform $\max[X(\omega)]$ over realizations of the noise. It is observed that the resulting distribution function is also dominated by a power law as the maximum amplitude is small. We have thus defined the bifurcation threshold to be located at the set of parameters for which the exponent of the power law is -1. Re-





sults of such a fit together with the fit performed on the stationary probability distribution function of x is shown in Fig. 5.8. The two determinations agree with each other.

Chapter 6

Correlation time near threshold

The approximate pitchfork and Hopf bifurcation lines derived in Chapters 3 and 4 are in great agreement with the numerical determination of the bifurcation thresholds even if the value of the time delay used extends the regime of small delay. We demonstrate in this chapter that this is because the value used for the time delay is smaller than the correlation time of the state variable. Furthermore, we note that the correlation time of Eq. (1.10) without delayed feedback ($b = 0$) and multiplicative noise only ($K = 0$) diverges with exponent -1 with respect to the control parameter of the equation [83]. We analyze in this chapter whether delayed feedback modifies this latter result. In order to do so, we apply the theory developed by Jung and Risken [83] to Eq. (1.10) with $K = 0$. This theory provides an integral representation of the correlation time of the state variable. The integral can be computed numerically. However, the theory needs the transition probabilities to be Markovian. We thus use the one dimensional expression resulting from the Stratonovich Taylor expansion under the assumption that the time delay is small introduced in Chapter 3 in order to compare the analytical predictions with the numerical determination of the correlation time. We show that non-Markovian effects in-

duce correlations which are not taken into account in the Jung-Risken theory, and we underline the need for a generalized theory with delay.

6.1 Correlation time

The correlation function and correlation time of Eq. (1.10) without delayed feedback ($b = 0$) and with multiplicative noise only ($K = 0$) were first studied by Stratonovich [131] by decoupling the correlation, and approximating higher-order correlation functions $C_n(t') = \langle x^{n-1}(t+t')x(t) \rangle - \langle x^{n-1} \rangle \langle x \rangle$ in terms of the usual correlation function $C_2(t')$. The correlation function and correlation time were further investigated numerically in [129, 132]. The analytical limit of the correlation time at small and large control parameter a are known [133, 134, 83]. Furthermore, an analytical expression for the correlation function and correlation time is provided in [83] by using a continued matrix method. This is the method that we have employed in our study and we refer to it as the Jung-Risken theory. Predictions of the correlation time have been verified by electronic analogue experiments [135, 136]. The study has also been generalized in [137] for stochastic differential equations with colored noise. The mathematical steps involved in the derivation of the correlation time according to the Jung-Risken theory are shown in Appendix D. We apply the results introduced in this appendix to the approximate Markovian expression associated to Eq. (1.10) as derived in Chapter 3. Systematic expansions at small and large noise intensities are also presented in Appendix D in order to derive a Padé approximant to the correlation time. Padé approximant is a rational function that approximates complex function, such as the integral representation of the correlation time. We briefly state results derived in Appendix D in this section and apply these to Eq. (1.10) under the assumption that the time delay is small.

The correlation time T of a stochastic process in its stationary state can be defined as the area under the correlation function normalized by the variance [138],

$$T = \frac{1}{C(0)} \int_0^\infty C(t') dt' , \quad (6.1)$$

where $C(t')$ is the correlation function,

$$C(t') = \langle \Delta x(t+t') \Delta x(t) \rangle , \quad (6.2)$$

and where $\Delta x = x - \langle x \rangle$. The Jung-Risken theory [83] demonstrates that given the Markovian process,

$$\dot{x}(t) = h(x) + g(x)\xi(t) , \quad (6.3)$$

where $\xi(t)$ is a Gaussian white noise process with mean $\langle \xi(t) \rangle = 0$ and correlation $\langle \xi(t)\xi(t') \rangle = 2D\delta(t-t')$, the correlation time of x is given by,

$$T = \frac{1}{C(0)} \int_0^\infty \frac{f^2(x')}{g^2(x')p_s(x')} dx' , \quad (6.4)$$

where

$$f(x) = - \int_0^x \Delta x' p_s(x') dx' , \quad (6.5)$$

where $g(x)$ is the coefficient of the noise of Eq. (6.3), and where $p_s(x)$ is its corresponding stationary probability distribution function. To apply the Jung-Risken theory to Eq. (1.10) with $K = 0$, we need the stationary probability distribution function from the Fokker-Planck equation associated to Eq. (1.10)

with $K = 0$ [Eq. (3.34)],

$$\begin{aligned} \frac{\partial}{\partial t} p(x, t) = & - \frac{\partial}{\partial x} \{ [(a + D)x + b\langle x_\tau | x \rangle - x^3] p(x, t) \} \\ & + D \frac{\partial^2}{\partial x^2} [x^2 p(x, t)] . \end{aligned} \quad (6.6)$$

Of course, this Fokker-Planck equation is not closed because of the presence of the non-Markovian term $\langle x_\tau | x \rangle$, as explained in Chapter 3. We thus use the approximate expression obtained under the assumption that the time delay is small,

$$\begin{aligned} \frac{\partial}{\partial t} p(x, t) = & - \frac{\partial}{\partial x} \{ [(\sigma + D)x - \gamma x^3] p(x, t) \} \\ & + D \frac{\partial^2}{\partial x^2} [x^2 p(x, t)] , \end{aligned} \quad (6.7)$$

where $\sigma = a + b[1 + \tau(a + b + D)]$ and $\gamma = (1 + b\tau)$. The approximate Fokker-Planck equation [Eq. (6.7)] is Markovian, and the known results from the Jung-Risken theory can be applied. In particular, the stationary probability distribution function of $x \in [0, \infty]$ satisfies $\dot{p}_s(x) = 0$ and is found to be

$$p_s(x) = 2(\beta\gamma)^{\beta\sigma} \Gamma^{-1}(\beta\sigma) |x|^{2\beta\sigma-1} e^{-\beta\gamma x^2} , \quad (6.8)$$

where $\beta = (2D)^{-1}$, and where $\Gamma(x)$ is the gamma function. In those terms, the stochastic threshold is located at $\sigma_c = 0$. Furthermore, the n^{th} stationary moment of the state variable is

$$\langle x^n \rangle_s = \int_0^\infty x^n p_s(x) dx = (\beta\gamma)^{-n/2} \Gamma^{-1}(\beta\sigma) \Gamma(\beta\sigma + n/2) . \quad (6.9)$$

Substitute Eq. (6.8) into Eq. (6.5) so that

$$f(x) = \langle x \rangle_s [P(\beta\sigma, \beta\gamma x^2) - P(\beta\sigma + 1/2, \beta\gamma x^2)] , \quad (6.10)$$

where $P(\eta, \omega)$ is the incomplete gamma function defined by

$$P(\eta, \omega) = \Gamma^{-1}(\eta) \int_0^\omega q^{\eta-1} e^{-q} dq . \quad (6.11)$$

Using the $n = 1$ and $n = 2$ moment of Eq. (6.9), together with $g(x) = D^{1/2}x$ and Eq. (6.10), the correlation time corresponding to the random process defined by Eq. (6.7) is

$$T = \frac{\beta(\beta\gamma)^{-\beta\sigma}\Gamma(\beta\sigma + 1)\Gamma^2(\beta\sigma + 1/2)}{\Gamma^2(\beta\sigma + 1) - (\beta\sigma)\Gamma^2(\beta\sigma + 1/2)} \times \int_0^\infty \frac{[P(\beta\sigma, \beta\gamma x^2) - P(\beta\sigma + 1/2, \beta\gamma x^2)]^2}{|x|^{2\beta\sigma+1}e^{-\beta\gamma x^2}} dx . \quad (6.12)$$

Equation (6.12) has to be evaluated numerically. Because of the singularity at $x = 0$, we perform the change of variable $x = \exp(z)$ prior to integration. The calculation has been verified by using several lower bound z_{min} and upper bound z_{max} ; no significant change was observed. The incomplete gamma function is calculated by using an ordinary continued fraction representation [139]. The limits of Eq. (6.12) are known [133, 134, 83]. At large σ or small D , the correlation time can be expanded in a power series,

$$T(\sigma, D) = \frac{1}{2\sigma} + \frac{7D}{16\sigma^2} + \frac{9D^2}{64\sigma^3} + \mathcal{O}\left[\frac{D^3}{\sigma^4}\right] , \quad (6.13)$$

whereas for small σ or large D ,

$$T(\sigma, D) = \frac{\pi}{2\sigma} - \frac{A}{D} + \mathcal{O}\left[\frac{\sigma}{D^2}\right] , \quad (6.14)$$

where $A = 1.5421\dots$. The mathematical steps involved in the derivation of both expansion are shown in Appendix D. A Padé approximant to Eq. (6.12) has also been proposed in [83]. The expression is

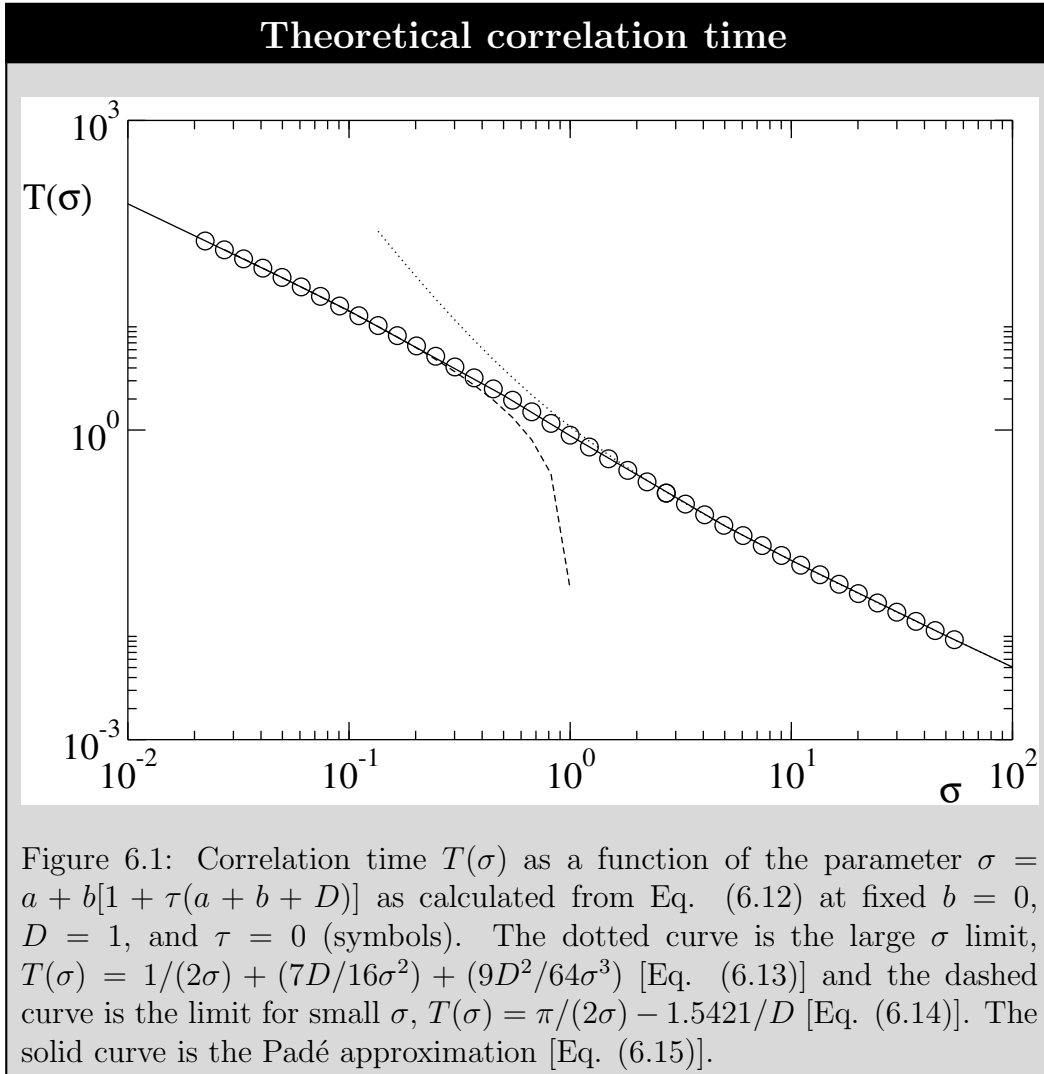
$$T(\sigma, D) = \frac{1}{2\sigma} + \frac{0.6037D\sigma + 1.0708D^2}{1.38\sigma^3 + 2.004D\sigma^2 + D^2\sigma}, \quad (6.15)$$

also shown in Appendix D. The correlation time T obtained from the numerical integration of Eq. (6.12) is shown in Fig. 6.1, together with its asymptotic limits of small and large σ . We also show the Padé interpolant. Equation (6.15) is expected to be valid in the limit of small time delay. We will compare this result with the correlation time computed from a direct numerical integration of Eq. (1.10) with $K = 0$ in the next section.

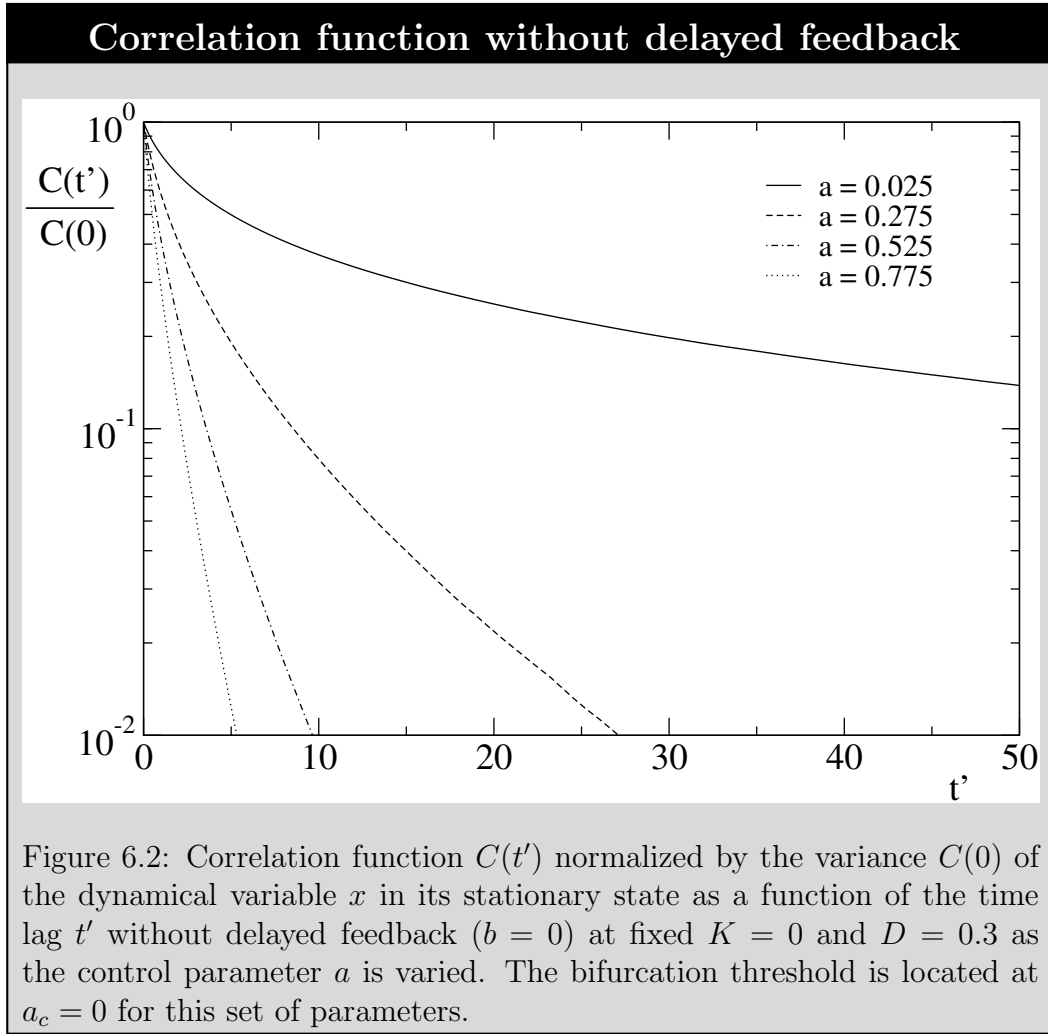
6.2 Numerical determination of the correlation time

The correlation function and correlation time are determined numerically with finite feedback, and compared to the approximation that follows from the Jung-Risken theory. We start to reproduce known results on the Stratonovich model [Eq. (1.10) with $b = 0$, $\gamma = 1$, and $K = 0$] in order to verify the methodology. The Stratonovich model is numerically integrated by using Eq. (2.2). The initial condition is a constant function in $[-\tau, 0]$ for each trajectory, with the constant being drawn from a Gaussian distribution of zero mean and variance 1. The time step used in the numerical integration is $\Delta t = 0.01$. The correlation function of the dynamical variable x ,

$$C(t') = \langle x(t+t')x(t) \rangle - \langle x \rangle^2, \quad (6.16)$$

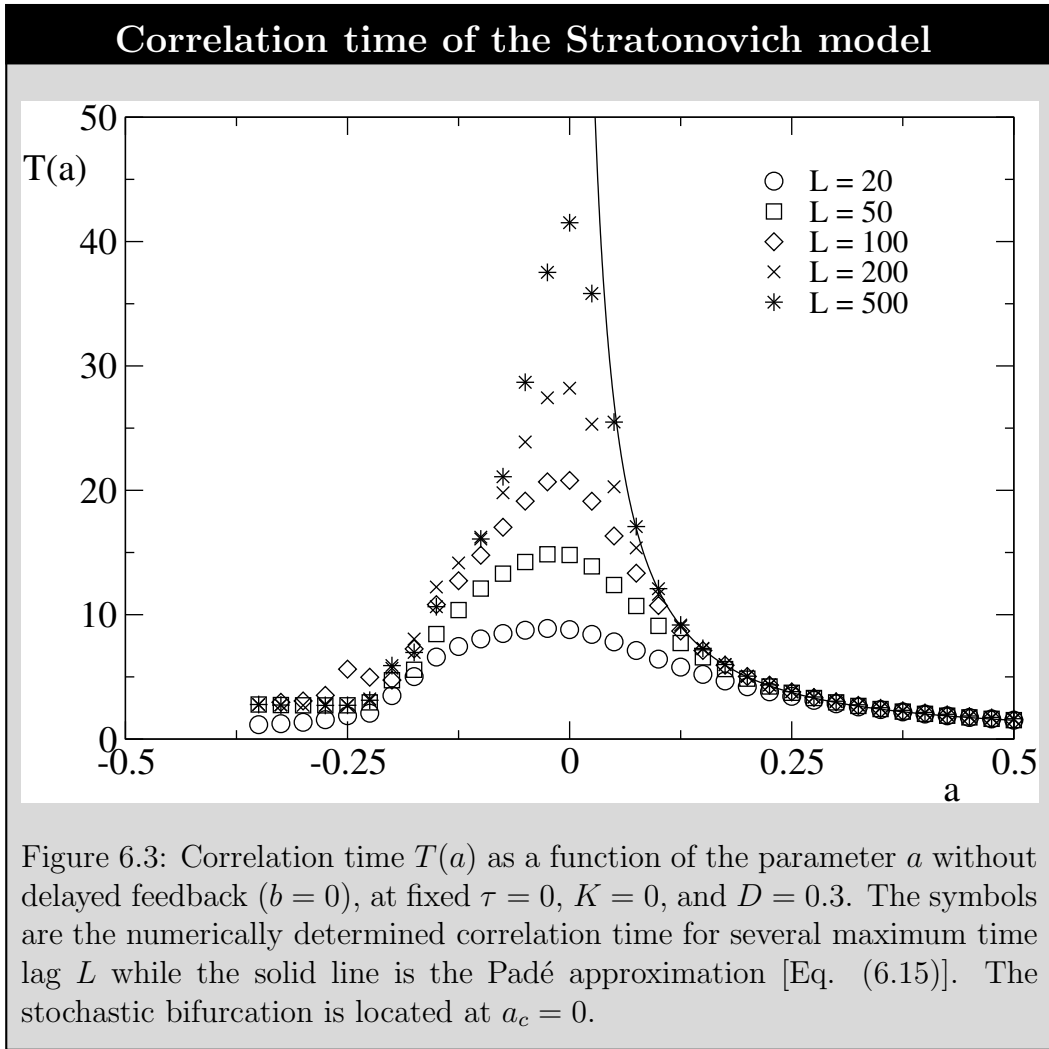


is computed in the time interval $t \in [t_{min}, t_{max}]$, with $t_{min} = 300$ and $t_{max} = 1400$. Trajectories have reached a stationary state in this time interval. Note that the lower bound t_{min} is larger than the largest correlation time that we have calculated. For a given trajectory, the correlation function is averaged over $N = 10^4$ values of $x(t_i)$, with $t_i = \{t_{min}, \dots, t_{min} + N\Delta t\}$, at fixed time lag t' . The correlation function is constructed for a time lag $t' \in [0, L]$, where L is the maximum time lag. The ensemble average is further constructed by considering 10^6 independent trajectories. The first moment of the state variable x in Eq. (6.16) is calculated in the time interval $t \in [t_{min}, t_{min} + L + N\Delta t]$.



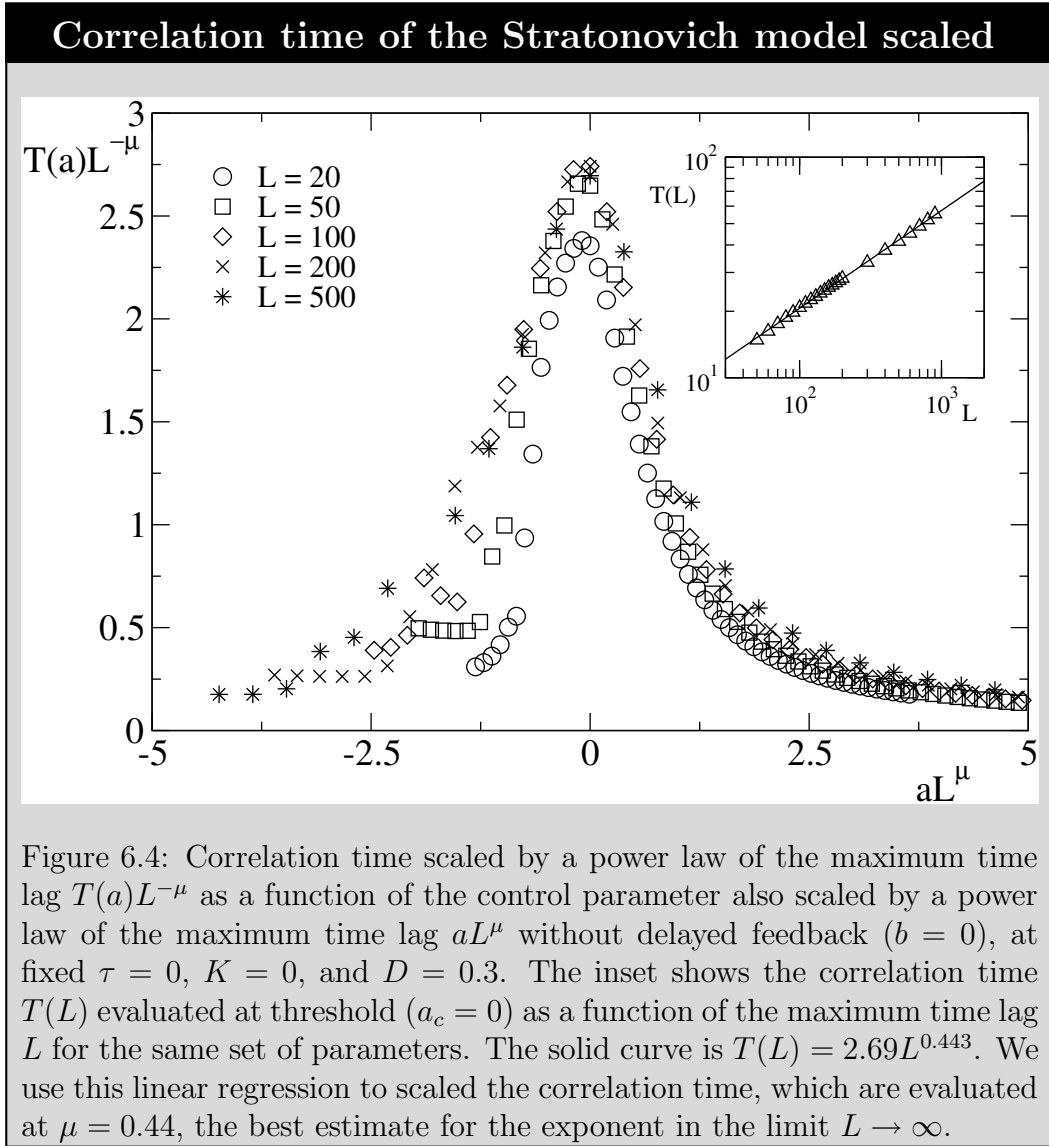
The correlation time is the area under the curve of the normalized correlation function. It is calculated according to Eq. (6.1) by using an integration time step of $\Delta t' = 0.01$. The normalized correlation function without delayed feedback ($b = 0$) is shown in Fig. 6.2 as the control parameter is varied.

Close to threshold, we expect that the correlation time will diverge. However, due to the finite time window of size L involved in the numerical integration, a true divergence cannot occur for purely numerical reasons. In order to analyze the divergence from the finite size of the integration domain, we repeat the determination of the correlation function for several values of the maximum time lag $L = \{20, 50, 100, 200, 500\}$, and study the extrapola-



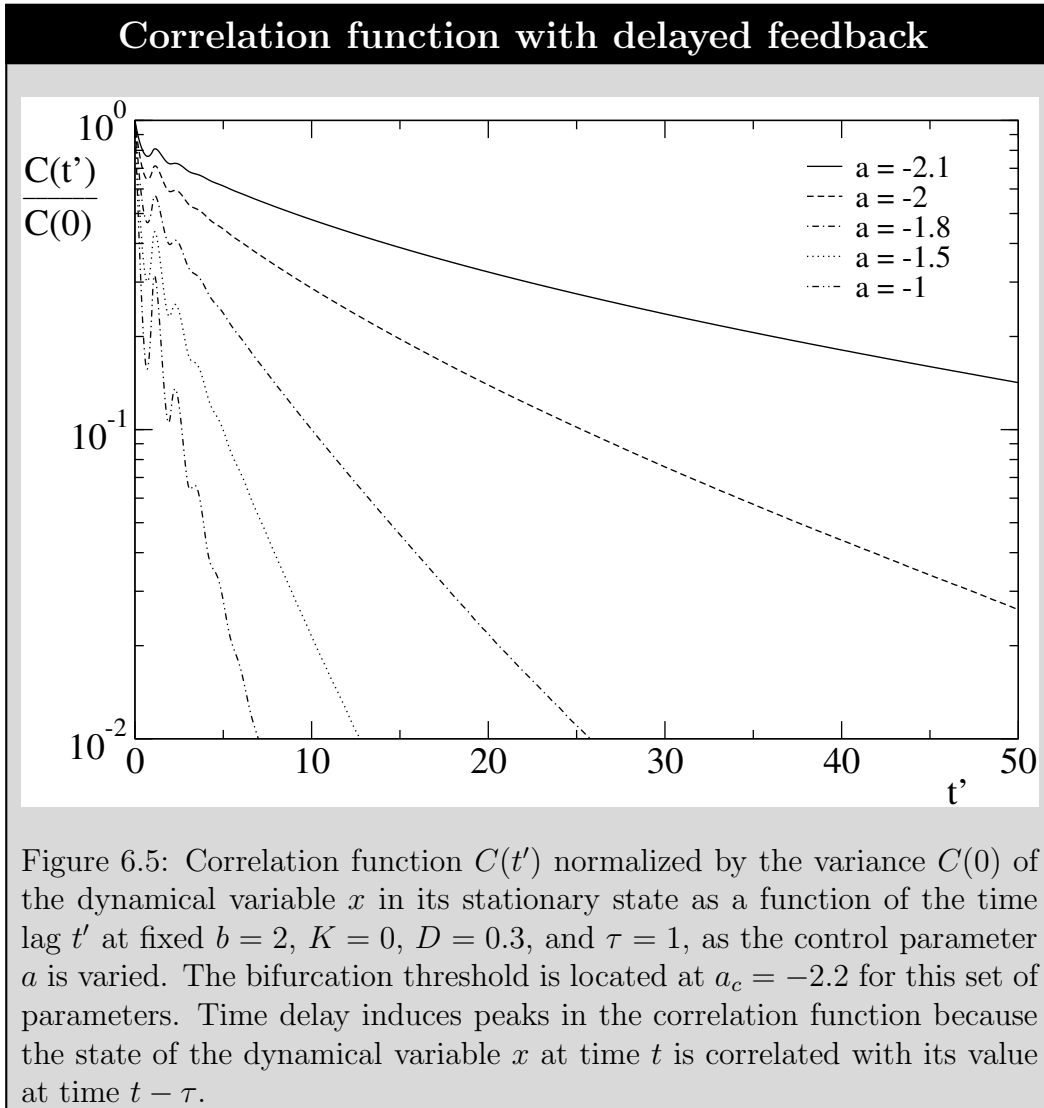
tion as $L \rightarrow \infty$. The procedure is repeated for different values of the control parameter a close to threshold.

The correlation time as calculated from the normalized correlation function in Fig. 6.2 is shown in Fig. 6.3. Away from the bifurcation threshold ($\sigma \gg \sigma_c = 0$), the normalized correlation function decays rapidly to zero. For large values of the control parameter, trajectories quickly saturate and fluctuate around their equilibrium value. The correlation time is small for this range of parameters and agrees well with the analytical prediction [Eq. (6.12)]. The decay of the normalized correlation function slows down as the bifurcation threshold is approached ($\sigma \sim \sigma_c$). In this range, one would have

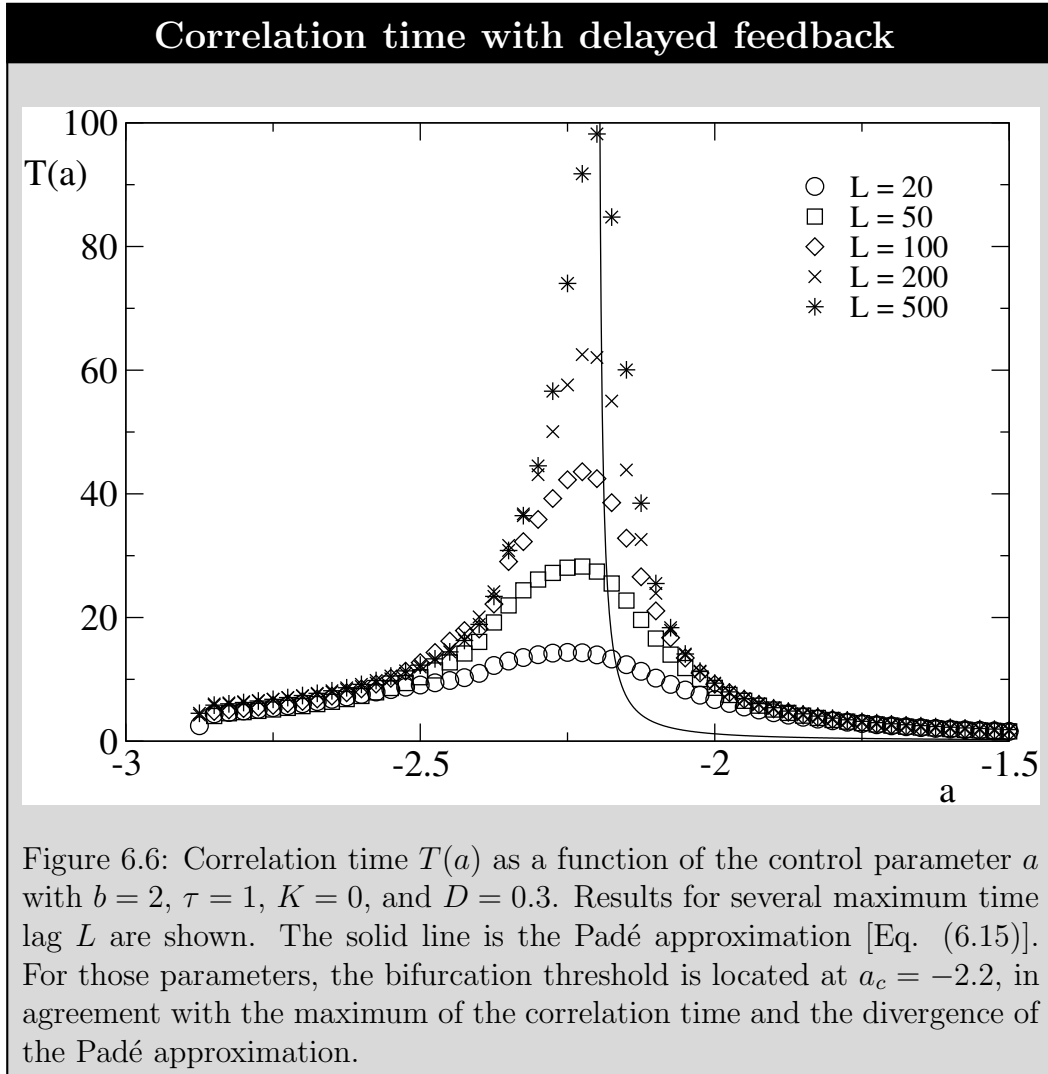


to integrate the normalized correlation function over a very long time lag window to approach the analytical prediction. We use instead scaling theory to overcome this limitation and to characterize the divergence of the correlation time. The correlation time is expected to diverge at threshold ($\sigma \sim \sigma_c$) for $L \rightarrow \infty$. We therefore write for finite L ,

$$T(\sigma, L) = L^{\mu} \tilde{T}(\sigma L^{\nu}) . \quad (6.17)$$

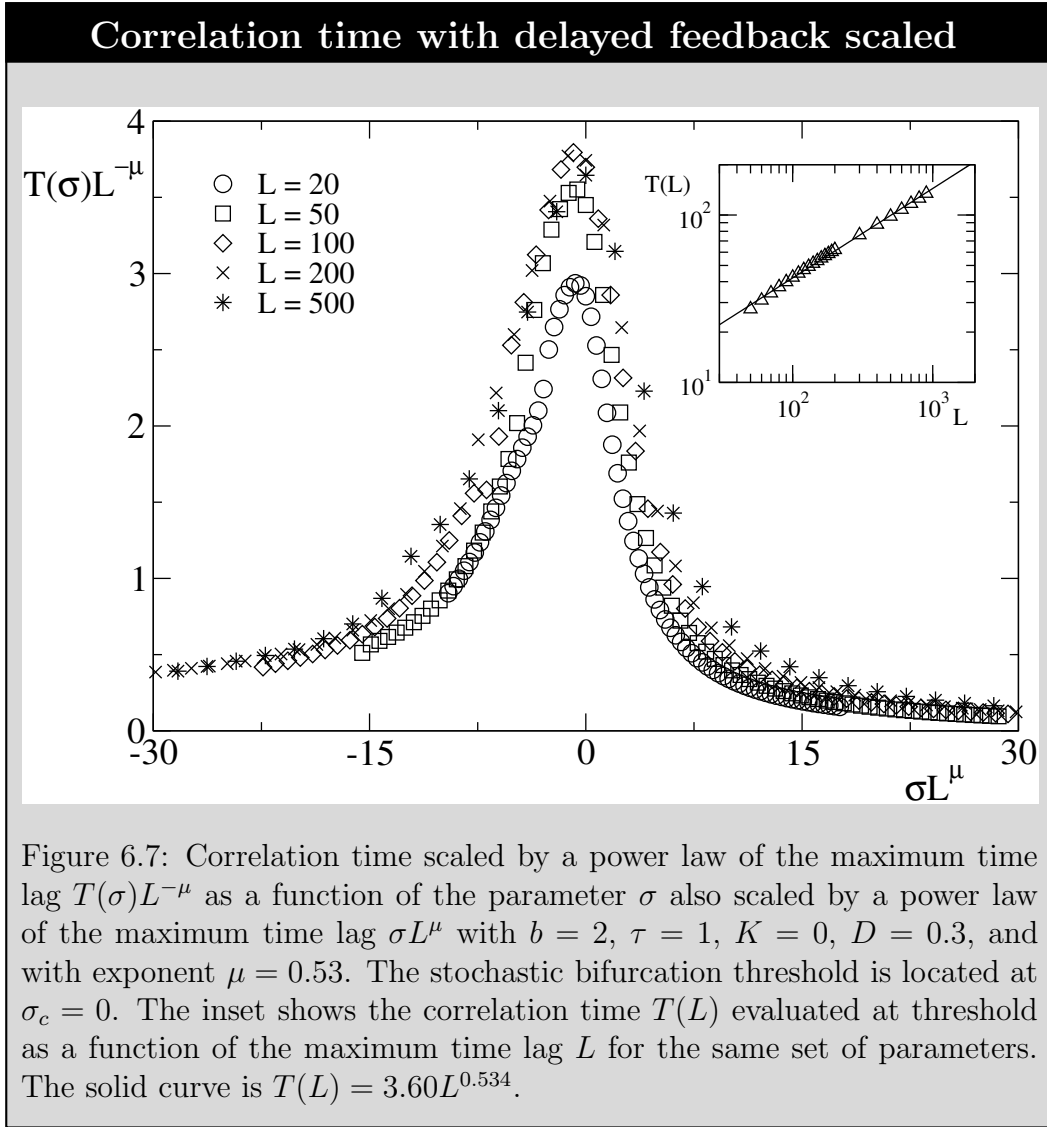


For finite σ and taking the limit $L \rightarrow \infty$, we have that $T \sim \sigma^{-\mu/\nu}$ if the scaling function is regular. Close to threshold, Eq. (6.14) predicts that the correlation time diverges with exponent $\mu/\nu = 1$. We show in Fig. 6.4 the scaled correlation time assuming only one unknown exponent for $L \in [50, 900]$. The value of the exponent μ is determined from the dependence of the correlation time on the maximum time lag evaluated at threshold ($\sigma_c = 0$). The extrapolation is shown in the inset of Fig. 6.4. The correlation time appears to follow a power law with the maximum time lag. Our best estimate for the exponent is $\mu = \nu = 0.44$. It is this value of the exponent that has been used to scale

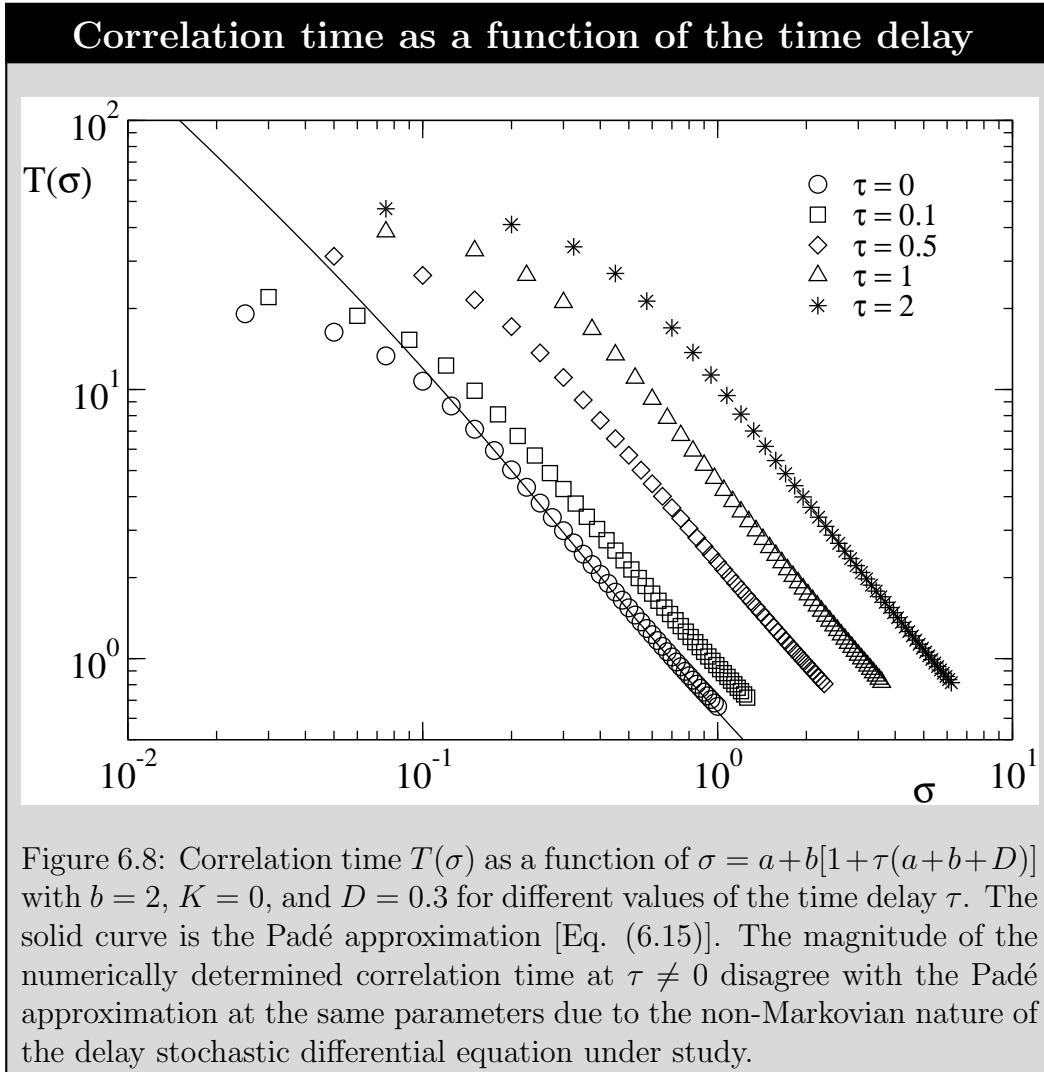


the correlation time according to Eq. (6.17), shown in Fig. 6.4. With this exponent, the curves of the correlation time calculated at different maximum time lag collapse to each other close to the bifurcation threshold. Our scaling analysis therefore agrees with the conclusion that the correlation time follows a power law divergence close to threshold, with exponent $T \sim \sigma^{-1}$.

The same analysis has been conducted for the case with delay $b \neq 0$. Equation (1.10) with $\gamma = 1$ and $K = 0$ is numerically integrated by using Eq. (2.2). Delayed feedback induces the presence of additional peaks in the normalized correlation function of the dynamical variable x as shown in Fig.



6.5. These peaks are a direct consequence of the correlation between the state of x at times t , $t - \tau$, $t - 2\tau$, etc. introduced by the delay. The correlation time with delayed feedback is calculated from a direct numerical integration of the governing equations and is shown in Fig. 6.6 for different values of L together with the Padé approximation given in Eq. (6.15). The analytical determination of the threshold agrees well with the location of the maximum of T in the figure. As was the case for no delay ($b = 0$), the maximum of the numerically determined correlation time increases with L . The scaling form [Eq. (6.17)] is tested again with the same condition $\mu = \nu$ that follows from



our analytic results for small τ . We show our scaling results with $\sigma_c = 0$ or $a_c = -2.2$ in Fig. 6.7. We further estimate $\mu \approx 0.53$ by fitting the correlation time as a function of $L \in [50, 900]$ (inset in the figure). This value of the exponent is quite close to the case of no delay. The correlation time curves calculated for different values of L collapse close to the bifurcation threshold as shown in Fig. 6.7. We therefore conclude that the correlation time diverges as $T \sim \sigma^{-1}$.

We note that the value of the correlation time predicted from Eq. (6.12) does not agree with our numerical determination, only the threshold location

and the exponent of the divergence of the correlation time. According to our analytic prediction, the correlation time depends on the delay τ through σ . This is not the case for our numerical results as T has a separate dependence on τ as shown in Fig. 6.8. Delayed feedback induces correlations between the state of the dynamical variable x at time t and $t-\tau$ and those correlations affect the value of the normalized correlation function. Those additional correlations are not included in the Jung-Risken theory applied to small delay because it assumes that the transition probabilities are Markovian.

Conclusions

A continuous model of a common gene regulatory network motif has been investigated in this thesis by means of the Langevin equation,

$$\dot{x}(t) = ax(t) + bx(t - \tau) - \gamma x^3(t) + x(t)\xi(t) + \eta(t) , \quad (7.1)$$

where a is a control parameter, b is the intensity of a feedback loop of time delay $\tau > 0$, γ is a constant, and where $\eta(t)$ and $\xi(t)$ are independent random processes normally distributed with mean $\langle \eta(t) \rangle = \langle \xi(t) \rangle = 0$ and correlation $\langle \eta(t)\eta(t') \rangle = 2K\delta(t - t')$ and $\langle \xi(t)\xi(t') \rangle = 2D\delta(t - t')$, where K and D are the intensity of the additive and multiplicative random processes, respectively. Equation (7.1) incorporates a time delay term modeling non-instantaneous biological process as well as parametric noise modeling fluctuations in reaction rates due to the environment. The underlying deterministic model exhibits both pitchfork and Hopf bifurcations. The bifurcation diagram for the stochastic case has been determined numerically from the stationary probability distribution function $p(x)$. Additive noise ($D = 0$) does not change the location of the bifurcation threshold, as opposed to multiplicative noise

($K = 0$).

We define the bifurcation threshold of the stochastic model as the point in model parameter space at which $p(x)$ changes from a delta function centered at the trivial state to a power law with an exponential cutoff at large x . In order to do so, we have obtained the Fokker-Planck equation associated with Eq. (7.1) (with $K = 0$)

$$\begin{aligned} \frac{\partial}{\partial t} p(x, t) = & - \frac{\partial}{\partial x} \{ [(a + D)x + b \langle x_\tau | x \rangle - x^3] p(x, t) \} \\ & + D \frac{\partial^2}{\partial x^2} [x^2 p(x, t)] . \end{aligned} \quad (7.2)$$

Due to the non Markovian nature of the process $x(t)$, Eq. (7.2) is not closed, but includes the average conditional drift,

$$\langle x_\tau | x \rangle = \int x_\tau p(x_\tau | x) dx_\tau . \quad (7.3)$$

We have expanded the conditional average in a stochastic Taylor series valid for small delay τ , and found,

$$\langle x_\tau | x \rangle = x [1 + \tau(a + b + D)] - \tau x^3 . \quad (7.4)$$

We have shown from this equation that the coupling of delayed feedback and parametric stochasticity shifts the bifurcations diagram relative to the deterministic model (this is in contrast with the case of parametric fluctuations without delayed feedback for which the location of the bifurcation is known to be independent of the intensity of the noise). In that range of parameters in which the bifurcation is direct, a small delay time expansion yields the desired stationary probability distribution function. By substituting Eq. (7.4) into Eq.

(7.2), a closed Markovian Fokker-Planck equation can be found,

$$\begin{aligned} \frac{\partial}{\partial t} p(x, t) = & - (1 + b\tau) \frac{\partial}{\partial x} \{ [(a + b + D)x - x^3] p(x, t) \} \\ & + D \frac{\partial^2}{\partial x^2} [x^2 p(x, t)] . \end{aligned} \quad (7.5)$$

The stationary probability distribution function of Eq. (7.5) is

$$p(x) = \begin{cases} \delta(x) & \text{if } \alpha \leq -1 \\ \frac{1}{2} \left(\frac{2D}{1+b\tau} \right)^{-\left(\frac{\alpha+1}{2}\right)} \Gamma^{-1} \left(\frac{\alpha+1}{2} \right) |x|^\alpha e^{-\frac{(1+b\tau)}{2D} x^2} & \text{if } \alpha > -1 \end{cases} . \quad (7.6)$$

where α is the exponent of the power law,

$$\alpha = \frac{(1 + b\tau)(a + b + D)}{D} - 2 . \quad (7.7)$$

The power law solution in Eq. (7.6) is not normalizable if $\alpha \leq -1$, and hence $p(x) = \delta(x)$ is the only admissible solution in this range. Hence, the bifurcation threshold is located at the point where $\alpha_c = -1$, or in terms of the parameter of the model,

$$a_c = -\frac{b[1 + \tau(b + D)]}{1 + b\tau} . \quad (7.8)$$

Equation (7.8) is only valid as $b\tau > -1$, corresponding to the direct pitchfork branch.

A multiple scale expansion has been developed to obtain the location of the Hopf bifurcation as this branch appears as a singular perturbation as $\tau \rightarrow 0$. We separate the time scale of the solution into a fast time scale t describing order 1 oscillations, and a slow time scale $\mathcal{T} = \epsilon^2 t$, where $0 < \epsilon \ll 1$, describing the time evolution of the amplitude of the oscillation, called also the envelope variables. Fast time scales are eliminated out of the equation by integrating

over a period of the oscillations. In terms of Eq. (7.1), we assume a solution of the form,

$$x(t, \mathcal{T}) = \epsilon A(\mathcal{T}) \cos(\omega t) + \epsilon B(\mathcal{T}) \sin(\omega t) , \quad (7.9)$$

where $A(\mathcal{T})$ and $B(\mathcal{T})$ are the envelope variables and where ω is the Hopf frequency. Substitution of Eq. (7.9) into Eq. (7.1) and integration over a period leads to a system of Langevin equations describing the slow time evolution of $A(\mathcal{T})$ and $B(\mathcal{T})$. Associated to this system of equations is a Fokker-Planck equation, which is uncoupled in polar coordinates. The normalizability condition described above applied to the stationary densities leads to the Hopf line,

$$-\left(\frac{a_c + D}{b}\right) = \cos\left(\tau\sqrt{b^2 - (a_c + D)^2}\right) . \quad (7.10)$$

The analytical method just introduced is quite general and can be applied to any stochastic differential equation with delayed feedback. We have tested the methodology on the van der Pol oscillator driven by parametric noise and augmented by delay term in the position and velocity of the oscillator. The location of the bifurcation threshold has been derived and agrees with results in the literature as $\tau = 0$.

Finally, the correlation time of the state variable x has been further investigated. It is known that the correlation time of Eq. (7.1) without delayed feedback ($b = 0$) diverges at threshold with exponent -1 with respect to the control parameter a . We have determined numerically that the same conclusion applies with delayed feedback ($b \neq 0$).

The results of this thesis suggest future paths that may be investigated. First, this thesis focuses on a continuous representation of a gene regulatory network by means of a Langevin equation. This representation is valid only if

the number of molecules involved in the network reactions is large. However, several gene networks are known to involve a limited number of copies of a given molecular species. A discrete representation would be more appropriate for those networks. This representation can be modeled by a Master equation. It could be interesting to know if the location and the nature of the bifurcation threshold are modified if the number of molecules is small. Note that the chemical reactions involved in the network could be investigated numerically with the Gillespie algorithm.

Furthermore, it has been underlined that the Jung-Risken theory is only valid as the transition probabilities are Markovian. Hence, the theory cannot be applied as it is to delay differential equations. However, it might be possible to expand the transition probability by assuming that the steps are small in order to generalize the Jung-Risken theory.

All through this thesis, time delay only appears in the drift coefficient of the stochastic equations considered. It is however possible to generalize the theoretical methods developed in this work in order to include time delay in the diffusion coefficient. This addition might make sense in biology as the intensity of the feedback loop might be also influenced by its environment and be a random number. For instance, this can be modeled by letting $b \rightarrow b + \zeta(t)$ in Eq. (1.10), where $\zeta(t)$ is a Gaussian white noise with mean $\langle \zeta(t) \rangle = 0$ and correlation $\langle \zeta(t)\zeta(t') \rangle = 2D'\delta(t - t')$. It is expected that such a modification will shift the location of the bifurcation diagram by an amount scaling with the intensity of the noise D' . Taylor expansion of this new term as well a multiple time scale expansion can also be performed in a straightforward way with the analytical methods introduced in this thesis.

Ito and Stratonovich calculus

Two interpretations of stochastic calculus have been introduced in the literature. One is due to Ito [33, 34] while the other one is from Stratonovich [35]. The two perspectives are equivalent to each other given the appropriate transformation rules. The main difference between the two is how the noise should be integrated. Before introducing both interpretations, let's introduce the concept of a *Gaussian white noise* [22, 42, 23]. It is a stochastic process $\xi(t)$ that satisfies the following properties,

1. $\langle \xi(t) \rangle = 0$.
2. $\langle \xi(t)\xi(t') \rangle = \delta(t - t')$.
3. All cumulants beyond the second vanish .

No well defined stochastic process with these properties exists. This random process is called white because it has a constant power spectral density. It is also Gaussian as the probability distribution function of a given realization of $\xi(t)$ is normally distributed. One can imagine $\xi(t)$ as a random sequence of small pulses, positive and negative, with short duration and small heights. Its

integral is called a Wiener process

$$W(t) = \int_0^t \xi(t') dt' . \quad (\text{A.1})$$

This process is neither stationary nor differentiable. A stochastic process $x(t)$ evolving in time through a differential equation understood in the Ito interpretation is usually written as ,

$$dx(t) = f[x(t)]dt + g[x(t)]dW(t) , \quad (\text{A.2})$$

where $f[x(t)]$ and $g[x(t)]$ are respectively the drift and diffusion coefficients, and where $dW(t)$ is the derivative of the Wiener process $W(t)$ with mean $\langle W(t) \rangle = 0$ and variance $\langle W^2(t) \rangle = 2Dt$ where $\langle \dots \rangle$ denotes an ensemble average over all the realizations of $W(t)$ and where D is the intensity of the noise. Equation (A.2) is called a Langevin equation. It defines the stochastic time evolution of a state variable. In the Ito convention, $x(t)$ in the diffusion coefficient $g[x(t)]$ is defined to be taken at the lower bound of the interval of the Wiener process. A stochastic process $x(t)$ is a solution to Eq. (A.2) if for all t and t_0 ,

$$x(t) = x(t_0) + \int_{t_0}^t f[x(t')] dt' + \int_{t_0}^t g[x(t')] dW(t') . \quad (\text{A.3})$$

The integral over the differential Wiener process $dW(t)$ is understood as,

$$\int_{t_0}^t g[x(t')] dW(t') = \text{ms-lim}_{n \rightarrow \infty} \sum_{i=1}^n g[x(t_{i-1})] [W(t_i) - W(t_{i-1})] , \quad (\text{A.4})$$

where ms-lim represents the *mean square limit*. Suppose that $X_n(\omega)$ is a sequence of random variables that are functions of ω and consider the mean

square deviation of $X_n(\omega)$ from $X(\omega)$. We say that X_n converges to X in the mean square sense if

$$\lim_{n \rightarrow \infty} \int p(\omega) [X_n(\omega) - X(\omega)]^2 d\omega = \lim_{n \rightarrow \infty} \langle (X_n - X)^2 \rangle = 0 . \quad (\text{A.5})$$

For this case, we thus have

$$\text{ms-lim}_{n \rightarrow \infty} X_n = X . \quad (\text{A.6})$$

Typically, a solution of Eq. (A.2) is understood as the discretized version of the stochastic differential equation,

$$x_{i+1} = x_i + f(x_i)\Delta t_i + g(x_i)\Delta W_i , \quad (\text{A.7})$$

where $x_i = x(t_i)$, $\Delta t_i = t_{i+1} - t_i$, and $\Delta W_i = W(t_{i+1}) - W(t_i)$, defined over a mesh of points t_i ,

$$t_0 < t_1 < t_2 < \dots < t_{n-1} < t_n = t . \quad (\text{A.8})$$

The solution is then formally constructed by letting the mesh size to go to zero.

Stratonovich introduced a different prescription to calculate the stochastic integral. A stochastic differential equation interpreted in the Stratonovich sense is usually written as

$$\dot{x}(t) = F[x(t)] + G[x(t)]\xi(t) , \quad (\text{A.9})$$

where $F[x(t)]$ and $G[x(t)]$ are respectively the drift and diffusion coefficient, and where $\xi(t) = dW(t)/dt$ is a Gaussian white noise. The value of $x(t)$ in the Stratonovich convention in the diffusion coefficient $G[x(t)]$ is the average of the values at the lower and upper bound of the interval. The solution of Eq. (A.9) is

$$x(t) = x(t_0) + S \int_{t_0}^t F[x(t')]dt' + S \int_{t_0}^t G[x(t')]dW(t') , \quad (\text{A.10})$$

where the S in front of the integrals refers to the Stratonovich interpretation and where the integral over the Wiener process is defined as

$$S \int_{t_0}^t G[x(t')]dW(t') = \text{ms-lim}_{n \rightarrow \infty} \sum_{i=1}^n G \left[\frac{x(t_i) + x(t_{i-1})}{2} \right] \times [W(t_i) - W(t_{i-1})] . \quad (\text{A.11})$$

Note that the dependence on $x(t)$ is averaged at the beginning and end of each interval.

Both the Ito and Stratonovich interpretation of stochastic calculus are equivalent. We derive next a relation between the two conventions. Consider a Langevin equation in the Ito convention Eq. (A.2). Write $x(t_i)$ in Eq. (A.11) as,

$$x(t_i) = x(t_{i-1}) + dx(t_{i-1}) , \quad (\text{A.12})$$

where $dx(t_{i-1})$ satisfies Eq. (A.7),

$$dx(t_{i-1}) = f[x(t_{i-1})](t_i - t_{i-1}) + g[x(t_{i-1})][W(t_i) - W(t_{i-1})] . \quad (\text{A.13})$$

Taylor expand the diffusive term in Eq. (A.11),

$$\begin{aligned}
G\left[\frac{x(t_i) + x(t_{i-1})}{2}\right] &= G\left[x(t_{i-1}) + \frac{dx(t_{i-1})}{2}\right] \\
&= G[x(t_{i-1})] + \frac{1}{2} \frac{\partial}{\partial x} G[x(t_{i-1})] dx(t_{i-1}) \\
&\quad + \frac{1}{4} \frac{\partial^2}{\partial x^2} G[x(t_{i-1})] d^2x(t_{i-1}) + \dots \\
&= G[x(t_{i-1})] + \left\{ \frac{1}{2} f[x(t_{i-1})] \frac{\partial}{\partial x} G[x(t_{i-1})] \right. \\
&\quad \left. + \frac{D}{2} g^2[x(t_{i-1})] \frac{\partial^2}{\partial x^2} G[x(t_{i-1})] \right\} (t_i - t_{i-1}) \\
&\quad + \frac{1}{2} g[x(t_{i-1})] \frac{\partial}{\partial x} G[x(t_{i-1})] [W(t_i) - W(t_{i-1})] ,
\end{aligned} \tag{A.14}$$

where we have used $d^2W(t) = 2Ddt$. Hence, we have derived,

$$\begin{aligned}
S \int_{t_0}^t G[x(t')] dW(t') &= \int_{t_0}^t G[x(t')] dW(t') \\
&\quad + D \int_{t_0}^t g[x(t')] \frac{\partial}{\partial x} G[x(t')] dt' ,
\end{aligned} \tag{A.15}$$

where the S in front of the integral in the left hand side of Eq. (A.15) refers to Stratonovich integral as opposed to the integrals in the right hand side which are Ito integrals. This formula gives a connection between the Ito and the Stratonovich interpretation of stochastic calculus. In fact, given the stochastic differential equation interpreted in the Stratonovich sense,

$$\dot{x}(t) = F[x(t)] + G[x(t)]\xi(t) , \tag{A.16}$$

it can be equivalently written as a stochastic differential equation interpreted in the Ito perspective,

$$dx(t) = \left\{ F[x(t)] + DG[x(t)] \frac{\partial}{\partial x} G[x(t)] \right\} dt + G[x(t)] dW(t) , \tag{A.17}$$

and vice and versa. Note that similar rules apply to multivariable Stratonovich and Ito stochastic differential equations.

Appendix **B**

Fokker-Planck equation

There is an associated Fokker-Planck equation to every Langevin equation [23, 73, 22]. While the Langevin equation defines the time evolution of a given state variable in time, the Fokker-Planck equation describes the time evolution of the probability of being in a specific state. Since a Langevin equation can be understood in either the Ito or Stratonovich interpretations, the derivation of the Fokker-Planck equation can also be done under either of the two perspectives. We are using both interpretations in this thesis but modified to include time delay. We thus review in this appendix the steps involved in both interpretations to obtain the Fokker-Planck equation associated to a Markovian Langevin equation.

B.1 Ito interpretation

We derive in this section the Fokker-Planck equation associated to a Langevin equation originally interpreted under the Ito convention [73, 87]. In order to do so, consider a Langevin equation interpreted under the Ito interpretation of stochastic calculus,

$$dx(t) = f[x(t)]dt + g[x(t)]dW(t) , \tag{B.1}$$

where $W(t)$ is a Wiener process with mean $\langle W(t) \rangle = 0$ and variance $\langle W^2(t) \rangle = 2Dt$ where $\langle \dots \rangle$ denotes an ensemble average over all the realizations of $W(t)$ and where D is the intensity of the noise. Consider an arbitrary function $G(x)$ defined on $[a, b]$ and that satisfies the following properties

$$\lim_{x \rightarrow a} G(x) = \lim_{x \rightarrow b} G(x) = 0, \quad (\text{B.2})$$

and

$$\lim_{x \rightarrow a} \frac{d}{dx} G(x) = \lim_{x \rightarrow b} \frac{d}{dx} G(x) = 0. \quad (\text{B.3})$$

With those properties, one can write

$$dG[x(t)] = G[x(t) + dx(t)] - G[x(t)]. \quad (\text{B.4})$$

One can then expand the quantity $G[x(t) + dx(t)]$ in a Taylor series around $x(t)$. Substitute Eq. (B.1) into Eq. (B.4) and keep terms up to the first order in dt ,

$$\begin{aligned} dG[x(t)] = & \left\{ f[x(t)] \frac{d}{dx} G[x(t)] + Dg^2[x(t)] \frac{d^2}{dx^2} G[x(t)] \right\} dt \\ & + g[x(t)] \frac{d}{dx} G[x(t)] dW(t). \end{aligned} \quad (\text{B.5})$$

Equation (B.5) is known as the Ito formula [22]. The ensemble average of $dG[x(t)]$ can be written as

$$\frac{d}{dt} \langle G[x(t)] \rangle = \left\langle f[x(t)] \frac{d}{dx} G[x(t)] + Dg^2[x(t)] \frac{d^2}{dx^2} G[x(t)] \right\rangle, \quad (\text{B.6})$$

where we have used $\langle W(t) \rangle = 0$. Use the definition of the ensemble average with $p(x, t)dx$, the probability that $x \in [x, x + dx]$ at time t ,

$$\int_a^b G(x) \frac{\partial}{\partial t} p(x, t) dx = \int_a^b G(x) \left\{ -\frac{\partial}{\partial x} [f(x)p(x, t)] + D \frac{\partial^2}{\partial x^2} [g^2(x)p(x, t)] \right\} dx, \quad (\text{B.7})$$

where the right-hand side has been integrated by parts with respect to x and where surface terms at $x = \pm\infty$ are zeroes. Since $G(x)$ is arbitrary, then

$$\frac{\partial}{\partial t} p(x, t) = -\frac{\partial}{\partial x} [f(x)p(x, t)] + D \frac{\partial^2}{\partial x^2} [g^2(x)p(x, t)], \quad (\text{B.8})$$

which is the Fokker-Planck equation associated to Eq. (B.1) under the Ito interpretation of stochastic calculus. The stationary probability distribution function $p_s(x)$ associated to Eq. (B.8) satisfies $\dot{p}_s(x) = 0$ and is,

$$p_s(x) = \mathcal{N} |g(x)|^{-2} \exp \left[\frac{1}{D} \int \frac{f(x')}{g^2(x')} dx' \right]. \quad (\text{B.9})$$

where \mathcal{N} is a normalization constant found by imposing conservation of probability over the whole space,

$$1 = \int_{-\infty}^{\infty} p_s(x) dx. \quad (\text{B.10})$$

The derivation of the Fokker-Planck equation using the Stratonovich interpretation is shown next.

B.2 Stratonovich interpretation

Derivation of the Fokker-Planck equation given a Langevin equation under the Stratonovich convention is well known [140]. We review the mathemati-

cal steps under the Stratonovich interpretation of stochastic calculus in this section. Consider a Langevin equation understood in the Stratonovich interpretation,

$$\frac{d}{dt}x(t) = f[x(t)] + g[x(t)]\xi(t) , \quad (\text{B.11})$$

where $f[x(t)]$ and $g[x(t)]$ are respectively the drift and diffusion coefficient, and where $\xi(t)$ is a gaussian white noise with mean $\langle \xi(t) \rangle = 0$ and correlation $\langle \xi(t)\xi(t') \rangle = 2D\delta(t-t')$, where D is the intensity of the randomness. In order to derive the Fokker-Planck equation associated to Eq. (B.11), consider the definition of the probability distribution function

$$p(x, t) = \langle \delta[x - x(t)] \rangle , \quad (\text{B.12})$$

where $x(t)$ is a solution of Eq. (B.11) corresponding to a definite realization of $\xi(t)$ and where the averaging is carried over the set of all realizations of $\xi(t)$. Taking the time derivative in both sides of Eq. (B.12),

$$\frac{\partial}{\partial t}p(x, t) = \left\langle \frac{\partial}{\partial t}\delta[x - x(t)] \right\rangle = - \left\langle \frac{d}{dt}x(t) \frac{\partial}{\partial x}\delta[x - x(t)] \right\rangle . \quad (\text{B.13})$$

The partial derivative involved in the last term of the right hand side of Eq. (B.13) can be taken outside the ensemble average since it is with respect to the non-random variable x . Substitute furthermore Eq. (B.11) into Eq. (B.13),

$$\frac{\partial}{\partial t}p(x, t) = - \frac{\partial}{\partial x} \langle \delta[x - x(t)] \{f[x(t)] + g[x(t)]\xi(t)\} \rangle . \quad (\text{B.14})$$

Consider the following identity [140],

$$\delta[x - x(t)]h[x(t)] \equiv \delta[x - x(t)]h(x) , \quad (\text{B.15})$$

where $h[x(t)]$ is an arbitrary function dependent of the stochastic process $x(t)$ and where $h(x)$ is the same function but dependent of the non-stochastic variable x . With this identity, the drift and diffusion coefficient can be taken outside the ensemble average of Eq. (B.14),

$$\frac{\partial}{\partial t} p(x, t) = -\frac{\partial}{\partial x} [f(x)p(x, t)] - \frac{\partial}{\partial x} \{g(x) \langle \delta[x - x(t)]\xi(t) \rangle\} , \quad (\text{B.16})$$

where we have used Eq. (B.12). To calculate the correlation function of the right-hand side of Eq. (B.16), use the Furutsu-Novikov theorem [103, 104],

$$\begin{aligned} \langle [\delta[x - x(t)]\xi(t)] \rangle &= \langle \delta[x(t) - x] \rangle \langle \xi(t) \rangle \\ &+ \int_0^t \langle \xi(t)\xi(t') \rangle \left\langle \frac{\delta}{\delta\xi(t')} \delta[x(t) - x] \right\rangle dt' . \end{aligned} \quad (\text{B.17})$$

By using the properties of the noise about its mean $\langle \xi(t) \rangle = 0$ and correlation $\langle \xi(t)\xi(t') \rangle = 2D\delta(t - t')$, Eq. (B.17) is

$$\langle [\delta[x - x(t)]\xi(t)] \rangle = D \left\langle \frac{\delta}{\delta\xi(t)} \delta[x(t) - x] \right\rangle . \quad (\text{B.18})$$

Moreover, from the property of the delta function, the right hand side of Eq. (B.18) is

$$\left\langle \frac{\delta}{\delta\xi(t)} \delta[x(t) - x] \right\rangle = - \left\langle \frac{\delta x(t)}{\delta\xi(t)} \frac{\partial}{\partial x} \delta[x(t) - x] \right\rangle . \quad (\text{B.19})$$

We evaluate the functional derivative involved in Eq. (B.19) with respect to $\xi(t')$ and then impose $t = t'$ [98]. In order to do so, integrate Eq. (B.11) with respect to time,

$$x(t) = x(t') + \int_{t'}^t ds \{f[x(s)] + g[x(s)]\xi(s)\} . \quad (\text{B.20})$$

Take then the functional derivative on both sides,

$$\frac{\delta x(t)}{\delta \xi(t')} = \int_{t'}^t ds \left\{ \frac{\partial f}{\partial x} \frac{\delta x(s)}{\delta \xi(t')} + \xi(s) \frac{\partial g}{\partial x} \frac{\delta x(s)}{\delta \xi(t')} + g[x(s)] \frac{\delta \xi(s)}{\delta \xi(t')} \right\}. \quad (\text{B.21})$$

Equation (B.21) must satisfy the *causality condition*. In fact, the stochastic process $x(t)$ depend functionally only on values of $\xi(t')$ which come earlier in terms of t in the interval $0 \leq t' \leq t$. It follows that the function derivative is zero outside this time interval,

$$\frac{\delta x(t)}{\delta \xi(t')} = 0 \quad , \quad \text{if } t' < 0 \text{ , or if } t' > t \text{ ,} \quad (\text{B.22})$$

which is called the causality condition. We further use the following property of the functional derivative,

$$\frac{\delta \xi(s)}{\delta \xi(t')} = \delta(s - t') \text{ ,} \quad (\text{B.23})$$

and integrate term proportional to the delta function to write Eq. (B.21),

$$\frac{\delta x(t)}{\delta \xi(t')} = H(t - t') \left\{ g[x(t')] + \int_{t'}^t ds \left[\frac{\partial f}{\partial x} \frac{\delta x(s)}{\delta \xi(t')} + \xi(s) \frac{\partial g}{\partial x} \frac{\delta x(s)}{\delta \xi(t')} \right] \right\} \text{ ,} \quad (\text{B.24})$$

where the causality condition has been taken into account by the introduction of the step function $H(t - t') = 1$ if $t \leq t'$ and $H(t - t') = 0$ otherwise. At $t = t'$, we have,

$$\frac{\delta x(t)}{\delta \xi(t)} = g[x(t)] \text{ .} \quad (\text{B.25})$$

Substitute Eq. (B.25) and Eq. (B.19) in Eq. (B.18),

$$\langle [\delta[x - x(t)]\xi(t)] \rangle = -D \frac{\partial}{\partial x} \langle g[x(t)]\delta[x(t) - x] \rangle \text{ .} \quad (\text{B.26})$$

Use the identity Eq. (B.15) to take the diffusion coefficient out of the ensemble average of Eq. (B.26) and use the definition of the probability distribution function [Eq. (B.12)] so that

$$\langle [\delta[x - x(t)]\xi(t)] \rangle = -D \frac{\partial}{\partial x} [g(x)p(x, t)] . \quad (\text{B.27})$$

Substituting Eq. (B.27) in Eq. (B.16) leads to the Fokker-Planck equation,

$$\frac{\partial}{\partial t} p(x, t) = -\frac{\partial}{\partial x} [f(x)p(x, t)] + D \frac{\partial}{\partial x} \left\{ g(x) \frac{\partial}{\partial x} [g(x)p(x, t)] \right\} , \quad (\text{B.28})$$

which can equivalently be written as

$$\begin{aligned} \frac{\partial}{\partial t} p(x, t) = & -\frac{\partial}{\partial x} \left\{ \left[f(x) + Dg(x) \frac{\partial g(x)}{\partial x} \right] p(x, t) \right\} \\ & + D \frac{\partial^2}{\partial x^2} [g^2(x)p(x, t)] . \end{aligned} \quad (\text{B.29})$$

The term proportional to D in the first term of the right hand side of Eq. (B.29) is called the noise-induced drift. It is a direct consequence of the Stratonovich interpretation of Eq. (B.11). The stationary solution of Eq. (B.29) satisfies $\partial_t p(x) = 0$ and leads to the solution,

$$p(x) = \mathcal{N} |g(x)|^{-1} \exp \left[\frac{1}{D} \int \frac{f(x')}{g^2(x')} dx' \right] , \quad (\text{B.30})$$

where \mathcal{N} is a normalization constant found by imposing conservation of probability,

$$1 = \int_{-\infty}^{\infty} p(x) dx . \quad (\text{B.31})$$

If the Langevin equation is additive, $g[x(t)] = 1$, and the Fokker-Planck equation [Eq. (B.29)] is

$$\frac{\partial}{\partial t} p(x, t) = -\frac{\partial}{\partial x} [f(x)p(x, t)] + D \frac{\partial^2}{\partial x^2} p(x, t) . \quad (\text{B.32})$$

The same expression would be obtained under the Ito interpretation. There is thus no difference between the Fokker-Planck equation derived either from the Ito or the Stratonovich interpretation if the noise is additive.

Appendix C

Integration method with delay

A second order numerical integration method is derived in this section in order to include delay in the algorithm. The derivation is based on a known second order numerical methods without delay [96]. Consider a Langevin equation of the form,

$$\dot{x}(t) = f[x(t)] + bx(t - \tau) + g[x(t)]\xi(t) + \eta(t) , \quad (\text{C.1})$$

where $f[x(t)]$ and $g[x(t)]$ are respectively the drift and the diffusion coefficient, where b is the intensity of the feedback loop, $\tau > 0$ is the time delay, and where $\xi(t)$ and $\eta(t)$ are two Gaussian white noises with mean $\langle \xi(t) \rangle = \langle \eta(t) \rangle = 0$ and correlation $\langle \xi(t)\xi(t') \rangle = 2D\delta(t-t')$, $\langle \eta(t)\eta(t') \rangle = 2K\delta(t-t')$, and $\langle \xi(t)\eta(t') \rangle = 0$, where D and K are respectively the intensity of the stochastic process $\xi(t)$ and $\eta(t)$. The algorithm focuses on cases where delayed feedback enters only linearly in Eq. (C.1), although it can be generalized for any function including time delay. Integrate Eq. (C.1) over the time interval $[t, t + \Delta t]$,

$$x(t + \Delta t) = x(t) + \int_t^{t+\Delta t} \{f[x(t')] + bx(t' - \tau) + g[x(t')]\xi(t') + \eta(t')\} dt' , \quad (\text{C.2})$$

and expands the drift $f[x(t')]$ and diffusion $g[x(t')]$ coefficient in power series around $x(t)$,

$$f[x(t')] \approx f_0[x(t)] + f_1[x(t)][x(t') - x(t)] , \quad (\text{C.3})$$

$$g[x(t')] \approx g_0[x(t)] + g_1[x(t)][x(t') - x(t)] , \quad (\text{C.4})$$

where the indices $\{0, 1\}$ are respectively the zeroth and first derivative with respect to x . The integrand $x(t')$ is found by further integrating Eq. (C.1),

$$x(t') = x(t) + \int_t^{t'} \{f[x(t'')] + bx(t'' - \tau) + g[x(t'')]\xi(t'') + \eta(t'')\} dt'' . \quad (\text{C.5})$$

Approximate the integrands by their value evaluated at the lower bound, i.e. $f[x(t'')] \approx f_0[x(t)]$, $x(t'' - \tau) \approx x(t - \tau)$, and $g[x(t'')] \approx g_0[x(t)]$,

$$\begin{aligned} x(t') = & x(t) + \{f_0[x(t)] + bx(t - \tau)\} (t' - t) + g_0[x(t)] \int_t^{t'} \xi(t'') dt'' \\ & + \int_t^{t'} \eta(t'') dt'' . \end{aligned} \quad (\text{C.6})$$

Substitute then Eq. (C.6) as well as Eqs. (C.3) and (C.4) into Eq. (C.2) leads to

$$\begin{aligned}
 x(t + \Delta t) = & x(t) + f_0[x(t)]\Delta t + g_0[x(t)] \int_t^{t+\Delta t} \xi(t')dt' \\
 & + f_1[x(t)] \left\{ \{f_0[x(t)] + bx(t - \tau)\} \frac{\Delta t^2}{2} \right. \\
 & \quad + g_0[x(t)] \int_t^{t+\Delta t} \int_t^{t'} \xi(t'')dt''dt' \\
 & \quad \left. + \int_t^{t+\Delta t} \int_t^{t'} \eta(t'')dt''dt' \right\} \\
 & + b \left\{ x(t - \tau)\Delta t + \{f_0[x(t - \tau)] + bx(t - 2\tau)\} \frac{\Delta t^2}{2} \right. \\
 & \quad + g_0[x(t - \tau)] \int_t^{t+\Delta t} \int_{t-\tau}^{t'-\tau} \xi(t'')dt''dt' \\
 & \quad \left. + \int_t^{t+\Delta t} \int_{t-\tau}^{t'-\tau} \eta(t'')dt''dt' \right\} \\
 & + g_1[x(t)] \left\{ \{f_0[x(t)] + bx(t - \tau)\} \int_t^{t+\Delta t} (t' - t)\xi(t')dt' \right. \\
 & \quad + g_0[x(t)] \int_t^{t+\Delta t} \int_t^{t'} \xi(t')\xi(t'')dt''dt' \\
 & \quad \left. + \int_t^{t+\Delta t} \int_t^{t'} \xi(t')\eta(t'')dt''dt' \right\} \\
 & + \int_t^{t+\Delta t} \eta(t')dt' .
 \end{aligned} \tag{C.7}$$

In order to calculate the integrals containing the random processes $\xi(t)$ and $\eta(t)$, we define

$$G_1(t, \Delta t) = \int_t^{t+\Delta t} \xi(t') dt' , \quad (\text{C.8})$$

$$G_2(t, \Delta t) = \int_t^{t+\Delta t} \int_t^{t'} \xi(t'') dt'' dt' , \quad (\text{C.9})$$

$$H_1(t, \Delta t) = \int_t^{t+\Delta t} \eta(t') dt' , \quad (\text{C.10})$$

$$H_2(t, \Delta t) = \int_t^{t+\Delta t} \int_t^{t'} \eta(t'') dt'' dt' . \quad (\text{C.11})$$

If $\eta(t)$ and $\xi(t)$ are two Gaussian processes of zero mean, G_1 , G_2 , H_1 , and H_2 , are also Gaussian variables of zero mean, and correlations

$$\langle G_1^2 \rangle = 2D\Delta t , \quad (\text{C.12})$$

$$\langle G_2^2 \rangle = \frac{2D}{3}\Delta t^3 , \quad (\text{C.13})$$

$$\langle G_1 G_2 \rangle = D\Delta t^2 , \quad (\text{C.14})$$

$$\langle H_1^2 \rangle = 2K\Delta t , \quad (\text{C.15})$$

$$\langle H_2^2 \rangle = \frac{2K}{3}\Delta t^3 , \quad (\text{C.16})$$

$$\langle H_1 H_2 \rangle = K\Delta t^2 , \quad (\text{C.17})$$

$$\langle G_1 H_2 \rangle = 0 , \quad (\text{C.18})$$

$$\langle G_2 H_1 \rangle = 0 . \quad (\text{C.19})$$

The three remaining integrals can be expressed in terms of G_1 and G_2 , and H_1 and H_2 , as

$$\int_t^{t+\Delta t} (t' - t)\xi(t')dt' = G_1(t, \Delta t)\Delta t - G_2(t, \Delta t), \quad (\text{C.20})$$

$$\int_t^{t+\Delta t} \int_t^{t'} \xi(t')\xi(t'')dt''dt' = \frac{1}{2}G_1^2(t, \Delta t), \quad (\text{C.21})$$

$$\int_t^{t+\Delta t} \int_{t-\tau}^{t'-\tau} \xi(t'')dt''dt' = G_2(t - \tau, \Delta t), \quad (\text{C.22})$$

$$\int_t^{t+\Delta t} (t' - t)\eta(t')dt' = H_1(t, \Delta t)\Delta t - H_2(t, \Delta t), \quad (\text{C.23})$$

$$\int_t^{t+\Delta t} \int_t^{t'} \eta(t')\eta(t'')dt''dt' = \frac{1}{2}H_1^2(t, \Delta t), \quad (\text{C.24})$$

$$\int_t^{t+\Delta t} \int_{t-\tau}^{t'-\tau} \eta(t'')dt''dt' = H_2(t - \tau, \Delta t), \quad (\text{C.25})$$

$$\int_t^{t+\Delta t} \int_t^{t'} \xi(t')\eta(t'')dt''dt' = 0. \quad (\text{C.26})$$

The Gaussian variables G_1 and G_2 as well as H_1 and H_2 can be simulated with four Gaussian random variables, $\Psi_1(t)$ and $\Psi_2(t)$, and $\Psi'_1(t)$ and $\Psi'_2(t)$, of zero mean and variance one:

$$G_1(t, \Delta t) = \sqrt{2D\Delta t}\Psi_1(t), \quad (\text{C.27})$$

$$G_2(t, \Delta t) = \sqrt{\frac{2D}{3}\Delta t^3} \left[\frac{\sqrt{3}}{2}\Psi_1(t) + \frac{1}{2}\Psi_2(t) \right], \quad (\text{C.28})$$

$$H_1(t, \Delta t) = \sqrt{2K\Delta t}\Psi'_1(t), \quad (\text{C.29})$$

$$H_2(t, \Delta t) = \sqrt{\frac{2K}{3}\Delta t^3} \left[\frac{\sqrt{3}}{2}\Psi'_1(t) + \frac{1}{2}\Psi'_2(t) \right]. \quad (\text{C.30})$$

Combining all our results, we write the iteration of our algorithm,

$$\begin{aligned}
x(t + \Delta t) = & x(t) + f_0[x(t)]\Delta t + f_1[x(t)] \left\{ \{f_0[x(t)] + bx(t - \tau)\} \frac{\Delta t^2}{2} \right. \\
& \left. + g_0[x(t)]G_2(t, \Delta t) + H_2(t, \Delta t) \right\} \\
& + b \left\{ x(t - \tau)\Delta t + \{f_0[x(t - \tau)] + bx(t - 2\tau)\} \frac{\Delta t^2}{2} \right. \\
& \left. + g_0[x(t - \tau)]G_2(t - \tau, \Delta t) + H_2(t - \tau, \Delta t) \right\} \quad (\text{C.31}) \\
& + g_0[x(t)]G_1(t, \Delta t) + g_1[x(t)] \left\{ \{f_0[x(t)] + bx(t - \tau)\} \times \right. \\
& \left. [G_1(t, \Delta t)\Delta t - G_2(t, \Delta t)] + \frac{1}{2}g_0[x(t)]G_1^2(t, \Delta t) \right\} \\
& + H_1(t, \Delta t) .
\end{aligned}$$

Consider Eq. (1.10) with additive noise ($D = 0$ and $K = 1$). We have $f_0[x(t)] = ax(t) - \gamma x^3(t)$, $f_1[x(t)] = a - 3\gamma x^2(t)$, $g_0[x(t)] = 1$, and $g_1[x(t)] = 0$, leading to,

$$\begin{aligned}
x(t + \Delta t) = & x(t) \left(1 + a\Delta t + \frac{1}{2}a^2\Delta t^2 \right) + H_1(t, \Delta t) \\
& + aH_2(t, \Delta t) + bH_2(t - \tau, \Delta t) - 3\gamma x^2(t)H_2(t, \Delta t) \\
& + bx(t - \tau)(1 + a\Delta t)\Delta t - \gamma x^3(t)(1 + 2a\Delta t)\Delta t \quad (\text{C.32}) \\
& + \frac{1}{2}b^2x(t - 2\tau)\Delta t^2 + \frac{3}{2}\gamma^2x^5(t)\Delta t^2 \\
& - \frac{3}{2}\gamma bx(t - \tau)x^2(t)\Delta t^2 - \frac{1}{2}b\gamma x^3(t - \tau)\Delta t^2 .
\end{aligned}$$

However, with multiplicative noise ($D = 1$ and $K = 0$), Eq. (1.10) has $f_0[x(t)] = ax(t) - \gamma x^3(t)$, $f_1[x(t)] = a - 3\gamma x^2(t)$, $g_0[x(t)] = x(t)$, and $g_1[x(t)] =$

1, and the algorithm is,

$$\begin{aligned}
x(t + \Delta t) = x(t) & \left[1 + a\Delta t + a^2 \frac{\Delta t^2}{2} + (1 + a\Delta t)G_1(t, \Delta t) \right. \\
& \left. + \frac{1}{2}(G_1(t, \Delta t))^2 \right] \\
& + bx(t - \tau) \left[\Delta t + a\Delta t^2 + \Delta t G_1(t, \Delta t) - G_2(t, \Delta t) \right. \\
& \left. + G_2(t - \tau, \Delta t) \right] \tag{C.33} \\
& - \gamma x^3(t) \left[2a\Delta t^2 + (G_1(t, \Delta t) + 1)\Delta t + 2G_2(t, \Delta t) \right] \\
& - \gamma x^2(t)x(t - \tau) \left(\frac{3b\Delta t^2}{2} \right) - \gamma x^3(t - \tau) \left(\frac{b\Delta t^2}{2} \right) \\
& + \gamma^2 x^5(t) \left(\frac{3\Delta t^2}{2} \right) + x(t - 2\tau) \left(b^2 \frac{\Delta t^2}{2} \right) .
\end{aligned}$$

Equations (C.32) and (C.33) are the algorithms used in this thesis to determine the bifurcation threshold of the equations considered.

Appendix **D**

Jung-Risken theory

The correlation function and correlation time of Markovian stochastic differential equation can be calculated exactly from the so-called Jung-Risken theory [83]. Consider a Langevin equation of the form

$$\dot{x}(t) = h(x) + g(x)\xi(t) , \quad (\text{D.1})$$

where $h(x)$ and $g(x)$ are respectively the drift and the diffusion coefficient and where $\xi(t)$ is a Gaussian white noise with mean $\langle \xi(t) \rangle = 0$ and correlation $\langle \xi(t)\xi(t') \rangle = 2D\delta(t-t')$, where D is the intensity of the noise. Equation (D.1) is understood under the Stratonovich interpretation of stochastic calculus. Its corresponding Fokker-Planck equation is given by Eq. (B.29). Define the Fokker-Planck operator \mathcal{L} as

$$\mathcal{L} = -\frac{\partial}{\partial x} \left[h(x) + Dg(x)\frac{\partial g(x)}{\partial x} \right] + D\frac{\partial^2}{\partial x^2}g^2(x) , \quad (\text{D.2})$$

so that the Fokker-Planck equation is

$$\frac{\partial}{\partial t}p(x,t) = \mathcal{L}p(x,t) . \quad (\text{D.3})$$

Assume also that $p(x, t)$ vanishes at the boundaries $x = 0$ and $x = \infty$. The stationary probability distribution function of Eq. (D.3) is given by Eq. (B.30). Furthermore, the moments of the stationary distribution $p(x)$ are defined by

$$\langle x^n \rangle = \int_0^\infty x^n p(x) dx . \quad (\text{D.4})$$

Define the correlation function $C(t')$ of the state variable x so that

$$C(t') = \langle \Delta x(t + t') \Delta x(t) \rangle , \quad (\text{D.5})$$

where $\Delta x = x - \langle x \rangle$. Several normalizations of the correlation function exist in the literature depending on the system under study. For example, the correlation function is normalized by the squared of the first moment in [82, 141, 142]. We choose to normalize the correlation function $C(t')$ by its variance $C(0) = \langle x^2 \rangle - \langle x \rangle^2$. This choice is also used in [129, 39]. The correlation time is defined as the area under the normalized correlation function,

$$T = \frac{1}{C(0)} \int_0^\infty C(t') dt' . \quad (\text{D.6})$$

We simplify the definition of the correlation time [Eq. (D.6)] in this appendix to obtain an expression that we can compute numerically. In order to do so, use the definition of the correlation function with respect to the joint probability density $p_2(x_1, t_1; x_2, t_2)$ [73]

$$C(t') = \int_0^\infty \int_0^\infty p_2(x_1, t + t'; x_2, t) \Delta x_1 \Delta x_2 dx_1 dx_2 . \quad (\text{D.7})$$

Introduce the transition probability $W(x_1, t' | x_2, 0)$ and the stationary probability distribution function $p(x_2)$ to rewrite the joint probability distribution

function as

$$p_2(x_1, t + t'; x_2, t) = W(x_1, t' | x_2, 0) p(x_2) . \quad (\text{D.8})$$

The transition probability $W(x_1, t' | x_2, 0)$ satisfies the Fokker-Planck equation

$$\frac{\partial}{\partial t} W(x_1, t' | x_2, 0) = \mathcal{L} W(x_1, t' | x_2, 0) . \quad (\text{D.9})$$

A formal solution of Eq. (D.9) with initial condition $W(x_1, 0 | x_2, 0) = \delta(x_1 - x_2)$ is

$$W(x_1, t' | x_2, 0) = e^{\mathcal{L}t'} \delta(x_1 - x_2) . \quad (\text{D.10})$$

Substitute Eq. (D.10) into Eq. (D.8) and use the resulting expression in Eq. (D.7). Integrate then by parts [134, 73] to obtain

$$C(t') = \int_0^\infty \Delta x_1 e^{\mathcal{L}t'} \Delta x_1 p(x_1) dx_1 . \quad (\text{D.11})$$

We make the change of variable $x_1 \rightarrow x$ to simplify the notation. We next define time-dependent terms in Eq. (D.11) as a new function

$$\hat{p}(x, t') = e^{\mathcal{L}t'} \Delta x p(x) . \quad (\text{D.12})$$

This new function satisfies the Fokker-Planck equation

$$\frac{\partial}{\partial t'} \hat{p}(x, t') = \mathcal{L} \hat{p}(x, t') , \quad (\text{D.13})$$

with initial condition $\hat{p}(x, 0) = \Delta x p(x)$. In those terms, Eq. (D.11) is

$$C(t') = \int_0^\infty \Delta x \hat{p}(x, t') dx . \quad (\text{D.14})$$

Substitute Eq. (D.14) into the definition of the correlation time, Eq. (D.6),

$$T = \frac{1}{C(0)} \int_0^\infty \Delta x dx \int_0^\infty \hat{p}(x, t') dt' , \quad (\text{D.15})$$

and define further a new function $\psi(x)$ so that

$$\psi(x) = \int_0^\infty \hat{p}(x, t') dt' . \quad (\text{D.16})$$

Integrate then the Fokker-Planck equation defined in Eq. (D.13) with respect to time and use the initial condition $\hat{p}(x, 0) = \Delta x p(x)$ to derive

$$-\Delta x p(x) = \mathcal{L}\psi(x) . \quad (\text{D.17})$$

Integrate then Eq. (D.17) with respect to x and use the formal form of the Fokker-Planck operator,

$$- \left[h(x) + Dg(x) \frac{\partial g(x)}{\partial x} \right] \psi(x) + D \frac{\partial}{\partial x} [g^2(x)\psi(x)] = f(x) , \quad (\text{D.18})$$

where

$$f(x) = - \int_0^x \Delta x' p(x') dx' . \quad (\text{D.19})$$

The homogeneous solution of Eq. (D.18) is the stationary probability distribution function and leads to a vanishing term. The inhomogeneous solution has the form

$$\psi(x) = p(x) \int_0^x \frac{f(x')}{g^2(x')p(x')} dx' . \quad (\text{D.20})$$

Substitute Eq. (D.20) into Eq. (D.15) and integrate by parts. It yields to a simple expression for the correlation time

$$T = \frac{1}{C(0)} \int_0^\infty \frac{f^2(x')}{g^2(x')p_s(x')} dx' . \quad (\text{D.21})$$

We use this simplified expression on Eq. (1.10) without delayed feedback ($b = 0$),

$$\dot{x}(t) = ax(t) - \gamma x^3(t) + \sqrt{D}x(t)\xi(t) , \quad (\text{D.22})$$

where a , γ , and D are constants, and where $\xi(t)$ is a Gaussian white noise with mean $\langle \xi(t) \rangle = 0$ and correlation $\langle \xi(t)\xi(t') \rangle = 2\delta(t-t')$. Results are known for this expression [83]. Its stationary probability density $p_s(x)$ is found from Eq. (B.30)

$$p(x) = 2(\beta\gamma)^{\beta a} \Gamma^{-1}(\beta a) |x|^{2\beta a - 1} e^{-\beta\gamma x^2} , \quad (\text{D.23})$$

where $\beta = (2D)^{-1}$, and where $\Gamma(x)$ is the gamma function. In those terms, the stochastic threshold is located at $a_c = 0$. Furthermore, the n^{th} moment of the state variable is

$$\langle x^n \rangle = \int_0^\infty x^n p(x) dx = (\beta\gamma)^{-n/2} \Gamma^{-1}(\beta a) \Gamma(\beta a + n/2) . \quad (\text{D.24})$$

Substitute Eq. (D.23) into Eq. (D.19) so that

$$f(x) = \langle x \rangle [P(\beta a, \beta\gamma x^2) - P(\beta a + 1/2, \beta\gamma x^2)] , \quad (\text{D.25})$$

where $P(\eta, \omega)$ is the incomplete gamma function defined by

$$P(\eta, \omega) = \Gamma^{-1}(\eta) \int_0^\omega q^{\eta-1} e^{-q} dq . \quad (\text{D.26})$$

Using the $n = 1$ and $n = 2$ moment of Eq. (D.24), together with $g(x) = D^{1/2}x$ and Eq. (D.25), the correlation time corresponding to the random process described by Eq. (D.22) is

$$T = \frac{\beta(\beta\gamma)^{-\beta a}\Gamma(\beta a + 1)\Gamma^2(\beta a + 1/2)}{\Gamma^2(\beta a + 1) - (\beta a)\Gamma^2(\beta a + 1/2)} \times \int_0^\infty \frac{[P(\beta a, \beta\gamma x^2) - P(\beta a + 1/2, \beta\gamma x^2)]^2}{|x|^{2\beta a + 1}e^{-\beta\gamma x^2}} dx . \quad (\text{D.27})$$

Equation (D.27) can be evaluated numerically. Moreover, one can expand Eq. (D.27) for large and small intensity of the noise D and derive a Padé approximant from the results of the expansion. Padé approximant is a tool to express a function originally in power series by a rational function [143]. We perform next this approximation. Consider first the expansion of the correlation time for small noise intensity. In order to do so, we use a scaled version of Eq. (D.22). In fact, perform first the change of variable $x = (a/\gamma)^{1/2}x'$ so that Eq. (D.22) is,

$$\left(\frac{a}{\gamma}\right)^{1/2} \frac{d}{dt}x'(t) = a \left(\frac{a}{\gamma}\right)^{1/2} x'(t) - \gamma \left(\frac{a}{\gamma}\right)^{3/2} x'^3(t) + \left(\frac{a}{\gamma}\right)^{1/2} x'(t)\xi(t) . \quad (\text{D.28})$$

Eliminate then γ from Eq. (D.28) and divide both sides by a . Rescale further time $t' = at$ and the intensity of the noise $D' = D/a$ to obtain the reduced equation

$$\dot{x}'(t') = x'(t') - x'^3(t') + x'(t')\xi'(t') , \quad (\text{D.29})$$

where $\xi'(t')$ is a Gaussian white noise with mean $\langle \xi'(t') \rangle = 0$ and correlation $\langle \xi'(t')\xi'(t'') \rangle = 2D'\delta(t' - t'')$. Consider then the stationary probability distribution function defined in Eq. (D.23). This quantity has extremum at

$x' = \pm\sqrt{1 - D'}$. Consider then the change of variable

$$q = 1 + \sqrt{D'}x' , \quad (\text{D.30})$$

and write the Fokker-Planck operator associated to Eq. (D.29),

$$\mathcal{L} = -\frac{\partial}{\partial q} [(1 + D')q - q^3] + D' \frac{\partial^2}{\partial q^2} q^2 , \quad (\text{D.31})$$

in terms of the new variable Eq. (D.30),

$$\begin{aligned} \mathcal{L} = & 2\frac{\partial}{\partial x}x + \frac{\partial^2}{\partial x^2} + (D')^{1/2} \left[\frac{\partial}{\partial x}(3x^2 - 1) + 2\frac{\partial^2}{\partial x^2}x \right] \\ & + D' \left[\frac{\partial}{\partial x}(x^3 - x) + \frac{\partial^2}{\partial x^2}x^2 \right] , \end{aligned} \quad (\text{D.32})$$

where we have made the change of variable $x' \rightarrow x$ to simplify the notation.

Furthermore, the adjoint of the Fokker-Planck operator [Eq. (D.32)] is,

$$\begin{aligned} \mathcal{L}^\dagger = & -2x\frac{\partial}{\partial x} + \frac{\partial^2}{\partial x^2} + (D')^{1/2} \left[-(3x^2 - 1)\frac{\partial}{\partial x} + 2x\frac{\partial^2}{\partial x^2} \right] \\ & + D' \left[-(x^3 - x)\frac{\partial}{\partial x} + x^2\frac{\partial^2}{\partial x^2} \right] . \end{aligned} \quad (\text{D.33})$$

We first compute the moments $M_n = \langle x^n \rangle$. Use the following identity

$$\int (\mathcal{L}^\dagger x^n) p(x) dx = 0 , \quad (\text{D.34})$$

together with

$$\begin{aligned} \mathcal{L}^\dagger x^n = & -2x(nx^{n-1}) + n(n-1)x^{n-2} \\ & + (D')^{1/2} [-(3x^2 - 1)(nx^{n-1}) + 2xn(n-1)x^{n-2}] \\ & + D' [(x - x^3)(nx^{n-1}) + x^2n(n-1)x^{n-2}] , \end{aligned} \quad (\text{D.35})$$

Coefficients $M_n^{(\nu)}$ of the moment							
$\nu \backslash n$	0	1	2	3	4	5	6
0	1	-1/4	1/2	-1/8	3/4	5/16	15/8
1	0	1/32	-1/16	3/16	-7/16		
2	0	5/128	5/64				

Table D.1: Coefficients $M_n^{(\nu)}$ of the expansion defined in Eq. (D.37) of the moment $M_n = \langle x^n \rangle$.

in order to obtain the relations,

$$0 = -2M_n + (n-1)M_{n-2} + (D')^{1/2} [(2n-1)M_{n-1} - 3M_{n+1}] + D' [nM_n - M_{n+2}] . \quad (\text{D.36})$$

To find the moments M_n , insert the following expansions,

$$M_{2n} = \sum_{\nu=0}^{\infty} (D')^{\nu} M_{2n}^{(\nu)} \quad (\text{D.37})$$

$$M_{2n+1} = \sqrt{D'} \sum_{\nu=0}^{\infty} (D')^{\nu} M_{2n+1}^{(\nu)} ,$$

in Eq. (D.36). The coefficients $M_n^{(\nu)}$ then obtained are shown in Tab. D.1. We can further obtain expansions for the correlation function $K(t')$ defined as

$$K(t') = \langle \Delta x^n(t+t') \Delta x(t) \rangle = \langle x^n(t+t') x(t) \rangle - \langle x^n \rangle \langle x \rangle . \quad (\text{D.38})$$

In fact, take the time derivative on both sides of Eq. (D.38) and use

$$\langle x^n(t+t')x(t) \rangle = \int x^n e^{\mathcal{L}t'} xp(x) dx , \quad (\text{D.39})$$

and

$$\frac{d}{dt'} \langle x^n(t+t')x(t) \rangle = \int (\mathcal{L}^\dagger x^n) e^{\mathcal{L}t'} xp(x) dx , \quad (\text{D.40})$$

to obtain an hierarchy of differential equations

$$\begin{aligned} \dot{K}_n = & n\{-2K_n + (n-1)K_{n-2} \\ & + (D')^{1/2} [(2n-1)K_{n-1} - 3K_{n+1}] + D' [nK_n - K_{n+2}] \} , \end{aligned} \quad (\text{D.41})$$

where $K_n = 0$ for $n \leq 0$. Terms involving the moments M_n vanish because of Eq. (D.36). The initial conditions of K_n are thus given by

$$K_n(0) = M_{n+1} - M_1 M_n . \quad (\text{D.42})$$

The initial condition $K_n(0)$ can be found by inserting the expansions

$$\begin{aligned} K_{2n}(0) &= \sqrt{D'} \sum_{\nu=0}^{\infty} (D')^\nu K_{2n}^{(\nu)}(0) \\ K_{2n+1}(0) &= \sum_{\nu=0}^{\infty} (D')^\nu K_{2n+1}^{(\nu)}(0) , \end{aligned} \quad (\text{D.43})$$

in Eq. (D.42). The coefficients $K_n^{(\nu)}(0)$ then obtained are shown in Tab. D.2. We then define the scaled correlation times $T'_n = aT_n$ according to Eq. (D.6), but not normalized by the variance,

$$T'_n = \int_0^{\infty} K_n(t') dt' . \quad (\text{D.44})$$

Coefficients $K_n^{(\nu)}(0)$ of the correlation function					
$\nu \backslash n$	1	2	3	4	5
0	1/2	0	3/4	1/2	15/8
1	-1/8	5/32	-15/32		
2	-1/16				

Table D.2: Coefficients $K_n^{(\nu)}(0)$ of the expansion defined in Eq. (D.43) of the correlation function $K(t') = \langle x^n(t+t')x(t) \rangle - \langle x^n \rangle \langle x \rangle$ evaluated at $t' = 0$.

With this definition, we obtain by using Eq. (D.41),

$$\begin{aligned}
 -K_n(0) = & n\{-2T'_n + (n-1)T'_{n-2} \\
 & + (D')^{1/2} [(2n-1)T'_{n-1} - 3T'_{n+1}] + D' [nT'_n - T'_{n+2}]\}.
 \end{aligned} \tag{D.45}$$

The correlation time T'_n are found by inserting the expansions

$$\begin{aligned}
 T'_{2n} &= \sum_{\nu=0}^{\infty} (D')^{\nu} T'_{2n}^{(\nu)} \\
 T'_{2n+1} &= \sqrt{D'} \sum_{\nu=0}^{\infty} (D')^{\nu} T'_{2n+1}^{(\nu)}.
 \end{aligned} \tag{D.46}$$

in Eq. (D.45). Results for these coefficients are shown in Tab. D.3. The correlation time T normalized by the variance, in terms of the original variables

Coefficients $T_n^{(\nu)}$ of the scaled correlation time					
$\nu \backslash n$	1	2	3	4	5
0	1/4	-3/16	3/8	-5/16	15/16
1	5/32	-1/64	-11/64		
2	-1/64				

Table D.3: Coefficients $T_n^{(\nu)}$ of the expansion of the scaled correlation time T_n , Eq. (D.46).

is,

$$T = \frac{T_1}{K_1(0)} = \frac{1}{2a} + \frac{7D}{16a^2} + \frac{9D^2}{64a^3} + \mathcal{O}\left(\frac{D^3}{a^4}\right). \quad (\text{D.47})$$

Note that Eq. (D.47) is independent of γ . Equation (D.47) constitutes the expansion of the correlation time for small noise intensity. The limit of Eq. (D.27) as the intensity of the noise D is large can also be obtained. In fact, consider the following identity [139],

$$P(\beta a, \beta \gamma x^2) = P(\beta a + 1, \beta \gamma x^2) + (\beta \gamma x^2)^{\beta a} e^{-\beta \gamma x^2} \Gamma^{-1}(\beta a + 1), \quad (\text{D.48})$$

where $P(\eta, \omega)$ is the incomplete gamma function defined as

$$P(\eta, \omega) = \int_0^\omega t^{\eta-1} e^{-t} dt. \quad (\text{D.49})$$

Use this identity to rewrite the function $f(x)$ [Eq. (D.25)] as follows,

$$f(x) = \langle x \rangle \left[P(\beta a + 1, \beta \gamma x^2) + (\beta \gamma x^2)^{\beta a} e^{-\beta \gamma x^2} \Gamma^{-1}(\beta a + 1) - P(\beta a + 1/2, \beta \gamma x^2) \right]. \quad (\text{D.50})$$

Substitution of Eq. (D.50) in the expression of the correlation time Eq. (D.21)

leads to three terms $T = T_1 + T_2 + T_3$,

$$T_1 = \frac{\langle x \rangle^2}{C(0)} \int_0^\infty (\beta \gamma x) \frac{\beta [P(\beta a + 1, \beta \gamma x^2) - P(\beta a + 1/2, \beta \gamma x^2)]^2}{2\Gamma^{-1}(\beta a)(\beta \gamma x^2)^{\beta a + 1} e^{-\beta \gamma x^2}} dx, \quad (\text{D.51})$$

$$T_2 = \frac{\langle x \rangle^2}{C(0)} \int_0^\infty (2\beta \gamma x) \frac{\beta \Gamma^{-1}(\beta a + 1)(\beta \gamma x^2)^{\beta a} e^{-\beta \gamma x^2}}{\Gamma^{-1}(\beta a)(\beta \gamma x^2)^{\beta a + 1} e^{-\beta \gamma x^2}} \times [P(\beta a + 1, \beta \gamma x^2) - P(\beta a + 1/2, \beta \gamma x^2)] dx, \quad (\text{D.52})$$

$$T_3 = \frac{\langle x \rangle^2}{C(0)} \int_0^\infty (\beta \gamma x) \frac{\beta \Gamma^{-2}(\beta a + 1)(\beta \gamma x^2)^{2\beta a} e^{-2\beta \gamma x^2}}{2\Gamma^{-1}(\beta a)(\beta \gamma x^2)^{\beta a + 1} e^{-\beta \gamma x^2}} dx. \quad (\text{D.53})$$

Consider the first term, Eq. (D.51). Make the change of variable $z = \beta \gamma x^2$ and define the integral

$$I_2(\beta) = \int_0^\infty z^{-(\beta a + 1)} e^z [P(\beta a + 1, z) - P(\beta a + 1/2, z)]^2 dz. \quad (\text{D.54})$$

In those terms, Eq. (D.51) is

$$T_1 = \frac{\beta}{2} \frac{\Gamma(\beta a + 1)\Gamma^2(\beta a + 1/2)}{[\Gamma^2(\beta a + 1) - (\beta a)\Gamma^2(\beta a + 1/2)]} I_2(\beta). \quad (\text{D.55})$$

The same change of variable is applied for the simplification of Eq. (D.52), but now defines the integral,

$$I_1(\beta) = \int_0^\infty z^{-1} [P(\beta a + 1, z) - P(\beta a + 1/2, z)] dz. \quad (\text{D.56})$$

In those terms, Eq. (D.52) reduces to

$$T_2 = \beta \frac{\Gamma^2(\beta a + 1/2)}{[\Gamma^2(\beta a + 1) - (\beta a)\Gamma^2(\beta a + 1/2)]} I_1(\beta). \quad (\text{D.57})$$

Finally, the same change of variable is also used for simplification of the third term. With this change, the infinite integral is the definition of the Γ function and so the third term reduces to

$$T_3 = \frac{1}{2a} \frac{\Gamma^2(\beta a + 1/2)}{[\Gamma^2(\beta a + 1) - (\beta a)\Gamma^2(\beta a + 1/2)]}. \quad (\text{D.58})$$

Combining Eqs. (D.55), (D.57), and (D.58), the expression for the correlation time is rewritten as

$$T(\beta) = \frac{\Gamma^2(\beta a + 1/2)}{[\Gamma^2(\beta a + 1) - (\beta a)\Gamma^2(\beta a + 1/2)]} \times \left[\frac{\beta}{2} \Gamma(\beta a + 1) I_2(\beta) + \beta I_1(\beta) + \frac{1}{2a} \right]. \quad (\text{D.59})$$

We now use the assumption that the intensity of the noise D is large to expand Eq. (D.59) such that,

$$T(\beta) = T(0) + \beta \left. \frac{\partial}{\partial \beta} T(\beta) \right|_{\beta=0} + \mathcal{O}(\beta^2). \quad (\text{D.60})$$

The first term of Eq. (D.60) is

$$T(0) = \frac{1}{2a} \frac{\Gamma^2(1/2)}{\Gamma^2(1)} = \frac{\pi}{2a}, \quad (\text{D.61})$$

where we have used the known values of the Γ function, $\Gamma(1/2) = \sqrt{\pi}$ and $\Gamma(1) = 1$. Consider then the second term of Eq. (D.60),

$$\begin{aligned} \left. \frac{\partial}{\partial \beta} T(\beta) \right|_{\beta=0} = & \frac{1}{2a} \left\{ \frac{2a\Gamma(1/2)\Gamma'(1/2)}{\Gamma^2(1)} \right. \\ & \left. - \frac{\Gamma^2(1/2)}{\Gamma^4(1)} [2a\Gamma(1)\Gamma'(1) - a\Gamma^2(1/2)] \right\} \\ & + \frac{\Gamma^2(1/2)}{\Gamma^2(1)} \left[\frac{1}{2}\Gamma(1)I_2(0) + I_1(0) \right], \end{aligned} \quad (\text{D.62})$$

where the sign ' in Eq. (D.62) denotes the first derivative with respect to β . The values of the derivative of the gamma function can be found by using the a tabulated function, the so-called digamma function $\psi(z)$ defined as

$$\psi(z) = - \int_0^\infty \frac{e^{-zt}}{1 - e^{-t}} dt. \quad (\text{D.63})$$

Note that by definition

$$\psi(z) = \frac{d}{dz} \ln [\Gamma(z)] = \frac{\Gamma'(z)}{\Gamma(z)}. \quad (\text{D.64})$$

In particular, $\psi(1/2) = -\kappa - 2\ln(2)$ and $\psi(1) = -\kappa$, where $\kappa = 0.5772\dots$ is the Euler-Mascheroni constant. Hence, we have

$$\left. \frac{\partial}{\partial \beta} T(\beta) \right|_{\beta=0} = \frac{\pi^2}{2} - 2\pi\ln(2) + \pi I_1(0) + \frac{\pi}{2} I_2(0). \quad (\text{D.65})$$

We then need only need to find the value of the integral $I_1(\beta)$ and $I_2(\beta)$ at zero. Consider the first integral,

$$I_1(0) = \int_0^\infty z^{-1} [P(1, z) - P(1/2, z)] dz, \quad (\text{D.66})$$

and integrate by parts,

$$I_1(0) = \ln|z| [P(1, z) - P(1/2, z)] \Big|_0^\infty - \int_0^\infty \ln|z| e^{-z} (1 - \Gamma^{-1}(1/2) z^{-1/2}) dz . \quad (\text{D.67})$$

By definition of the incomplete gamma function, $P(1, 0) = P(1/2, 0) = 0$ and $P(1, \infty) = P(1/2, \infty) = 1$, and so only the second term of Eq. (D.67) contributes. Furthermore, use the following identity [144],

$$\int_0^\infty \ln|z| z^{\nu-1} e^{-\mu z} dz = -\frac{1}{\mu^\nu} \Gamma(\nu) [\psi(\nu) + \ln|\mu|] , \quad (\text{D.68})$$

so that Eq. (D.67) simplifies to

$$I_1(0) = - \int_0^\infty \ln|z| e^{-z} [1 - \Gamma^{-1}(1/2) z^{-1/2}] dz = -2\ln(2) . \quad (\text{D.69})$$

Finally, consider the integral $I_2(\beta)$ as defined in Eq. (D.54) and evaluate it at the origin,

$$I_2(0) = \int_0^\infty z^{-1} e^z [P(1, z) - P(1/2, z)]^2 dz . \quad (\text{D.70})$$

Note that the incomplete gamma function can be expressed as [139],

$$P(1, x) = 1 - e^{-x} , \quad (\text{D.71})$$

and

$$P(1/2, x) = 2\pi^{-1/2} \int_0^{\sqrt{x}} e^{-u^2} du = \text{erf}(\sqrt{x}) , \quad (\text{D.72})$$

where $\text{erf}(x)$ is the error function. The value of $I_2(0)$ can thus be evaluated numerically by using a continued fraction representation of the error function.

This leads to

$$I_2(0) = 0.4401 . \quad (\text{D.73})$$

Combining Eqs. (D.61) and (D.73) and substitute in Eq. (D.60), we thus obtain the expansion of the correlation time for large value of the noise intensity,

$$T = \frac{\pi}{2a} - \frac{A}{D} + \mathcal{O}\left(\frac{a}{D^2}\right) , \quad (\text{D.74})$$

where $A = 1.5421\dots$. Note that the correlation time diverges with respect to the control parameter with exponent -1. The expansion of the correlation time at small [Eq. (D.47)] and large [Eq. (D.74)] intensity of the noise can be combined together to derive the Padé approximant associated to Eq. (D.27). Padé approximant is a tool to express a function originally in power series by a rational function [143]. This method provides an analytical rational function that approximates the integral representation of the correlation time with the appropriate limit. In terms of the scaled correlation time $T' = aT$, assume a solution of the form,

$$T' = a_0 + \frac{a_1 D' + a_2 D'^2}{b_0 + b_1 D' + b_2 D'^2} = c_0 + c_1 D' + c_2 D'^2 , \quad (\text{D.75})$$

where $c_0 = 1/2$, $c_1 = 7/16$ and $c_2 = 9/64$. Equation (D.75) leads to a set of equations to solve,

$$a_0 = c_0 , \quad (\text{D.76})$$

$$a_1 = b_0 c_1 , \quad (\text{D.77})$$

$$a_2 = b_0 c_2 + c_1 b_1 , \quad (\text{D.78})$$

Furthermore, we impose the following limits determined from Eqs. (D.47) and (D.74),

$$\lim_{D' \rightarrow \infty} T' = a_0 + a_2 = \frac{\pi}{2} \quad (\text{D.79})$$

and

$$\frac{\partial}{\partial \beta} T'(\beta) = -2A . \quad (\text{D.80})$$

where $A = 1.5421$. The last condition implies that

$$a_1 - a_2 b_1 = -A . \quad (\text{D.81})$$

Then we have

$$a_2 = \frac{\pi}{2} - a_0 = 1.0708\dots , \quad (\text{D.82})$$

$$a_1 = \frac{c_1}{c_1^2 + c_2 a_2} (a_2^2 - A c_1) = 0.6037\dots , \quad (\text{D.83})$$

$$b_0 = \frac{a_1}{c_1} = 1.3800\dots , \quad (\text{D.84})$$

$$b_1 = \frac{A + a_1}{a_2} = 2.0040\dots , \quad (\text{D.85})$$

Combine Eqs. (D.82), (D.83), (D.84), (D.85), and $a_0 = 1/2$ and substitute in Eq. (D.75). In terms of the parameters of the model, the correlation time is

$$T = \frac{1}{2a} + \frac{0.6037Da + 1.0708D^2}{1.38a^3 + 2.004Da^2 + aD^2} . \quad (\text{D.86})$$

Equation (D.86) constitutes the Padé approximant of the correlation time associated to Eq. (D.22).

Bibliography

- [1] N. A. Campbell, J. B. Reece, L. A. Urry, M. L. Caine, S. A. Wasserman, P. V. Minorsky, and R. B. Jackson, *Biology*. San Francisco: Benjamin Cummings, 9th ed., 2010.
- [2] H. Lodish, A. Berk, C. A. Kaiser, M. Krieger, M. P. Scott, A. Bretscher, H. Ploegh, and P. Matsudaira, *Molecular Cell Biology*. New York: W. H. Freeman, 6nd ed., 2008.
- [3] B. Alberts, A. Johnson, J. Lewis, M. Raff, K. Roberts, and P. Walter, *Molecular Biology of the Cell*. New York: Garland Science, 5th ed., 2007.
- [4] X. Zhou, *Computational systems bioinformatics : methods and biomedical applications*. New Jersey: World Scientific, 2008.
- [5] S. Russel, *Microarray innovations : technology and experimentation*. Boca Raton: CRC Press, 2009.
- [6] M. Ptashne, *A genetic switch: Phage lambda and higher organisms*. New York: Cell Press and Blackwell Scientific, 2nd ed., 1992.
- [7] E. H. Davidson, J. P. Rast, P. Oliveri, A. Ransick, C. Caletani, C. Yuh, T. Minokawa, G. Amore, V. Hinman, C. Arenas-Mena, O. Otim, C. T.

- Brown, C. B. Livi, P. Y. Lee, R. Revilla, A. G. Rust, Z. J. Pan, M. J. Schilstra, P. J. C. Clarke, M. I. Arnone, L. Rowen, R. A. Cameron, D. R. McClay, L. Hood, and H. Bolouri, "A genomic regulatory network for development," *Science*, vol. 295, p. 1669, 2002.
- [8] R. Albert and H. G. Othmer, "The topology of the regulatory interactions predicts the expression pattern of the drosophila segment polarity genes," *J. Theor. Biol.*, vol. 223, p. 1, 2003.
- [9] G. von Dassow, E. Meir, E. M. Munro, and G. M. Odell, "The segment polarity network is a robust development module," *Nature*, vol. 406, p. 188, 2000.
- [10] M. Kanehisa and S. Goto, "Kegg : Kytot encyclopedia of genes and genomes," *Nucl. Acid Res.*, vol. 28, p. 27, 2000.
- [11] P. D. Karp, M. Arnaud, J. Collado-Vides, J. Ingraham, I. T. Paulsen, and M. H. Saier, "The e. coli ecocyc database: no longer just a metabolic pathway database," *ASM News*, vol. 70, p. 25, 2004.
- [12] R. D. Leclerc, "Survival of the sparsest: robust gene networks are parsimonious," *Mol. Syst. Biol.*, vol. 4, p. 213, 2008.
- [13] H. H. McAdams and A. Arkin, "Simulation of prokaryotic gene circuits," *Ann. Rev. Biophys. Biomolecul. Struct.*, vol. 27, p. 199, 1998.
- [14] M. I. Arnone and E. H. Davidson, "The hardwiring of development: organization and function of genomic regulatory systems," *Development*, vol. 124, p. 1851, 1997.

-
- [15] H. Jeong, B. Tombor, R. Albert, Z. N. Oltvai, and A. L. Barabasi, “The large-scale organization of metabolic networks,” *Nature*, vol. 407, p. 651, 2000.
- [16] H. Bolouri and E. H. Davidson, “Transcriptional regulatory cascades in development: Initial rates, not steady state, determine network kinetics,” *Proc. Natl. Acad. Sci. USA*, vol. 100, p. 9371, 2003.
- [17] H. H. McAdams and A. Arkin, “Stochastic mechanisms in gene expression,” *Proc. Natl. Acad. Sci. USA*, vol. 94, p. 814, 1997.
- [18] M. B. Elowitz, A. J. Levine, E. D. Siggia, and P. S. Swain, “Stochastic gene expression in a single cell,” *Science*, vol. 297, p. 1183, 2002.
- [19] W. J. Blake, M. Kaern, C. R. Cantor, and J. Collins, “Noise in eukaryotic gene expression,” *Nature*, vol. 422, p. 6932, 2003.
- [20] S. A. Kauffman, “Metabolic stability and epigenesis in randomly constructed genetic nets,” *J. Theor. Biol.*, vol. 22, p. 437, 1969.
- [21] S. A. Kauffman, *The Origins of Order: Self-Organization and Selection in Evolution*. USA: Oxford University Press, 1993.
- [22] C. W. Gardiner, *Handbook of Stochastic Methods for Physics, Chemistry and the Natural Sciences*. Berlin: Springer-Verlag, 2nd ed., 1997.
- [23] N. G. van Kampen, *Stochastic processes in Physics and Chemistry*. Amsterdam: Elsevier, 1981.
- [24] D. Gillespie, “Exact stochastic simulation of coupled chemical reactions,” *J. Comp. Phys.*, vol. 22, p. 403, 1977.

-
- [25] K. Ito and M. Nisio, "On stationary solutions of stochastic differential equation," *J. Math, Kyoto Univ.*, vol. 4, p. 1, 1964.
- [26] H. J. Kushner, *Stochastic stability and control*. New York: Academic, 1967.
- [27] I. I. Gihman and A. V. Skorohod, *Stochastic differential equations*. New York: Springer-Verlag, 1972.
- [28] T. T. Soong, *Random differential equations in science and engineering*. New York: Academic, 1973.
- [29] L. Arnold, *Stochastic Differential Equations : Theory and Applications*, vol. 1 and 2. New York: Academic, 1974.
- [30] A. Freidman, *Stochastic differential equations and applications*, vol. 1 and 2. New York: Academic, 1975.
- [31] K. Ikeda and S. Watanabe, *Stochastic differential equations and diffusion processes*. New York: North-Holland, 1981.
- [32] T. C. Gard, *Introduction to stochastic differential equations*. New York: Dekker, 1988.
- [33] K. Ito, "Differential equations determining a markoff process (in japanese)," *J. Pan-Japan Math. Coll.*, vol. 18, p. 261, 1942.
- [34] K. Ito, *Differential equations determining a Markoff process (in english)*. New York: Springer-Verlag, 1986.
- [35] R. L. Stratonovich, *Introduction to the Theory of Random Noise vol. 1*. New York and London: Gordon and Breach, 1963.

-
- [36] S. E. A. Mohammed, *Stochastic functional differential equations*. Boston: Pitman, 1984.
- [37] V. B. Kolmanovskii and V. R. Nosov, *Stability of functional differential equations*. New York: Academic, 1986.
- [38] P. E. Kloeden and E. Platen, *The Numerical Solution of Stochastic Differential Equations*. New York: Springer-Verlag, 1991.
- [39] W. Horsthemke and R. Lefever, *Noise Induced Transitions: Theory and Applications in Physics, Chemistry, and Biology*. Berlin: Springer-Verlag, 1984.
- [40] A. R. Bulsara, K. Lindenberg, V. Seshardi, K. E. Shuler, and B. J. West, "Stochastic processes with non-additive fluctuations : I. Ito and Stratonovich calculus and the effects of correlations," *Physica A*, vol. 97, p. 211, 1979.
- [41] A. R. Bulsara, K. Lindenberg, V. Seshardi, K. E. Shuler, and B. J. West, "Stochastic processes with non-additive fluctuations : II. Some applications of Ito and Stratonovich calculus," *Physica A*, vol. 97, p. 234, 1979.
- [42] N. G. van Kampen, "Ito versus Stratonovich," *J. Stat. Phys.*, vol. 24, p. 175, 1981.
- [43] J. Smythe, F. Moss, P. V. E. McClintock, and D. Clarkson, "Ito versus Stratonovich revisited," *Phys. Lett. A*, vol. 97, p. 95, 1983.
- [44] M. C. Mackey and I. G. Nechaeva, "Solution moment stability in stochastic differential delay equations," *Phys. Rev. E.*, vol. 52, no. 4, pp. 3366–3376, 1995.

-
- [45] P. S. Swain, M. B. Elowitz, and E. D. Siggia, “Intrinsic and extrinsic contributions to stochasticity in gene expression,” *Proc. Natl. Acad. Sci. U.S.A.*, vol. 99, p. 12795, 2002.
- [46] J. M. Raser and E. K. O’Shea, “Control of stochasticity in eukaryotic gene expression,” *Science*, vol. 304, p. 1811, 2004.
- [47] D. Volfson, J. Marciniak, W. J. Blake, N. Ostroff, L. S. Tsimring, and J. Hasty, “Origins of extrinsic variability in eukaryotic gene expression,” *Nature*, vol. 439, p. 861, 2006.
- [48] T. Shibata, “Fluctuating reaction rates and their applications to problems of gene expression,” *Phys. Rev. E*, vol. 67, p. 061906, 2003.
- [49] T. Shibata, “Reducing the master equations for noisy chemical reactions,” *J. Chem. Phys.*, vol. 119, p. 6629, 2003.
- [50] R. E. Bellman and K. L. Cooke, *Differential-Difference Equations*. New York: Academic Press, 1963.
- [51] R. D. Driver, “A functional differential system of neutral type arising in a two-body problem of classical electrodynamics,” in *Nonlinear differential equations and nonlinear mechanics*, (New York), Academic, 1963.
- [52] A. Halanay, *Differential equations, stability, and oscillations, time lags*. New York: Academic, 1966.
- [53] J. K. Hale, *Functional differential equations*. New York: Springer-Verlag, 1971.

-
- [54] L. E. El'sgol'ts and S. B. Norkin, *Introduction to the theory and application of differential equations with deviating arguments*. London: Academic Press, 1973.
- [55] J. K. Hale, *Theory of functional differential equations*. New York: Springer-Verlag, 1977.
- [56] R. D. Driver, *Ordinary and Delay Differential Equations*, vol. 20. New York: Springer, 1977.
- [57] T. Saaty, *Modern nonlinear equations*. New York: Dover Publications, 1981.
- [58] F. A. Hopf, D. Kaplan, H. M. Gibbs, and R. L. Shomaker, "Bifurcations to chaos in optical bistability," *Phys. Rev. A*, vol. 25, p. 2172, 1982.
- [59] K. Ikeda and K. Matsumoto, "High-dimensional chaotic behavior in systems with time-delayed feedback," *Physica D*, vol. 29, p. 223, 1987.
- [60] H.-J. Zhang, J.-H. Dai, P. Wang, F.-L. Zhang, G. Xu, and S.-P. Yang, "Chaos in liquid crystal optical bistability," in *Directions in Chaos* (B.-L. Hao, ed.), (Singapore), pp. 46–89, World Scientific, 1988.
- [61] A. Longtin and J. Milton, "Complex oscillations in the human pupil light reflex with mixed delayed feedback," *Math. Biosci.*, vol. 90, p. 183, 1988.
- [62] A. Longtin, J. Milton, J. E. Bos, and M. C. Mackey, "Noise and critical behavior of the pupil light reflex at oscillation onset," *Phys. Rev. A*, vol. 41, p. 6992, 1990.

-
- [63] C. M. Marcus and R. M. Westervelt, "Stability of analog neural networks with delay," *Phys. Rev. A*, vol. 39, p. 347, 1989.
- [64] J. G. Milton, A. Longtin, A. Beuter, M. C. Mackey, and L. Glass, "Complex dynamics and bifurcations in neurology," *J. Theor. Biol.*, vol. 138, p. 129, 1989.
- [65] C. M. Marcus and R. M. Westervelt, "Stability and convergence of analog neural networks with multiple-time-step parallel dynamics," *Phys. Rev. A*, vol. 42, p. 2410, 1990.
- [66] A. Longtin, "Noise-induced transitions at a hopf bifurcation in a first-order delay-differential equation," *Phys. Rev. A*, vol. 44, p. 4801, 1991.
- [67] M. Mackey and L. Glass, "Oscillation and chaos in physiological control systems," *Science*, vol. 197, p. 287, 1977.
- [68] L. Glass and M. Mackey, *From Clocks to Chaos : The rhythms of life*. NJ: Princeton University Press, 1988.
- [69] J. Bélair and M. C. Mackey, "Consumer memory and price fluctuations in commodity markets: An integrodifferential model," *J. Dyn. Diff. Eqns.*, vol. 1, p. 299, 1989.
- [70] M. C. Mackey, "Commodity price fluctuations: Price dependent delays and nonlinearities as explanatory factors," *J. Econ. Theory*, vol. 48, p. 497, 1989.
- [71] A. T. Bharucha-Reid, *Elements of the theory of Markov processes and their applications*. New York: McGraw-Hill, 160.

-
- [72] A. Papoulis, “Brownian movement and markoff processes,” in *Probability, Random Variables, and Stochastic Processes*, (New York), p. 515, McGraw-Hill, 1984.
- [73] H. Risken, *The Fokker-Planck Equation: Methods of solutions and Applications*. Berlin: Springer, 1989.
- [74] D. Bratsun, D. Volfson, L. S. Tsimring, and J. Hasty, “Delayed-induced stochastic oscillations in gene regulation,” *Proc. Natl. Acad. Sci. USA*, vol. 102, no. 41, p. 14593, 2005.
- [75] P. Smolen, D. Baxter, and J. Bryne, “Modeling circadian oscillations with interlocking positive and negative feedback loops,” *J. Neurosci.*, vol. 21, p. C6644, 2001.
- [76] K. Sriram and M. S. Gopinathan, “A two variable delay model for the circadian rhythm of *Neurospora Crassa*,” *J. Theor. Biol.*, vol. 231, p. C23, 2004.
- [77] T. Galla, “Intrinsic fluctuations in stochastic delay systems: Theoretical description and application to a simple model of gene regulation,” *Phys. Rev. E*, vol. 80, p. 021909, 2009.
- [78] J. Guckenheimer and P. Holmes, *Nonlinear Oscillations, Dynamical Systems, and Bifurcations of Vector Fields*. New York: Springer, 2nd ed., 1983.
- [79] Y. A. Kuznetsov, *Elements of Applied Bifurcation Theory*. New York: Springer, 2nd ed., 1998.

-
- [80] S. H. Strogatz, *Nonlinear dynamics and chaos with applications to Physics, Biology, Chemistry and Engineering*. New York: Perseus Books, 1994.
- [81] A. Schenzle and H. Brand, “Multiplicative stochastic processes in statistical physics,” *Phys. Rev. A*, vol. 20, p. 1628, 1979.
- [82] R. Graham and A. Schenzle, “Carleman imbedding of multiplicative stochastic processes,” *Phys. Rev. A*, vol. 25, p. 1731, 1982.
- [83] P. Jung and H. Risken, “Correlation functions and correlation times for models with multiplicative white noise,” *Z. Phys. B*, vol. 59, p. 469, 1985.
- [84] L. E. El’sgol’ts, *Introduction to the theory differential equations with deviating arguments*. New York: Holden-Day, 1966.
- [85] M. C. Mackey and I. G. Nechaeva, “Noise and stability in differential delay equations,” *J. Dyn. Diff. Eqns.*, vol. 6, p. 395, 1994.
- [86] T. D. Frank, “Delay Fokker-Planck equations, Novikov’s theorem, and Boltzmann distributions as small delay approximations,” *Phys. Rev. E*, vol. 72, p. 011112, 2005.
- [87] S. Guillouxic, I. L’Heureux, and A. Longtin, “Small delay approximation of stochastic delay differential equations,” *Phys. Rev. E*, vol. 59, p. 3970, 1999.
- [88] S. Guillouxic, I. L’Heureux, and A. Longtin, “Rate processes in a delayed, stochastically driven, and overdamped system,” *Phys. Rev. E*, vol. 61, p. 1906, 2000.

-
- [89] R. D. Driver, D. W. Sasser, and M. L. Slater, “The equation $x'(t) = ax(t) + bx(t - \tau)$ with “small” delay,” *Amer. Math. Monthly*, vol. 80, p. 990, 1973.
- [90] R. Kuske, “Multi-scale analysis of noise-sensitivity near a bifurcation,” in *IUTAM Symposium on Nonlinear Stochastic Dynamics* (N. S. Namachchivaya and Y. Lin, eds.), (Dordrecht, The Netherlands), p. 492, Kluwer Academic Publishers, 2003.
- [91] M. M. Klosek, “Multiscale analysis of effects of additive and multiplicative noise on delay differential equations near a bifurcation point,” *Acta Phys. Pol. B*, vol. 35, no. 4, pp. 1387–1405, 2004.
- [92] M. M. Klosek and R. Kuske, “Multiscale analysis of stochastic delay differential equations,” *Multiscale Model. Simul.*, vol. 3, no. 3, pp. 706–729, 2005.
- [93] P. H. Baxendale, “Stochastic Duffing-van der Pol oscillator,” in *IUTAM Symposium on Nonlinear Stochastic Dynamics* (N. S. Namachchivaya and Y. K. Lin, eds.), (Dordrecht, The Netherlands), p. 492, Kluwer Academic Publishers, 2003.
- [94] P. H. Baxendale, “Stochastic averaging and asymptotic behavior of the stochastic Duffing-van der Pol equation,” *Stoch. Proc. Appl.*, vol. 113, pp. 235–272, 2004.
- [95] T. D. Frank, “Delay Fokker-Planck equations, perturbation theory, and data analysis for nonlinear stochastic systems with time delays,” *Phys. Rev. E*, vol. 71, p. 031106, 2005.

-
- [96] R. F. Fox, "Second-order algorithm for the numerical integration of colored-noise problems," *Phys. Rev. A*, vol. 43, p. 2649, 1991.
- [97] G. E. P. Box and M. E. Muller, "A notes on the generation of random normal deviates," *Annals of Math. Stat.*, vol. 29, p. 610, 1958.
- [98] M. San Miguel and R. Toral, "Stochastic effects in physical systems," in *Instabilities and nonequilibrium Structures, VI*, (The Netherlands), Kluwer Academic, 2000.
- [99] W. Hornsthemke and R. Lefever, "Noise-induced transition," in *Noise in nonlinear dynamical systems. Volume 2 : Theory of noise induced processes in special applications* (F. Moss and P. V. E. McClintock, eds.), (Great Britain), p. 388, Cambridge University Press, 1989.
- [100] H. Haken, *Synergetics: Introduction and Advanced Topics*. Berlin, Heidelberg, New York: Springer-Verlag, 1978.
- [101] E. M. Lifshitz and L. P. Pitaevskii, *Statistical Physics*. Oxford: Pergamon, 1980.
- [102] F. Drolet and J. Viñals, "Adiabatic reduction near a bifurcation in stochastically modulated systems," *Phys. Rev. E*, vol. 57, p. 5036, 1998.
- [103] K. Furutsu, "On the theory of radio wave propagation over inhomogeneous earth," *J. Res. NBS*, vol. D-67, p. 39, 1963.
- [104] E. A. Novikov, "Functional and the random force method in turbulence theory," *Sov. Phys. JETP*, vol. 20, p. 1290, 1965.

-
- [105] J. Lei and M. C. Mackey, “Stochastic differential delay equation, moment stability, and application to hematopoietic stem cell regulation system,” *SIAM L. Appl. Math.*, vol. 67, p. 387, 2007.
- [106] R. M. Corless, G. H. Gonnet, D. E. G. Hare, D. J. Jeffrey, and D. Knuth, “On the lambert W function,” *Adv. Computational Maths*, vol. 5, p. 329, 1996.
- [107] E. M. Wright, “The linear difference-differential equation with constant coefficients,” *Proc. Royal Soc. Edinburgh A*, vol. 62, p. 387, 1949.
- [108] P. E. Kloeden and E. Platen, “Stratonovich and Ito stochastic Taylor expansion,” *Math. Nachr.*, vol. 151, p. 33, 1991.
- [109] R.-H. Shao and Y. Chen, “Stochastic resonance in time-delayed bistable systems driven by weak periodic signal,” *Physica A*, vol. 388, p. 977, 2009.
- [110] H. Zhang and D. Li, “Stochastic time-delayed systems driven by correlated noises: Steady-state analysis,” *Physica A*, vol. 388, p. 3017, 2009.
- [111] M. Lücke, “Noise in nonlinear dynamical systems,” in *Theory of noise induced processes in special applications* (F. Moss and P. McClintock, eds.), (Cambridge, England), Cambridge University Press, 1989.
- [112] E. V. Appleton and B. van der Pol, “On a type of oscillation-hysteresis in a simple triode generator,” *Philosophical magazine*, vol. 43, p. 177, 1922.
- [113] A. Maccari, “The response of a parametrically excited van der Pol oscillator to a time delay state feedback,” *Nonlinear Dyn.*, vol. 26, p. 105, 2001.

-
- [114] A. Maccari, "Vibration control for the primary resonance of the van der Pol oscillator by a time delay state feedback," *Int. J. Nonlinear Mech.*, vol. 38, p. 123, 2003.
- [115] A. Maccari, "Delayed feedback control for a parametrically excited van der Pol oscillator," *Phys. Scr.*, vol. 76, p. 526, 2007.
- [116] J. Xu and K. W. Chung, "Effects of time delayed position feedback on a van der Pol-Duffing oscillator," *Physica D*, vol. 180, p. 17, 2003.
- [117] J. C. Ji and C. H. Hansen, "Stability and dynamics of a controlled van der Pol-Duffing oscillator," *Chaos Soliton Fract.*, vol. 28, p. 555, 2006.
- [118] X. Li, J. C. Ji, C. H. Hansen, and C. Tan, "The response of a Duffing-van der Pol oscillator under delayed feedback control," *J. Sound Vibrat.*, vol. 291, p. 644, 2006.
- [119] C. Mayol, R. Toral, and C. R. Mirasso, "Derivation of amplitude equations for nonlinear oscillators subject to arbitrary forcing," *Phys. Rev. E*, vol. 69, p. 066141, 2004.
- [120] M. Gaudreault, F. Drolet, and J. Viñals, "Analytical determination of the bifurcation thresholds in stochastic differential equations with delayed feedback," *Phys. Rev. E*, vol. 82, p. 051124, 2010.
- [121] E. School, A. G. Balanov, and N. Janson, "Controlling stochastic oscillations close to a hopf bifurcation by time-delayed feedback," *Stoch. Dyn.*, vol. 5, p. 281, 2005.
- [122] D. S. Goldobin, "Coherence versus reliability of stochastic oscillators with delayed feedback," *Phys. Rev. E*, vol. 78, p. 060104, 2008.

-
- [123] X. L. Yang and Z. K. Sun, “Research on parametric resonance in a stochastic van der Pol oscillator under multiple time delayed feedback,” *Int. J. Nonlinear Mech.*, vol. 45, p. 621, 2010.
- [124] Y. Jin and H. Hu, “Principal resonance of a duffing oscillator with delayed state feedback under narrow-band random parametric excitation,” *Nonlinear Dyn.*, vol. 50, p. 213, 2007.
- [125] K. A. Wisenfeld and E. Knobloch, “Effect of noise on the dynamics of a nonlinear oscillator,” *Phys. Rev. A*, vol. 26, p. 2946, 1982.
- [126] E. Knobloch and K. A. Wisenfeld, “Bifurcations in fluctuating systems : the center-manifold approach,” *J. Stat. Phys.*, vol. 33, no. 3, pp. 611–637, 1983.
- [127] F. Baras, M. M. Mansour, and C. van der Broeck, “Asymptotic properties of coupled nonlinear langevin equations in the limit of weak noise. II: Transition to a limit cycle,” *J. Stat. Phys.*, vol. 28, p. 577, 1982.
- [128] V. Seshadri, B. West, and K. Lindenberg, “Stability properties of nonlinear systems with fluctuating parameters,” *Physica A*, vol. 107, p. 219, 1981.
- [129] J. M. Sancho, M. San Miguel, S. L. Katz, and J. D. Gunton, “Analytical and numerical studies of multiplicative noise,” *Phys. Rev. A*, vol. 26, pp. 1589–1609, 1982.
- [130] M. Gaudreault, F. Lépine, and J. Viñals, “Pitchfork and Hopf bifurcation thresholds in stochastic equations with delayed feedback,” *Phys. Rev. E*, vol. 80, p. 061920, 2009.

-
- [131] R. L. Stratonovich, *Introduction to the Theory of Random Noise vol. 2*. New York and London: Gordon and Breach, 1963.
- [132] J. Sancho, R. Mannella, P. McClintock, and F. Moss, "Relaxation times in a bistable system with parametric white noise : Theory and experiment," *Phys. Rev. A*, vol. 32, p. 3639, 1985.
- [133] S. Faetti, C. Festa, L. Fronzoni, P. Grigolini, F. Marchesoni, and V. Palleschi, "Multiplicative stochastic processes : on the correlation time as a function of noise intensity," *Phys. Lett.*, vol. 99A, no. 1, p. 25, 1983.
- [134] A. Hernandez-Machado, M. San Miguel, and J. Sancho, "Relaxation time of processes driven by multiplicative noise," *Phys. Rev. A*, vol. 29, p. 3388, 1984.
- [135] R. Mannella, S. Faetti, P. Grigolini, P. V. E. McClintock, and F. E. Moss, "The effect of multiplicative noise on the relaxation time of a real non-linear physical system : a comparison of experiment and theory for the random growing rate model (RGRM)," *J. Phys. A: Math. Gen.*, vol. 19, p. L699, 1986.
- [136] R. Mannella, S. Faetti, P. Grigolini, and P. McClintock, "On the relaxation of fluctuations in the steady state of the stratonovich model," *J. Phys. A : Math. Gen.*, vol. 21, p. 1239, 1988.
- [137] J. Casademunt, R. Mannella, P. McClintock, F. Moss, and J. Sancho, "Relaxation times of non-markovian processes," *Phys. Rev. A*, vol. 35, p. 5183, 1987.

-
- [138] W. Horstehmke and R. Lefever, *Noise-Induced Transitions : Theory and Applications in Physics, Chemistry, and Biology*. Berlin, Heidelberg: Springer, 1984.
- [139] M. Abramowitz and I. A. Stegun, *Handbook of mathematical functions*. New York: Dover publ., 1964.
- [140] V. I. Klyatskin and V. I. Tatarskii, “Diffusive random process approximation in certain nonstationary statistical problems of physics,” *Usp. Fiz. Nauk*, vol. 110, p. 499, 1973.
- [141] R. Short, L. Mandel, and R. Roy, “Correlation functions of a dye laser: Comparison between theory and experiment,” *Phys. Rev. Lett.*, vol. 49, p. 647, 1982.
- [142] P. Lett, R. Short, and L. Mandel, “Photon statistics of a dye laser far below threshold,” *Phys. Rev. Lett.*, vol. 52, p. 341, 1984.
- [143] G. A. Baker, *Padé approximants*. Cambridge, New York: Cambridge University Press, 2nd ed., 1996.
- [144] L. Gradshteyn and M. Ryzhik, *Tables of integrals series and products*. New York: Academic press, 1965.